The Developing Rhesus Monkey Microbiome

By

NOAH ALEXANDER SIEGEL

DISSERTATION

Submitted in partial satisfaction of the requirements for the degree of

DOCTOR OF PHILOSOPHY

in

Immunology

in the

OFFICE OF GRADUATE STUDIES

of the

UNIVERSITY OF CALIFORNIA
DAVIS

Approved:

(Lisa A. Miller), Chair

(Andreas Baumler)

(Barbara Shacklett)

Committee in Charge

2023

The Developing Rhesus Monkey Microbiome

by

Noah Alexander Siegel

To the cherished individuals in my life - my family, friends, and mentors.

Acknowledgements

> He is a wise man who does not grieve for the things which he has not, but rejoices for those which he has.
>
> Epictetus

I want to thank Dr. Lisa Miller, my advisor, for her unwavering support and encouragement throughout my PhD journey. She has challenged me to push past my limits and has provided me with invaluable opportunities for growth as a scientist. I am grateful for the collaborative and inspiring environment she has created, where ideas are freely exchanged, and everyone works together towards common goals. I would also like to extend my thanks to my committee members, Dr. Barbara Shacklett and Dr. Andreas Baümler, for their expert guidance and advice that helped me navigate through my research findings.

I would like to express my gratitude to the funding sources that made this project possible. Their contributions have been instrumental in turning this project from an idea to a reality. The R01 grant enabled us to acquire the necessary supplies, materials, and samples for our research into the effects of neonatal antibiotics on lung pulmonary immunity. Additionally, the grant allowed us to obtain the animals required to conduct the study. The grant also provided us with reagents such as DNA extraction kits and various services, including DNA sequencing and untargeted metabolomics. Moreover, I was fortunate to receive the P51 Diversity Fellowship at the start of my graduate studies. The fellowship provided me with a stipend and supported my training in Bioinformatics through courses offered at the UC Davis Genome Center.

I want to express my sincere gratitude to all of my labmates for their unwavering

support. In particular, I would like to extend a special thanks to Alexa Rindy, our former lab manager, whose guidance and organizational skills were invaluable in steering this project. Taylor Westmont, whose project is also rooted in the same grant, has been a valuable resource, an exceptional colleague, and a dear friend. I also deeply appreciate Diwash Shrethsa, who consistently lent a listening ear and offered valuable feedback on the coding efforts invested in this project.

I am grateful to Matt Rolston, who trained me in generating the sequencing libraries that played a foundational role in this project while I was at the Host Microbe Systems Core at UC Davis. His constant support and reassurance that I could complete this project during those long days and nights at the HMSC were essential. Additionally, I would like to thank Aaron Para from the CNPRC IT department for his generous help troubleshooting various computer issues, from failed hard drives to software installation glitches.

I am thankful to Jessica Drushell, the Graduate Group in Immunology coordinator, who has always been there to answer my questions and provide guidance on navigating graduate school whenever I needed extra assistance. I appreciate the close friendships I made in graduate school; the companionship of Gustavo Garcia, JW Roh, Sonny Elizaldi, and Carlos Carrasco will be valued for years to come. I would also like to express my gratitude to my parents, Marsha and Boris Siegel, for encouraging my interests and teaching me to think critically about the world. Lastly, I am grateful to my fiancée, Viki Haghani, for supporting me through the ups and downs of my PhD, including the recent global viral pandemic.

Noah Alexander Siegel
September 2023
Immunology

Abstract

The microbiome is vital for maintaining good health, with disruptions carrying significant consequences. Antibiotics, diseases, environmental changes, and biological sex can perturb the microbiome, contributing to chronic illnesses. Antibiotic use is a substantial disruptor, highlighting the need to pinpoint specific microbial species and their functions for targeted therapies. Our research examined the microbiome, utilizing 16S sequencing to gain deeper insights into microbial communities at the species level and infer their functional capacity. Early-life antibiotic exposure was found to have a lasting impact on the microbiome, with a more pronounced effect observed in males than females. These effects extended to the respiratory microbiome, demonstrating the interconnectedness of microbiome composition with physiological factors. Furthermore, our research delved into predicted metagenomic pathways in the gut and lung microbiomes, revealing shifts in metabolic functions with antibiotic treatment, particularly in pathways linked to short-chain fatty acid metabolism, highlighting the potential consequences of such alterations on host health. Advances in microbiome research stress the importance of considering sex-specific differences in microbiome responses, leading to tailored health interventions. In conclusion, this research substantiates the role of the microbiome in maintaining health and the potential impact of disruptions on the immune system. Our findings emphasize the need for targeted therapeutic strategies to mitigate the consequences of microbiome disturbances, thus advancing health and well-being.

Contents

List of Tables

List of Figures

Chapter 1

Exploring the Complex Relationship Between the Microbiome and Health: Implications for Antibiotic Use and Sex Differences

> In the field of observation, chance favours only the prepared mind.
>
> Louis Pasteur

Abstract

The human microbiome is critical in maintaining good health, and disturbances can have significant consequences. Factors such as antibiotics, disease, tobacco smoke, and environmental changes can reduce bacterial diversity and alter microbial composition,

contributing to chronic illnesses. In addition, the immune system is essential for maintaining microbiome homeostasis, and changes to the immune system can both cause or result from microbiome disruption. Notably, antibiotic use is a significant factor that can disrupt the microbiome. Therefore, identifying specific microbial species and their functions in health and disease is crucial for developing targeted treatments. Furthermore, biological sex can impact the microbiome, and future studies need to account for this when analyzing data. The use of animal models such as rhesus macaque and murine models can help us understand the role of the microbiome in health and disease. Ultimately, a better understanding of the interplay between biological sex, the microbiome, and the immune system can lead to targeted therapies that can mitigate the adverse effects of microbiome disruption and improve human health.

Introduction

The human body harbors a collection of microorganisms called the microbiome, the gut microbiome being the most extensively studied. Its crucial role in human health includes food digestion and immune system influence. However, disrupting the microbiome can have severe consequences (Kozyrskyj et al. 2016, Yildiz et al. 2018, Gao et al. 2019). Antibiotics, commonly used to treat bacterial infections, can significantly impact the gut microbiome by reducing bacterial diversity and altering its composition (Lamberte and van Schaik 2022).

The respiratory microbiome is gaining increasing attention due to its potential role in respiratory diseases, such as asthma, chronic obstructive pulmonary disease, and pneumonia (Biesbroek et al. 2014b, Biesbroek et al. 2014a, Marsland et al. 2015, He et al. 2017, Wang et al. 2017, Kuek and Lee 2020). Alterations in respiratory microbiome diversity,

such as increased abundances of potentially pathogenic bacteria, have been observed in respiratory infections (Yildiz et al. 2018), while chronic respiratory diseases that may contribute to disease development and exacerbation have been linked to changes in the respiratory microbiome (Huang et al. 2015, Mammen and Sethi 2016). Environmental factors like diet and air pollution can also impact the gut and respiratory microbiota. For instance, a high-fat, low-fiber diet can alter the gut microbiome's composition, reducing bacterial diversity (Cox et al. 2014). Air pollution from PM2.5 and NO2 pollution are associated with reduced Ružička dissimilarity, a measure of beta-diversity, suggesting a possible interplay between the nasal microbiota of human infants and air pollution (Gisler et al. 2021).

Biological factors also play a role in microbiome composition; recent research has highlighted sex differences in microbiome composition across various body sites, including the gut and respiratory tract (Kim et al. 2019, Jo et al. 2021, Valeri and Endres 2021). Women have a higher abundance of specific bacterial genera in the gut, such as *Bacteroides* and *Prevotella*, while men have a higher abundance of other taxa, such as *Allobaculum* and *Anaeroplasma* (Kim et al. 2019). Hormonal fluctuations may influence these differences, with estrogen promoting the growth of certain gut bacteria associated with health benefits (Peng et al. 2020). Sex-specific differences in gut microbiome composition may contribute to differences in disease susceptibility and outcomes, including autoimmune diseases, obesity, and colorectal cancer (Markle et al. 2013, Kim et al. 2020, Daly et al. 2022).

This review aims to comprehensively introduce the gut and respiratory microbiomes during health and disease, including the significance of sex differences in microbiome maturation. Finally, we discuss the use of animal models to study the microbiome.

Gut Microbiome

The gut microbiome is a complex ecosystem that comprises trillions of microorganisms, including bacteria, viruses, fungi, and archaea (Lloyd-Price et al. 2016). Vaginally-born human infants start to develop their microbiome when exiting the birthing canal. They are coated with vaginal microbes, while cesarian-born infants are first introduced to their mother's skin microbes (Rautava et al. 2012). There is a debate regarding the persistence of a placental microbiome due to the inconsistent and unreliable nature of sampling methods (Kuperman et al. 2020). However, much of the current literature demonstrates that infants are not exposed to microbes in the womb under healthy conditions (de Goffau et al. 2019, Kuperman et al. 2020). Breast milk from mothers provides essential nutrients for an infant's microbiome development after birth (Harmsen et al. 2000). The infant gut microbiota undergoes frequent changes until around 3 years of age when it begins to resemble a stable phenotype with high abundances of bacteria from various phyla, including *Firmicutes*, *Bacteroidetes*, *Proteobacteria*, *Actinobacteria*, *Fusobacteria*, and *Cyanobacteria* (Nobel et al. 2015, Marsland et al. 2015). Work on murine models from the Blaser group highlights the importance of this initial colonization, showing that early-life disruption of the microbiota in mice can lead to a long-term alteration in the composition of the gut microbiome (Cox et al. 2014).

Rhesus monkeys are another useful model for studying the gut microbiome as the infant human and rhesus monkey microbiomes overlap considerably, with *Bifidobacteria* being one of the predominant taxa present. Specifically it was found that infant primate gut microbiome is significantly enriched for *Bifidobacterium*, *Ureaplasma*, *Collinsella*, *Catenibacterium*, *Holdemanella*, *Anaerostipes*, *Roseburia*, *Bacteroides*, *Dorea*, and *Senegalimassilia* and deficient in *Anaeroplasma*, *Prevotellacaea gen.*, *Sphaerochaeta*, and *Fibrobacter*

relative to old macaques (Janiak et al. 2021). Similar results were obtained by both the Rhoades group in which they identified enrichment of *Campylobacter*, *Bifidobacterium*, *Catenibacterium*, *Succinivibrio*, and *Helicobacter* in infant rhesus monkeys (Rhoades et al. 2019) and the Slupsky team where infants were enriched for *Bifidobacterium* and *Blautia* (Hasegawa et al. 2018). These findings coincide with what is observed in human studies in that the gut microbiome tends to be enriched for *Bifidobacterium* during infancy and its abundance wanes during adulthood. Despite significant overlap between many taxa of the microbiome of rhesus monkeys and humans, the rhesus microbiome resembles more of a hunter-gatherer phenotype than that of a typical western microbiome (Rhoades et al. 2019).

The microbial density of the gut microbiome is far greater than any other mucosal site (Huttenhower et al. 2012). Being a well-studied mucosal site, researchers have demonstrated that the gut microbiome can modulate other mucosal sites and play a crucial role in regulating the gut-lung axis (van Nimwegen et al. 2011, Trompette et al. 2014). Although the gut and lungs are spatially far apart, they can communicate via the blood and lymphatic system (He et al. 2017). The gut microbiota produces short-chain fatty acids (SCFAs) that have been shown to influence the immune system and inflammation (Sivaprakasam et al. 2016).

Some of the most studied SCFA are acetate, propionate, and butyrate; these molecules are by-products of bacterial metabolism of indigestible dietary fibers in the gut (Pascale et al. 2018). Butyrate is one of the most extensively studied SCFA due to its immune capabilities (Vinolo et al. 2011). Among its many properties, butyrate has been demonstrated to limit NF-κB activation in macrophages residing in the lamina propria in human patients living with ulcerative colitis (Lührs et al. 2002). More recently, butyrate has been found to reduce neutrophil inflammatory cytokine production in Inflammatory

Bowel Disease (IBD) patients (Li et al. 2021). The researchers conducted *in vivo* DSS colitis mouse experiments in the same study. They found that histone deacetylase (HDAC) activity was responsible for promoting the inflammatory properties of neutrophils in IBD patients. Blockage with the pan HDAC inhibitor trichostatin A recapitulated the effect of butyrate, thus perpetuating the role of butyrate as an anti-inflammatory mediator in the gut. SCFAs also modulate the development of regulatory T cells (Tregs) that play a role in suppressing the immune response (Park et al. 2015).

Alteration of the gut microbiome through probiotics and fecal microbiome transplants (FMT) can have global effects on the body. In mice, nasal administration of *Lactobacillus casei* or *Lactobacillus rhamnosus* can reduce symptoms of influenza infection and dampen viral titers (Marsland et al. 2015). Breastfeeding acts as a form of probiotic in that it helps seed the infant's immature microbiome. The oligosaccharides of breast milk serve as a nutrient source for specific microbes such as *Lactobacillus* (Kim and Yi 2020). In addition to providing sugars, breast milk contains secretory IgA and other anti-microbial factors (Park et al. 2015, Roager and Licht 2018, Kim and Yi 2020). While probiotics can facilitate the development of a healthy microbiome, colonization of opportunistic pathogens such as *Clostridioides difficile*, a diarrhea and colitis-causing bacteria, can disrupt the microbiome. Asymptomatic carriers of this bacterium experience a reduction in the abundance of *Bacteroidetes* and *Firmicutes* and an overabundance of *Proteobacteria* (Zhang et al. 2015). The United States Food and Drug Administration (USFDA) has recently approved Rebyota, the first FMT product to treat recurrent *Clostridioides difficile* (Kempler 2022).

Lung Microbiome

The lung microbiome is a relatively new area of research, but important insights have already been revealed into the role of microorganisms in lung health and disease such as less stable respiratory microbiomes of infants at 2 years are characerized by a trajectory towards Haemophilus and Streptococcus-dominated profiles (Biesbroek et al. 2014a). Due to the reduced cost of sequencing and the introduction of culture-independent methods such as 16s sequencing, researchers can discover more information on the respiratory microbiota (Moffatt and Cookson 2017). Once initially thought to be sterile, it is now accepted that the respiratory microbiome is home to a diverse community of microorganisms, including bacteria, viruses, fungi, and other microorganisms (Baughman et al. 1987, Thorpe et al. 1987, Moffatt and Cookson 2017). Various factors, such as age, sex, smoking status, and environmental exposures, influence the composition of the lung microbiome (Koppen et al. 2015, Chen et al. 2020). The composition also depends upon the location along the respiratory tract. For example, the nasal microbiome has significant overlap with skin microbes and tends to comprised primarily or aerobic bacteria where as the lower has significant anerobic microbial populations such as *Prevotella sp.* and *Veillonella sp.* (Dickson et al. 2017).

The respirory microbiome of mice is highly variable and connections to the human microbiome are difficult to make due to mice being caprophagic. The family *Erysipelotrichaceae*, a microbiome enriched in the feces, is also found in the respiratory microbiome (Dickson et al. 2018). Another study confirmed the presence of the genera *Ochrobactrum* and *Rhodococcus* in the normal murine respiratory microbiome sampling by BAL (Kostric et al. 2018). Like human studies, the rhesus macaque respiratory microbiome is less studied than the gut microbiome. Of what few respiratory microbiome

studies there for rhesus macaques, all focus on adult populations (Janiak et al. 2021, Rhoades et al. 2022). Unlike humans, whose lung microbiome is primarily comprised of *Corynebacterium spp.*, *Dolosigranulum spp.*, and *Moraxella spp.* (Peterson et al. 2016) the rhesus monkey lung microbiome primarily contains the genus *Tropheryma* as a dominant community member however the genera *Streptococcus*, *Fusobacterium*, and *Actinobacillus* are also seen across lung samples (Rhoades et al. 2022).

Upper airway Microbiome

The upper respiratory tract, which consists of the nasal passages and pharynx, is responsible for transporting air from and to the lower respiratory tract. This area is commonly referred to as the nasopharynx and is also a physical barrier that can prevent potential pathogens from seeding the lower lung (Zhao et al. 2023). The nasopharynx is the point where the respiratory tract meets the external environment and can be impacted by external factors, including the type of feeding, such as breastfeeding versus formula feeding (Biesbroek et al. 2014b).

Under normal conditions, a healthy nasal cavity is enriched with microbes such as, but not limited to, *Corynebacterium spp.*, *Dolosigranulum spp.*, and *Moraxella spp.* (Peterson et al. 2016). The nasal, like the gut microbiome, can also be impacted by the method of delivery, as shown by Bosch et al., where they collected 112 nasopharynx swabs from healthy term infants either delivered vaginally or cesarian and compared the nasal microbiome composition between the mode of birth. They found the infants delivered vaginally had their nasal microbiomes colonized by a more diverse set of microbes, including *Corynebacterium* and *Dolosigranulum*, during the first week of life compared to infants born cesarian (Bosch et al. 2016).

Lower airway microbiome

The lower lung microbiome is distinct from the nasopharyngeal microbiome, harboring more anaerobic microbes (Huffnagle et al. 2017). The lung is a less hospitable environment to bacteria proliferation than the gut, as the gut's function is to acquire and absorb nutrients from ingested food, thus supporting a high microbial density. Conversely, the lack of microbes in the lower lung is due to its maintaining the bronchial epithelial fluid lining, which promotes gas exchange rather than nutrient acquisition. Due to this purpose, the adult human airway has a surface area roughly 40 times larger than the skin's (Weibel 1963). The composition of microbes in the lower airways includes gram-negative bacteria, such as *Provotella* and *Veillonella* (Hilty et al. 2010), and gram-positive bacteria, like *Coprococcus* and *Dorea* (Tong et al. 2019). Samples of microbial communities from this site are highly contaminated as one has to go through the upper respiratory tract to collect a sample. A bronchoscope usually accomplishes this task (Dickson et al. 2017). The lower microbial density of the distal airways also makes collecting sufficient amounts for analysis challenging (Segal et al. 2013, Bassis et al. 2015). Despite current issues in studying the lower lung microbiome, research suggests that the lower respiratory microbiome is seeded through microaspiration or inhaling bacteria from the air (Huxley et al. 1978, Gleeson et al. 1997, Dickson et al. 2017).

Under healthy conditions, the microbiome of the lower lung should be sparse; however, bacterial communities can plume during diseased states such as COPD and cystic fibrosis, leading to further respiratory issues (Mammen and Sethi 2016, Zhao et al. 2023). Furthermore, whether the lower respiratory microbiome is transient or persistent is debatable (Dickson et al. 2018). However, the abundance of innate-immune features such as mucociliary clearance (Kuek and Lee 2020), pulmonary surfactant (SPD, SPB) (Se-

ungHye and Mallampalli 2015), and innate immune cells (macrophages and neutrophils) (Grimaldi et al. 2002, Hewitt and Lloyd 2021) suggests the lower lung environment prevents bacteria from establishing a niche.

Gut-Lung Axis

Changes in the microbiome are observed in lung diseases such as cystic fibrosis, asthma, and chronic obstructive pulmonary disease (COPD), indicating essential cross-talk between mucosal sites in the human body (Zhang et al. 2020). The gut-lung axis is a bidirectional communication system between the gut and lung microbiomes that influences host health and disease.

Although most studies on the gut-lung axis investigate how the gut affects the lung microbiome, it is crucial to note that respiratory infection causes disturbances in the gut microbiota (Yildiz et al. 2018). Various mechanisms mediate the gut-lung axis, including migrating immune cells between the gut and lung, circulating microbial metabolites, and releasing cytokines and other signaling molecules. One study found that group 3 innate lymphoid cells (ILC3) in the gut responded to a *Streptococcus pneumonia* infection by migrating from the gut to the lung, mediating IL22-dependent host defense in mice. In this same study, disrupting the microbiome with antibiotics diminished this response. Thus, demonstrating that protective ILC3 influx depended on the sensing of commensal microbes in the gut by dendritic cells that in turn mediated ILC3 migration to the lungs (Gray et al. 2017). Another study investigating the effect of microbiome ablation via antibiotics on the response to influenza infection in mice found that antibiotic treatment impaired DC homeostasis and migration. As a result, animals treated with antibiotics had reduced CD4 and CD8 T-cell activation (Ichinohe et al. 2011).

GUT-LUNG AXIS

The metabolites such as tryptophan and SCFAs derived from the gut can enter circulation via the portal vein or lymphatic system, thus exerting protective properties such as immune regulation (Roager and Licht 2018, Zhang et al. 2020). Mouse studies have confirmed that fermentation products of dietary fibers, primarily SCFAs, can protect against allergic airway inflammation by modulating immune function (Marsland et al. 2015). In a recent study, the gut microbiome of neonates was investigated, and the researchers found that bacterial epoxide hydrolase genes were elevated in infants who develop atopy or asthma during childhood. Further investigation using a murine model found that when mice in an asthma challenge model were treated with the metabolite 12,13-diHOME, a product of epoxide hydrases, a reduction in regulatory T-cells was observed (Levan et al. 2019).

Ablation or disruption of the gut microbiome can have distant effects on pulmonary immunity in the lung. Thus reconstitution of the gut microbiome with healthy microbes has the ability to treat or alleviate the severity of respiratory disease. In a 10-month randomized, double-blind, parallel, and placebo-controlled study, scientists demonstrated that oral *Bifidobacterium longum BB53* significantly reduced the incidence of respiratory illnesses throughout the study (Lau et al. 2017). Furthermore, studies on mice have shown that oral administration of probiotics can induce antigen-specific T cells, which have been found to help dampen allergic responses (Marsland et al. 2015). In particular, this phenomenon has been observed with inactivated *Mycobacterium vaccea* (Zuany-Amorim et al. 2002), *Lactobacillus rhamnusus* (Feleszko et al. 2007, Jang et al. 2012), and *Bifidobacterium breve* (Sagar et al. 2014). Given the close relationship between the gut and lung microbiomes, it is likely that probiotics made to control respiratory disease will be utilized in the future.

Sex differences

Data on sex differences in non-human primates remains sparse, but the physiological similarities to humans make them excellent models for studying sex differences in the microbiome. Recent studies report no sex difference in gut microbiome diversity, precisely alpha diversity (Adriansjach et al. 2020, Janiak et al. 2021). The finding is not specific to the gut as the study, which characterized the microbiomes of free-ranging rhesus macaques, reached a similar column in the oral microbiome (Janiak et al. 2021). Physiological studies on the sex-dependent effects of microbiome alteration, such as research from the Gao group, suggest antibiotic exposure has no significant effect on weight gain in both males and females in rhesus macaques. Their study evaluated antibiotic usage as a binary variable, meaning that the number of courses was not considered. Although this study sheds light on how antibiotic exposure impacts weight in rhesus monkeys across the life span, the lack of information regarding response to antibiotic regimens makes its findings hard to extrapolate to human populations where multiple courses of antibiotics are frequent (Sidener et al. 2017).

The ease of mechanistic studies is one benefit of using murine models over human and non-human primate studies. We can observe how multiple factors can impact the microbiome using murine studies. In adult mice, environmental factors such as high-fat diet and antibiotic treatment have less of an impact on the gut microbiome than sex (Peng et al. 2020, Stepanauskaite et al. 2023, Zhu et al. 2023). The microbiome of male mice differs heavily from that of females, and Peng et al., 2020 demonstrated this was independent of diet. In their study, which investigated the impact of environmental factors and sex on the microbiome, the researchers found increased abundance of the genera *Parabacteroides*, *Lactobacillus*, *Bacteroides*, and *Bifidobacterium* in females relative to males (Peng et al.

2020).

Recent human studies have revealed sex-specific differences in the composition and function of the microbiome, highlighting the role of sex hormones in shaping the microbial landscape (Gomez et al. 2015, Baars et al. 2018, Gao et al. 2019, Zhang et al. 2021). Estrogen, testosterone, and their intermediates facilitate differences in the microbiome. Men have a more stable testosterone level, while women have fluctuating estrogen levels (Klein 2000, Valeri and Endres 2021). These hormonal differences might explain why women have a more diverse and variable microbiome than men and if these different microbiomes, in turn, can give rise to sex differences in the immune response. Such differences are observed with females tending to develop autoimmune diseases more frequently (Gomez et al. 2015). At the same time, males are more regularly plagued by increased intensity and prevalence of bacterial, parasitic, and viral infections (Klein 2000).

Estrogen and testosterone have been shown to affect the gut microbiome and immune cells directly. For example, β-estradiol has been demonstrated to promote the transformation of dendritic cells to produce IL-12 and IFN-γ by driving the development of $CD11b^{+}CD11c^{+}$ DCs which have increased expression of MHCII, CD40, and CD86 from BM precursors (Siracusa et al. 2008). This increased activation, in turn, activates pathways for pro-inflammatory cytokines. Similarly, when B cells are exposed to a sustained concentration of estradiol, polyclonal B cells' activation and prolongation in B cells' survival are observed (Grimaldi et al. 2002). Estrogen has been shown to influence the composition and diversity of the gut microbiome in women, with higher levels of estrogen associated with a higher abundance of *Lactobacillus* species and a lower abundance of *Bacteroides* species (Kozyrskyj et al. 2016).

On the other hand, testosterone is associated with increased diversity and richness and a higher abundance of *Clostridia* and *Ruminococcaceae* species in the gut microbiome of

males (Flores et al. 2012). A recent study showed, using regression analysis, that the abundance of Firmicutes and *Lachnospirales* demonstrated a negative correlation with testosterone levels (Liu et al. 2022). *Comamonas testosteroni* can digest androgens, suggesting that microbes can feed off testosterone (Chen et al. 2016). Testosterone has also been shown to modulate the immune system, which can affect the microbiome (Yoon and Kim 2021). Dihydrotestosterone (DHT) and estradiol, intermediates of estrogen and testosterone, can impact the gut microbiome. DHT, a testosterone metabolite, increases the abundance of *Lactobacillus* species (Markle et al. 2013), while estradiol, an estrogen metabolite, can regulate gut permeability and impacts the gut microbiome's composition and function (Valeri and Endres 2021).

These findings suggest that sex hormones can influence the microbiome and may contribute to sex-specific differences in susceptibility to diseases such as inflammatory bowel disease, colorectal cancer, and urinary tract infections. Further research is needed to fully understand the mechanisms underlying these sex-specific differences and to develop targeted interventions that can modulate the microbiome in a sex-specific manner.

Microbiome disruption

Microbiome disruption can occur through many avenues, including antibiotics, disease development, tobacco smoke, and environmental changes. One can only discuss the topic of microbiome disruption by acknowledging the immune system's influence on the microbiome's homeostasis. Changes in the immune system are often the cause and the result of microbiome disruption. One study demonstrated that changes in microbial composition were associated with distinct changes in host immune tone after studying lower airway samples from infants (Pattaroni et al. 2018).

MICROBIOME DISRUPTION

Antibiotics are widely used to treat bacterial infections, and their efficacy in combating infectious diseases has improved public health. However, antibiotics also significantly impact the microbiome, notably the gut microbiome. Antibiotics can disrupt the balance of the gut microbiome by reducing the diversity of bacterial species and altering the microbiome's composition. This disruption can lead to the overgrowth of opportunistic pathogens, which can cause infections and increase the risk of antibiotic resistance (Blaser 2016). Studies have also shown that antibiotic use can lead to long-term changes in the gut microbiome, which may increase the risk of certain diseases, including inflammatory bowel disease (Manichanh et al. 2010, Cho et al. 2012, Korpela et al. 2016, Turta and Rautava 2016, Bokulich et al. 2016).

The gut microbiome has been extensively studied, and its disruption is linked to various health conditions, including inflammatory bowel disease, obesity, and diabetes (Jovel et al. 2018). Gastrointestinal infections, such as those caused by *Salmonella* and *Campylobacter*, can also disrupt the gut microbiome (Jacobson et al. 2018, Rouhani et al. 2020). These infections can lead to changes in the composition and diversity of the gut microbiome, which may persist long after the infection has resolved (Khan et al. 2019). In some cases, gastrointestinal infections can lead to chronic conditions, such as inflammatory bowel disease, which is associated with long-term gut microbiome changes (Seyedian et al. 2019). A nationwide case–control study had findings that suggested that enteric infections may induce the microbiome dysbiosis that contributes to the development of inflammatory bowel disease (Axelrad et al. 2019).

There is growing interest in the potential role of the respiratory tract microbiome in respiratory diseases, such as asthma, chronic obstructive pulmonary disease (COPD), and pneumonia. Respiratory infections, such as those caused by RSV, influenza, and *Pseudomonas aeruginosa*, can also disrupt the respiratory microbiome (Collie et al. 2015,

Groves et al. 2018). These infections can alter the composition of the respiratory microbiome, leading to an increase in potentially pathogenic bacteria (Dickson et al. 2014). Moreover, respiratory infections can lead to inflammation, further disrupting the microbiome and impairing lung function in mice (Liu et al. 2021). Chronic respiratory diseases, such as asthma and COPD, are also associated with changes in the respiratory microbiome, which may contribute to developing or exacerbating these conditions (Huang et al. 2015). Tobacco smoke is a well-known risk factor for respiratory diseases, including lung cancer and COPD. Tobacco smoke can also disrupt the respiratory microbiome by altering the composition and diversity of the microbiome (Öberg et al. 2011, Mayhew et al. 2018). Environmental factors like diet and pollution can also impact the gut and respiratory microbiome. Studies have shown that a high-fat, low-fiber diet can alter the gut microbiome's composition, reducing bacterial diversity (Trompette et al. 2014, Cox et al. 2014, Stepanauskaite et al. 2023). Pollution, notably air pollution, has additionally been linked to changes in the respiratory microbiome, with studies showing that exposure to air pollution can alter the composition and diversity of the microbiome (Gao et al. 2017, Fouladi et al. 2020). These disruptions can lead to an increase in potentially pathogenic bacteria, a reduction in bacterial diversity, and changes in the microbiome.

Conclusion

The human microbiome plays a crucial role in maintaining the host's health, and disrupting this microbial ecosystem can have significant consequences for human health. Microbial imbalance can stem from various sources, such as antibiotic usage, respiratory and gastrointestinal infections, tobacco smoke exposure, and environmental factors. Such disruptions can lead to a reduction in bacterial diversity, an increase in potentially

pathogenic bacteria, and changes in microbial composition, which may contribute to the development of chronic diseases such as inflammatory bowel disease, obesity, diabetes, asthma, and chronic obstructive pulmonary disease.

Antibiotic use is one of the most significant factors that disrupt the microbiome. While antibiotics are effective in combating bacterial infections, they can reduce the diversity of bacterial species and alter the microbiome's composition, leading to the overgrowth of opportunistic pathogens and increasing the risk of antibiotic resistance. Therefore, the use of antibiotics must be carefully considered and balanced against the potential consequences of disrupting the microbiome. Lastly, biological sex should be considered a factor when covering topics related to microbiome alteration, as it is becoming increasingly evident that sexual dimorphisms influence the microbiome. Future research should focus on identifying specific microbial species and their functions in health and disease, considering the sex-specific effects of microbiome changes and associated diseases, on developing targeted treatments for microbiome-associated conditions in males and females.

In conclusion, the human microbiome is a complex ecosystem that plays a crucial role in human health, and disrupting this microbial community can have significant consequences. Understanding the complex interplay between the microbiome and the immune system and identifying specific microbial species' functions can lead to the development of targeted therapies to mitigate the adverse effects of microbiome disruption and improve human health.

Chapter 2

Early-life antibiotic treatment results in persistent microbiome alterations in association with sex

No data is clean, but most is useful.

Dean Abbott

Abstract

Background: Antibiotic treatment commonly occurs shortly after birth and is administered to infants suspected of having an infection. However, this antibiotic treatment can alter the developing microbiome, which can have detrimental effects on host health. Sex differences in the microbiome are often unexamined or unreported, leaving a gap in knowledge about whether sex influences the response to perturbations of the microbiome. We hypothesized that antibiotic treatment during infancy would cause persistent

changes to the developing microbiome and alter host physiology and that these effects could be sex-dependent. Using an infant rhesus macaque model to recapitulate human pediatric populations, we assessed how early-life administration of antibiotics impacted the development of the gut microbiome during the first 6 months of life. **Results:** Infant rhesus macaques were administered an antibiotic cocktail during the first week of life, with controls receiving saline during the same time period. Antibiotic-treated infants had higher weight and neutrophil-to-lymphocyte ratio z-scores compared to controls, an effect that was influenced by sex. Accordingly, we observed sexually dimorphic changes in α-diversity and taxa abundance in response to antibiotic treatment, with more significant differences observed between antibiotic-treated and control males compared to female groups. Metagenomic pathways of the gut microbiome examined using picrust showed that metabolic functional differences were altered with antibiotic treatment, particularly pathways related to short-chain fatty acid metabolism. **Conclusions:** We found that early-life antibiotic exposure resulted in persistent changes to physiology and the gut microbiome. These effects of antibiotics were sex-dependent, with differences more prevalent in males and not females. Our data demonstrates the importance of examining sex-dependent differences and that future studies should take sex into account when determining the effects of an altered microbiome on health.

Introduction

Infections can cause significant morbidity and mortality in infants, in part due to their immature immune responses (PrabhuDas et al. 2011, Ruf and Knuf 2014). Clinicians commonly administer antibiotics shortly after birth to mitigate the potential risk of sepsis (Raymond et al. 2017). However, the actual rates of neonatal sepsis are significantly lower

compared to the frequency of antibiotic treatment. In an analysis of antibiotic use in a neonatal intensive care unit, 99.8% of infants received at least one dose of an antibiotic, while only 5% of suspected infections were confirmed with positive blood cultures (Cantey et al. 2015). Antibiotics can disrupt the commensal microbiota, the community of microbes that colonize the human body. The gut microbiota is resilient against external perturbations, but this commensal microbial community can be significantly altered if exposed to antibiotics early in its development. Antibiotic-induced alterations in the adult microbiota are relatively transient, while the effects of antibiotics on the infant microbiota may have a much longer and more significant impact. The infant microbiota may be particularly susceptible to perturbations, as the microbiota has not yet reached a stable phenotype.

A relatively sterile unborn child becomes coated with microbes during the birthing process (Vangay et al. 2015, Tamburini et al. 2016). The microbiome "matures" during early life, undergoing successional changes in composition and resembling an adult-like microbiome by about 2 to 3 years of age. In addition to altering the microbiome composition, antibiotics delay this microbiome maturation (Bokulich et al. 2016). The health and developmental consequences of these alterations in the microbiome are poorly understood. It is known that early life antibiotic treatment can impact the growth of infants. There is a greater risk of obesity later in life following infant treatment to antibiotics (Bailey et al. 2014, Vangay et al. 2015), and more recently, antibiotics have been shown to impact height and weight gain during the first years of life (Kamphorst et al. 2019, Uzan-Yulzari et al. 2021). While antibiotics are commonly associated with increased weight gain, it has been demonstrated that the timing of antibiotic treatment can influence whether an infant has increased or decreased weight gain with age. These effects on weight can be sex-dependent and are more apparent in male infants (Uzan-Yulzari

et al. 2021). Sex-dependent effects of antibiotics could suggest either sex differences in the microbiome or in response to alterations of the microbiome. Unfortunately, sex differences in the infant microbiome are often not reported, though sex differences in the microbiome have been shown to exist in infants (Cong et al. 2016), adults (Mueller et al. 2006, Ding and Schloss 2014, Haro et al. 2016), and in animal models (Yurkovetskiy et al. 2013, Haro et al. 2016, Johnson et al. 2020) . Whether there are sex differences in the infant microbiome following antibiotic treatment has not been reported.

Since much of what is known about antibiotics and the microbiome comes from epidemiological studies (Ding and Schloss 2014, Mueller et al. 2015, Cong et al. 2016), we set out to investigate the longitudinal effect of early-life antibiotic treatment on the infant rhesus macaque microbiome in a controlled setting. We were interested in how long antibiotics would disrupt the infant microbiome, whether we would observe sex differences in response to antibiotics and hypothesized that antibiotic treatment during infancy would cause persistent changes to the developing microbiome and alter host physiology. Since antibiotics have been shown to influence weight gain (Kamphorst et al. 2019, Uzan-Yulzari et al. 2021), we assessed infant weights throughout this study; additionally, as the immune system is also developing and maturing alongside the microbiome (Vangay et al. 2015, Tamburini et al. 2016). Therefore, we examined whether antibiotic treatment was associated with altered developmental trajectories of circulating white blood cells. We found that antibiotics altered the microbiome for up to six months after antibiotic treatment and that sex could influence its effects on the microbiome and physiology. These results indicate that sex is an important variable to consider in microbiome studies, as the response to external perturbations may differ by sex.

Materials and Methods

Rhesus Macaques.

Infant colony-bred Indian rhesus macaques (Mucaca mulatta) born and housed at the California National Primate Research Center (CNPRC) were used in this study. The animals were negative for simian immunodeficiency virus (SIV), simian T lymphotropic virus (STLV), and simian retrovirus (SRV), and they did not have a history of pharmacological or dietary intervention with known influences on the microbiome. All animals were healthy for the duration of the study. Animals were enrolled in the study on a tapered schedule and, although samples were collected once per month, the exact age in days of each animal may have differed slightly. Age in months and age in days are used to assess differences on continuous and discrete scales.

Diet, housing, and antibiotics.

All animals were housed indoors and breast-fed by their respective dams until weaning age at 5 months. Infant monkeys were assigned to a control group (n=8; male n=3, female n=5) and antibiotic (ABX) treatment group (n=10; male n=5, female n=5). Antibiotics or saline were administered to animals for 7 consecutive days. We previously found that intramuscular (I.M.) administration of a broad-spectrum antibiotic cocktail on postnatal days 1-7 results in an altered intestinal microbiome in rhesus monkeys (data not shown). Control animals were not administered antibiotics of any kind. In contrast, the antibiotic-treated animals received an intramuscular (I.M.) broad-spectrum antibiotic cocktail containing Gentamicin (5 mg/kg), Ampicillin (50 mg/kg), and Vancomycin (15 mg/kg) daily at postnatal days 4 or 5 for 7 days. This cocktail was used because it

is commonly administered to human infants suspected of having an infection, making the dosage and regimen in this study clinically relevant. Control animals were given a saline injection as a substitute for antibiotics via the same administration route, age, and antibiotic course duration.

Collection of Clinical Data.

Animal weights were measured at least once per month. CBC differentials were conducted by the California National Primate Research Center research services staff. Animals were anesthetized with ketamine hydrochloride (5-30 mg/kg) for femoral venipuncture. CBC differentials were performed on EDTA anticoagulated blood using a Sysmex XT2000i and blood chemistry was performed using Beckman AU480 chemistry analyzer.

Microbiome Profiling.

DNA extraction.

The fecal microbiota was assessed in total DNA from fecal swabs (Copan fecal swabs). Fecal swabs were collected monthly for 6 months and stored in Copan collection tubes at -80°. Swabs were thawed on ice and vortexed in Clary-Blair media until homogenous. Aliquots of approximately 200 µl were used for total bacterial DNA extraction. DNA was isolated using the Qiagen DNeasy PowerSoil kit (Qiagen) with the following modifications. After adding buffer C1, samples were incubated at 65° for 10 min and then subjected to homogenization using a Qiagen TissueLyser (Qiagen) for 10 min at 20 cycles per second. The samples were then turned 180 degrees and subjected to further homogenization for an additional 10 min at 20 cycles per second, per the manufacturer's recommendation. Samples were eluted in 60 µl of buffer C6.

PCR amplification.

Amplification of the V3-V4 domain of the 16S rRNA gene was performed using a DNA template and primers 319F (F stands for forward) [TCGTCGGCAGCGTCAGATGTG-TATAAGAGACAG(spacer)GTAC TCCTACGGGAGGCAGCAGT] and 806R (R stands for reverse) [GTCTCGTGGGCTCGGAGATGTGTATAAGAGACAG(spacer)CCGGA CTACNVGGGTWTCTAAT] using a two-step PCR procedure. In step one of the amplification procedure, both forward and reverse primers contained an Illumina tag sequence, a variable length spacer to increase diversity and improve the quality of the sequencing run, a linker sequence, and the 16S target sequence. Each PCR contained 1U Kapa2G Robust Hot Start Polymerase (Kapa Biosystems), 1.5 mM MgCl2, 0.2 mM final concentration of deoxynucleotide triphosphate (dNTP) mix, 0.2 µl final concentration of each primer, and 1 µl of DNA for each sample. PCR conditions were as follows: an initial incubation of 95° for 45 s, 50° for 30 s, 72° for 30 s, and a final extension of 72° for 3 min. In step two, each sample was barcoded with a unique forward and reverse barcode combination using forward and reverse primers with an Illumina P5 adaptor sequence, a unique 8-nucleotide (nt) barcode, a partial matching sequence of the forward adaptor used in step one and reverse primers with an Illumina P7 adaptor, unique 8-nt barcode, and a partial matching sequence of the reverse adaptor used in step 1. The PCR in step two contained 1 U Kapa2G Robust Hot Start polymerase (Kapa Biosystems). 1.5 mM MgCl2, 0.2 mM final concentration dNTP mix, 0.2 µM final concentration of each uniquely barcoded primer, and 1 µl of the product from the PCR in step one diluted at 7:1 ratio in water. PCR conditions were as follows: (i) an initial incubation at 95° for 3 min; (ii) 8 cycles, with 1 cycle consisting of 95° for 30 s, 58° for 30 s, and 72° for 30 s; and (iii) a final extension step of 72° for 3 min. The final product was quantified on a Qubit instrument using the Qubit Broad Range DNA kit

(Invitrogen), and individual amplicons were pooled in equal concentrations. The pooled library was cleaned utilizing Ampure XP beads (Beckman Coulter). The library was quantified via qPCR followed by 300-bp paired-end sequencing using an Illumina Miseq instrument in the Genome DNA Technologies Core, University of California, Davis.

Bioinformatics.

All samples were sequenced on an Illumina MiSeq platform at the Genome DNA Technology Core at the University of California, Davis. Analysis began with demultiplexing sequence reads. Demultiplexing of the raw FASTQ files and adapter trimming of sequences were performed using dbcAmplicons version 0.8.5. (https://github.com/msettles/dbcAmplicons). The unmerged forward and reverse reads were imported into QIIME2 version 2020.8 (https://docs.qiime2.org/2020.8/), and amplicon sequencing variants (ASVs) were determined following the DADA2 analysis pipeline (Callahan et al. 2016). Snakemake (Köster and Rahmann 2012) was used as workflow manager to manage the QIIME2 environment (https://github.com/nasiegel88/tagseq-qiime2-snakemake-1). Each sequence was assigned to its given samples based on the given barcode. Reads that did not match any barcode were discarded (failed to meet minimum quality thresholds). Barcoded forward and reverse sequencing reads were quality filtered and merged. Sequences that were only observed one time or only in a single sample were also discarded. Chimeras were detected and filtered from paired end reads. Comparison of clustered sequences was performed against SILVA 138. All data generated in this study utilize the same instrumentation, technician reference database, packages, and pipeline. Data processing and filtering and trimming of reads.

The data were filtered as follows: ambiguous phyla were removed, phyla with a mean prevalence of less than 10 were removed. Taxa were agglomerated at the genus level if

possible and all taxa without genus-level taxonomic assignments were retained. Samples with less than 5000 reads were removed.

Statistical analysis.

All R packages involved in analyses were installed in R 4.0.3 and managed by the R package manager, renv (version 0.12.5) unless otherwise stated. Statistical analysis of microbial communities was performed primarily using the Bioconductor package Phyloseq (version 1.34.0). Differential abundance analyses were performed using Linear discriminant analysis effect size (LEfSe) as described in the literature (Segata et al. 2011). Alpha diversity indices were computed in Qiime2 and measured as Shannon index, Pielou's evenness, observed ASVs, and phylogenetic diversity. Alpha diversity indices were analyzed with the permuspliner function in SplinectomeR (version 0.1.0), a permutation-based package in R that uses weighted local polynomials (loess splines) to test for group differences in longitudinal data (Shields-Cutler et al. 2018). This method is less sensitive to the limitations of using aggregate data over time. We performed 1000 permutations. Metagenomic analysis of Picrust2 predicted Kegg pathways was analyzed in Statistical Analysis of Metagenomic Profiles (STAMP, version 2.1.3). Differences in bacterial pathway % mean proportions were assessed with Welch's t-test and significance was taken at $p < 0.05$. All mixed effects models used in this study were fitted using the R package lmerTest (3.1-3). Animal weights and CBC concentrations were transformed into z-scores using the study mean and study average to calculate z-scores. Animal weight was measured across early development with treatment, sex, and age as fixed effects and animals as random effects. Neutrophil to lymphocyte ratio was measured across early development with treatment, sex, and age as fixed effects and animals as random effects. Loess spines were used to account for the non-linear relationship between CBC concen-

tration and age as previously described in the literature (Pembrey et al. 2008). Splines were permuted using the Spline base R package (version 4.0.3).

Data availability.

Raw reads were deposited to the Sequence Read Archive (insert project number) and are available on Open Science Framework (https://osf.io/87gsx/). The figures and code present in this study can be found on GitHub (https://github.com/lmillergrp/siegel_et_al_2021).

Results

Study Design.

Infant rhesus macaques enrolled in this study were born and raised indoors. Antibiotic-treated infants received a broad-spectrum antibiotic cocktail of ampicillin, gentamicin, and vancomycin during the first week of life, with controls receiving saline. The antibiotic cocktail in our study is commonly used in clinical settings, making it a relevant model of antibiotic-induced dysbiosis in pediatric populations. All infants were breastfed by their mothers until weaned at approximately 5 months of age. We collected fecal swabs, weights, and blood monthly from postnatal days 4 or 5 until 6 months of age (Fig. 2.1).

Effect of early-life antibiotic treatment on clinical parameters.

We aimed to determine if there were any physiological changes specific to antibiotic-treated animals. We measured the CBC trajectory from postnatal days 4 or 5 until

6 months of age. A non-linear mixed-effects model was used to determine if antibiotic treatment and sex significantly impacted neutrophil-to-lymphocyte ratio (NLR) for age z-scores. We observed a significant effect of treatment and sex on NLR-for-age z-scores over six months, with antibiotic-treated animals having fluctuating NLR z-scores and control animals having a steady decline in NLR-for-age z-scores (p=0.006) (Fig. 2.2a, Table. 2.1). Other lymphocyte and leukocyte z-scores were assessed, but significant differences were not observed (Supp. Fig. 2.1a-2.1d).

Given that previous studies implicated an altered microbiome to changes in weight (Cho et al. 2012, Nobel et al. 2015, Cox and Blaser 2015, Bokulich et al. 2016), we interrogated whether treatment and sex had a significant effect on weight over 6 months. Animal weights were transformed into z-scores, and a linear mixed-effects model was constructed to ascertain the impact of sex and early-life antibiotic treatment on weight-for-age z-scores. There was a significant impact of sex and age on weight-for-age z-scores (p=0.027) (Fig. 2.2b, Table. 2.2). Similarly, sex and treatment also significantly impacted weight over the first six months of life (p=0.017) (Fig. 2.2b, Table. 2.2).

Microbiome composition.

16s rRNA sequencing revealed the most abundant phyla during the first six months to be Firmicutes, Proteobacteria, Actinobacteria, and Bacteriodota (Fig. 2.3a). Despite the top four taxa's dominant abundances during early life, we observed several phyla that made up less than 1% of the total composition (Fig. 2.3b). Independent of antibiotic treatment, Firmicutes made up most of the fecal microbiome composition every month and consistently increased in proportion while the phyla Proteobacteria, Actinobacteria, and Bacteriodota decreased in proportion, albeit to a lesser extent for Bacteriodota (Fig. 2.3b). The changes in the abundances of Firmicutes, Pro-

teobacteria, Actinobacteria, and Bacteriodota occurred primarily in antibiotic-treated infant males (Fig. 2.4b, 2.4e, 2.4h, 2.4k). Firmicutes abundance was significantly reduced in antibiotic-treated males at 2 and 3 months, while few alterations were observed in females (Fig. 2.4b, 2.4c). Actinobacteria had low abundance regardless of antibiotic treatment. Despite antibiotic treated infants having increased abundance of Actinobacteria relative to controls, and more pronounced changes in males, by 6 months of age, Actinobacteria were readily undetectable regardless of previous antibiotic treatment (Fig. 2.4g, 2.4h, 2.4i). Bacteriodota was most resilient to persistent alterations after antibiotic treatment (Fig. 2.4d-2.4f).

Differential abundance of taxa and microbiome diversity.

We assessed the microbiome's diversity on discrete (monthly) and continuous (daily) scales to understand whether the diversity of the microbiome of antibiotic-treated and control infants differed over 6 months and where those differences were most pronounced. Using Loess splines, we demonstrate that early-life antibiotics persistently altered the microbiome's alpha diversity, with significant alterations observed in males but not females (Fig. 2.5a, 2.5b, 2.5c). A longitudinal effect of early-life antibiotic treatment on alpha diversity was not observed (Supp. Fig. 2.2). We observed that male infants have reductions alpha diversity at months 1 and 2, following antibiotic treatment, although these results did not reach significance. However, by 6 months of age, antibiotic-treated males had increased alpha diversity compared to control males (Fig. 2.5d, 2.5e, 2.5f). Similar findings were not observed in female infants, further implicating sex as a critical factor in the persistent effects of early-life antibiotic treatment. Linear discriminant analysis effect size (LEfSe) was used to assess differential abundance of taxa at each month and to assess subsequent compositional differences in taxa abundance post-early-life antibiotic treatment.

Variation in bacteria differential abundance between control and antibiotic-treated infants primarily resided at 6 months of age (Fig. 2.6a-2.6c). We observed most of the differentially abundant taxa from the phyla *Proteobacteria*, *Firmicutes*, and *Bacteriodota*, including *o_bradymonadales* and *o_delsulfuromonadia* for *Proteobacteria*; *o_oscillospirales*, *f_lachnospiraceae*, and *f_oscillospiraceae* for *Firmicutes*; and *f_rikenellaceae* for *Bacteriodota* in antibiotic-treated infants. Although control infants had fewer differentially abundant taxa, they were observed to have increased proportions of short-chain fatty acid-producing bacteria from *f_lactobacillaceae* and another unclassified taxon from the Lactobacillus group (Fig. 2.6a).

Next, we questioned whether there were sex differences in bacterial differential abundance. We observed prominent differences in the overall number of differentially abundant taxa between antibiotic-treated males and females and control males and females at 6 months, suggesting that the effects of early-life antibiotic treatment do not become substantial until later in life (Fig. 2.6b, 2.6c). These differences could be associated with the instability of the fecal microbiome at such a young age. The number of differentially abundant taxa between antibiotic-treated males and females differed between control males and females (Fig. 2.6b, 2.6c). Control males and females possessed comparable numbers of differentially abundant taxa with different taxa increased in each group (Fig. 2.6b). The results were strikingly different from antibiotic-treated males and females, which had 20 and 2 differentially abundant taxa, respectively (Fig. 2.6c).

Taxa from the phyla *Firmicutes*, *Bacteriodota*, *Proteobacteria*, *Actinobacteria*, and *Cyanobacteria* were increased in antibiotic treated males, including *f_erysipelotrichia* from *Firmicutes*; *f_prevotellaceae* from *Bacteriodota*; o_rickettsiales from *Proteobacteria*; *g_eggerthella* and *g_enterohabdus* from *Actinobacteriota*; and *f_coriobacteriaceae*, *o_gastroanerophilales*, and *g_vampirovibrio* from *Cyanobacteria* (Fig. 2.6b). Conversely,

antibiotic-treated females had increased taxa abundances from the phyla *Firmicutes*, specifically *g_allisonella* (Fig. 2.6b). Bacteria from the phylum *Fibrobacterota* made up most of the differentially abundant phyla in control males. Also, males had increased *g_eubacterium* at month 6, whereas control females primarily had increased abundances of bacteria from the phyla *Proteobacteria*, including *o_pasteurellales* and *f_pasteurellaceae*; and *Firmicutes*, specifically *g_faecalibacterium*. Additionally, control females had increased taxa abundances from the order lactobacillus, including *g_weissel* and *f_leuconostocaceae* (Fig. 2.6b, 2.6c).

Similar to what was observed at six months of age, we report many differentially abundant taxa after the first week of life (at month 0) in control animals (Fig. 2.5a). Furthermore, control females had higher proportions of *Actinobacteria*, of which *g_bifidobacteria* is a part, at months two and four (Fig. 2.5b, 2.5d). The number of differentially abundant taxa at months 0-5 was relatively small compared to the differences observed at six months, suggesting that the temporal changes in the microbiome after early-life antibiotic treatment are most pronounced later in life. Taxa that were often increased at months 0-5 in antibiotic-treated infants were *Actinobacteria* and *g_bifidobacteria*. Control infants had significantly increased proportions of *g_campylobacter* and *g_helicobacter* pronounced at 1 month (Fig. 2.6b). Captive rhesus monkeys are commonly colonized with helicobacter suggesting the bacteria is part of the normal microbiota of rhesus macaques (Fernandez et al. 2002).

The metagenomic function of the developing microbiome.

Given that many taxa have redundant metabolic processes, we aimed to determine if changes in predicted metagenomic function accompanied the observed changes in the microbiome composition. We used Phylogenetic Investigation of Communities by Re-

construction of Unobserved States 2 (picrust2) to interrogate the mean proportion of differentially abundant bacteria metabolic pathways (Douglas et al. 2020). Variation in predicted metagenomic pathways occurred between antibiotic-treated and control infants (Fig. 2.7a); however, fewer differences in metabolic pathways were observed between sex (Fig. 2.7b, 2.7c). 6 months of age was characterized by the most pronounced changes in bacteria metabolic pathways. Of note, pathways known to convert pyruvate to short-chain fatty acids, such as acetate, were observed to be reduced in infants treated with antibiotics during the first week of life (Fig. 2.7a). A pathway responsible for converting pyruvate to acetate was significantly increased in control infants relative to antibiotic-exposed infants.

Despite the majority of metagenomic differences occurring primarily at six months of age, we also observed metagenomic functional changes throughout the study. For example, the first week of life was when most differences in predicted metabolic pathways were observed between antibiotic-treated and control infants (Supp. Fig. 2.6a) compared to other ages. However, by 1-month of age, much of the differences in metagenomic pathways between antibiotic-treated and control infants were resolved, suggesting a slight but temporary return to normal microbiome function (Supp. Fig. 2.6b-2.6f). Four months of age was when most differences in metagenomic pathways between sexes in the control group were observed (Supp. Fig. 2.8e) however, fewer differences in metagenomics function were observed between sexes in the antibiotic group (Supp. Fig. 2.7a-2.7c).

Discussion

The effects of early life antibiotic treatment on the developing infant microbiome are poorly defined. Additionally, the sex-dependent effects of antibiotics are often not ex-

amined. To address this, we set out to investigate the impact of antibiotic treatment during the first week of life on physiology and the microbiome in a longitudinal manner. We found that the most abundant phyla in the infant rhesus macaque microbiome were *Firmicutes*, *Proteobacteria*, *Actinobacteria*, and *Bacteriodota* (Fig. 2.2a). This finding is comparable with that of Rhoades et al. 2019, which demonstrated that the developing rhesus microbiome is primarily *Firmicutes* and *Bacteriodota* (Rhoades et al. 2019). Similarly, they found that *Actinobacteria* decreased with age, which we also observed (Fig. 2.3g, 2.3h, 2.3i). Antibiotic treatment influenced the temporal abundance of these phyla, with more pronounced changes in antibiotic treated males than control males (Fig. 2.3). Changes in alpha diversity were also significantly impacted in antibiotic-treated males (Fig. 2.5b, 2.5e). While alpha diversity was initially lower in antibiotic-treated males relative to control males, it was significantly higher by 6-months of age. These results concur with a recent study which showed that human infants exposed to antibiotics early in life developed an altered microbiome composition and increased alpha diversity that surpasses the control group by about two years of age (Uzan-Yulzari et al. 2021).

We found that antibiotic administration during the first week of life was associated with alterations in weight-for-age z-scores, with antibiotic-treated infants having a trend towards higher weight-for-age z-scores during 5 and 6 months of age (Fig. 2.4b). While antibiotic treatment alone was not associated with alterations in weight-for-age z-scores, sex and antibiotic treatment together did (Table 2.2) , indicating that the effects of antibiotics on weight-for-age z-scores are sex-dependent. Other studies that have examined the effects of antibiotics on growth have also found sex differences in weight gain following antibiotic treatment (Cox et al. 2014, Uzan-Yulzari et al. 2021). The timing of antibiotic exposure matters, as antibiotic treatment during the first few weeks of life

is associated with decreased weight gain with age, while antibiotic treatment later in infancy and childhood is associated with increased weight gain (Kamphorst et al. 2019, Uzan-Yulzari et al. 2021). Unlike others, we found that antibiotic treatment during the first week of life was associated with a trend towards increased weight with age. Such a difference could be partially attributable to our study's duration, as we assessed weights during the first six months of life while other studies monitored weight for the first few years of life (Kamphorst et al. 2019, Uzan-Yulzari et al. 2021). Our study also took place in a controlled environment in contrast to epidemiological studies where there can be variability in the type of antibiotics infants receive and the duration of treatment. Uzan-Yulzari et al., 2021 demonstrated that increased antibiotic treatment during infancy causes significant changes in weight-for-age z scores relative to untreated controls (Uzan-Yulzari et al. 2021). Thus, the effects of antibiotics on weight may be influenced by the type and duration of antibiotic treatment. Of the clinical parameters we examined, the most significant difference we found between antibiotic-treated infants and controls was in the NLR-for-age z-score (Fig. 2.4a, Table 2.1). Antibiotic-treated infants had fluctuating NLR-for-age z-scores, initially lower during early-life and then higher than control infants around five to six months of age. Control infants had decreased NLR-for-age z-scores with age. NLR is a marker of subclinical inflammation; thus, an increase in NLR-for-age z-scores could suggest mild inflammation. Antibiotics have been shown to influence inflammation, though generally in a more acute fashion (Knoop et al. 2016). However, the microbiome was also altered at 6 months of age in our infants and could provoke inflammation, even months after antibiotic treatment.

Although control infants had fewer differentially abundant taxa, they were observed to have increased proportions of short-chain fatty acid-producing bacteria from Lactobacillaceae and another unclassified taxon from the Lactobacillus group (Fig. 2.6a). Metage-

nomic analysis of the microbiome further supported this difference, as pathways related to short-chain fatty acid (SCFA) metabolism were reduced in antibiotic-treated infants compared to controls (Fig. 2.7a). Short-chain fatty acids have anti-inflammatory properties, in addition to many other health benefits (Park et al. 2015, Tang and Offermanns 2017, Ratajczak et al. 2019, Venegas et al. 2019). Antibiotic-treated infants did have greater microbiome diversity at six months compared to controls, and it is conventionally thought that greater diversity of the microbiome is more beneficial for health. Various diseases are associated with reduced microbiome diversity (DiGiulio et al. 2015, Wlodarska et al. 2015, Needell and Zipris 2016, Tremlett et al. 2017, Levy et al. 2017, Weiss and Hennet 2017). However, this is not always the case, as higher diversity of the vaginal microbiome is associated with pre-term birth (Biagi et al. 2016) and inflammation (Anahtar et al. 2015). Our results suggest that although antibiotic-treated infants have increased diversity metrics relative to control infants, not all the taxa contributing to increased diversity are necessarily beneficial.

LEfSe analysis (Fig. 2.6a) showed that the most significant differences in bacteria differential abundance between antibiotic-treated infants and controls were at six months of age, in accordance with our finding that the most significant differences in alpha diversity were seen at that age. The number of differentially abundant taxa was similar between control males and females (Fig. 2.6c), which was not the case in antibiotic-treated infants. Antibiotic-treated males had twenty differentially abundant taxa, while antibiotic-treated females had two (Fig. 2.6b). While it has been demonstrated that there are sex differences in the microbiome, it has not previously been shown that antibiotics can have a sex-dependent effect on the microbiome. Aside from pre-existing sex differences in the microbiome, the only environmental factor that has been shown to exert sex-dependent effects on the microbiome is diet. Analysis and re-analysis of microbiome studies demon-

strated that sex*diet interactions could modify the microbiome (Bolnick et al. 2014). Administration of an oligofructose supplement caused reduced fecal community richness in males, while increasing it in females (Shastri et al. 2015). The effects of diet on the microbiome can be sex-dependent, and thus it is not unsurprising that antibiotics can also affect the microbiome in a sex-dependent manner. Although we found compositional differences in the microbiome with respect to sex, few metagenomic functions differed between the sexes. We could not detect differences in metagenomic pathways for every month (Supp. Fig. 2.7, Supp. Fig. 2.8).

Our study has limitations, for example, the samples size for control males was small (n=3) which limited our ability to detect statistically significant differences. Changes in metabolic functions will need to be confirmed by examining differences in circulating levels of metabolites. While we have data supporting the differences during infancy, we cannot say whether these antibiotic-induced alterations persist into adulthood. Furthermore, while we have detected sex differences in the microbiome and response to antibiotic treatment, this data does not reveal the mechanism by which this is happening. Sex differences in the microbiome could be influenced by genetics, differences in mucosal immunity, and sex hormone (Yurkovetskiy et al. 2013, Org et al. 2016).

In summary, our results indicate that antibiotic treatment during the first week of life in infant rhesus macaques can have lasting effects on the microbiome months after treatment at a compositional and functional level. Furthermore, antibiotic treatment impacted weight-for-age z-scores, an effect influenced by sex. We also found that there were sex-dependent effects of antibiotics on the microbiome, with changes most pronounced in antibiotic-treated male infants. Our study is the first to report sex-dependent changes in the microbiome following antibiotic treatment. These findings indicate the possibility that other environmental factors could have sex-dependent effects on the microbiome.

ACKNOWLEDGMENTS

As the microbiota plays a vital role in various aspects of health, it will be essential to consider sex as a variable that can impact the influence of changes in the microbiome.

Acknowledgments

This publication was made possible by an NIEHS-funded diversity supplement awarded to Noah Siegel (P51OD011107). Its contents are solely the responsibility of the authors and do not necessarily represent the official views of the NIEHS or NIH. We want to acknowledge the significant contributions of the CNPRC staff for assistance in the completion of this project, including Paul-Michael Sosa, Sarah Davis, Anne Gibbons, and Don Canfield.

Disclosure

The authors have no relevant affiliations or financial involvement with any organization or entity with a financial interest in or financial conflict with the subject matter or materials discussed in the manuscript.

Figures

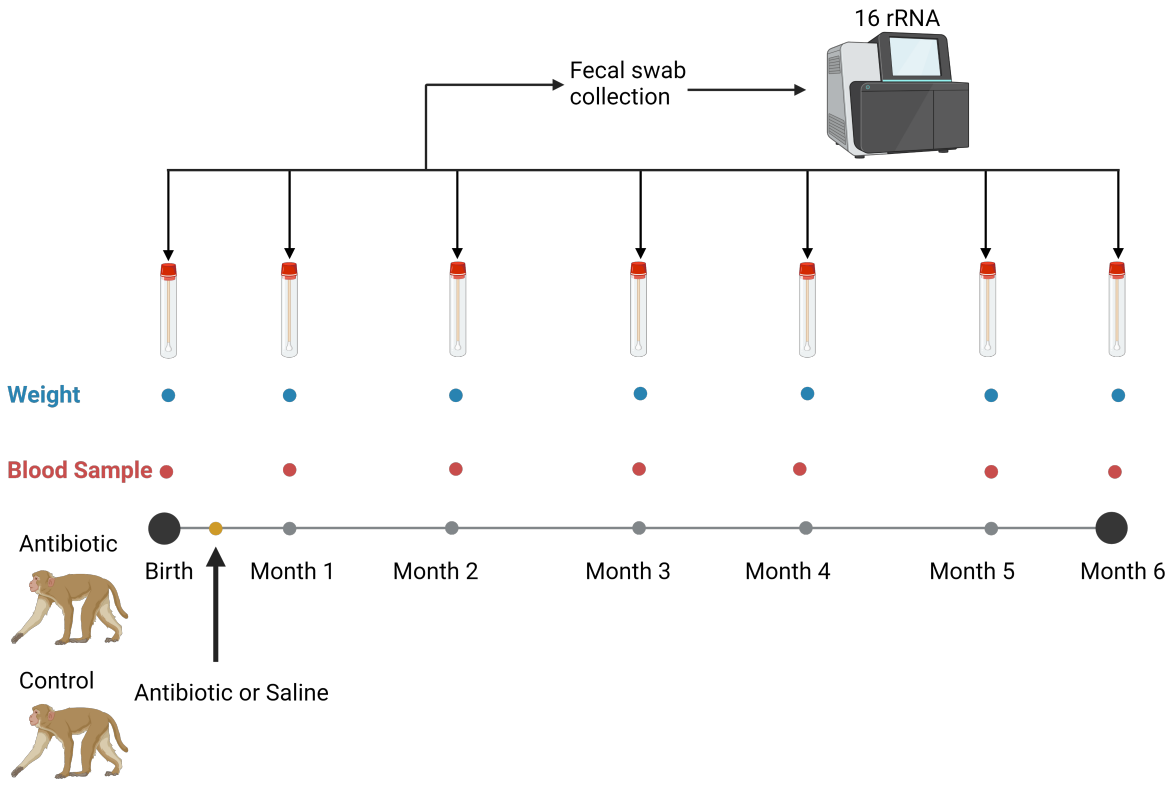

Figure 2.1: Experimental Design. Study design (Fig. 1)

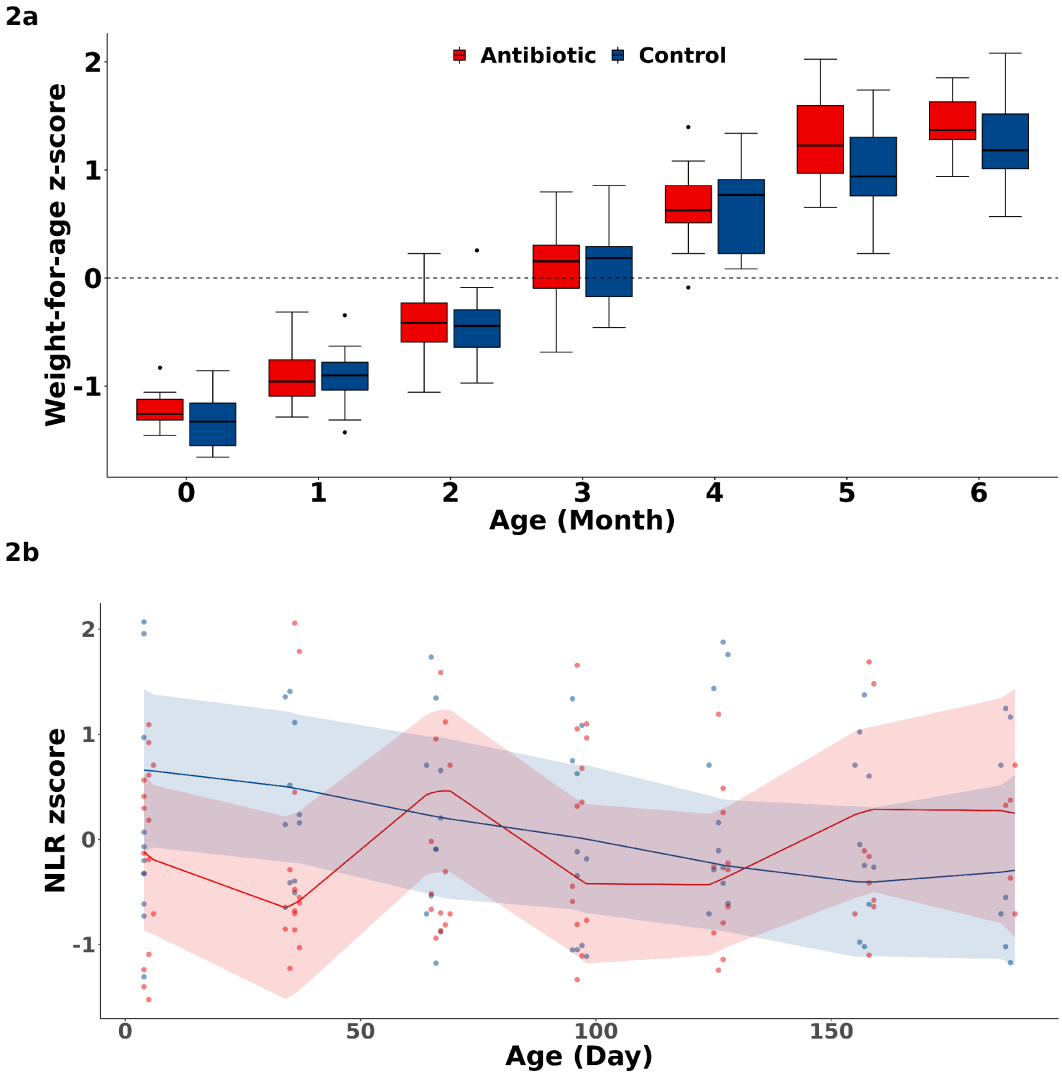

Figure 2.2: Early-life antibiotics causes persistent physiological changes in neutrophil-to-lymphocyte ratio and weight. Mixed effects model of Neutrophil-to-lymphocyte ratio over the first 6 months of life (age measured in days). Weight increase over the first 6 months of life (age measured in days) (Fig. 2a). The area around the splines in the NLR model represent 95% confidence intervals. The weight model is represented by age in months for simplicity (Fig. 2b). Error bars in weight mixed effected model represent the standard error of the mean. Age in days and sex were included as covariates the NLR and weight mixed effects models. Sample sizes were as follows: Antibiotic exposed infants (n=14), Control infants (n=12), Antibiotic exposed males (n=9), antibiotic exposed females (n=5), control males (n=6), and control females (n=6). We were able to include an additional 8 animals for our regression analyses for months 0-5 bringing the total samples size to 26 for those time points.

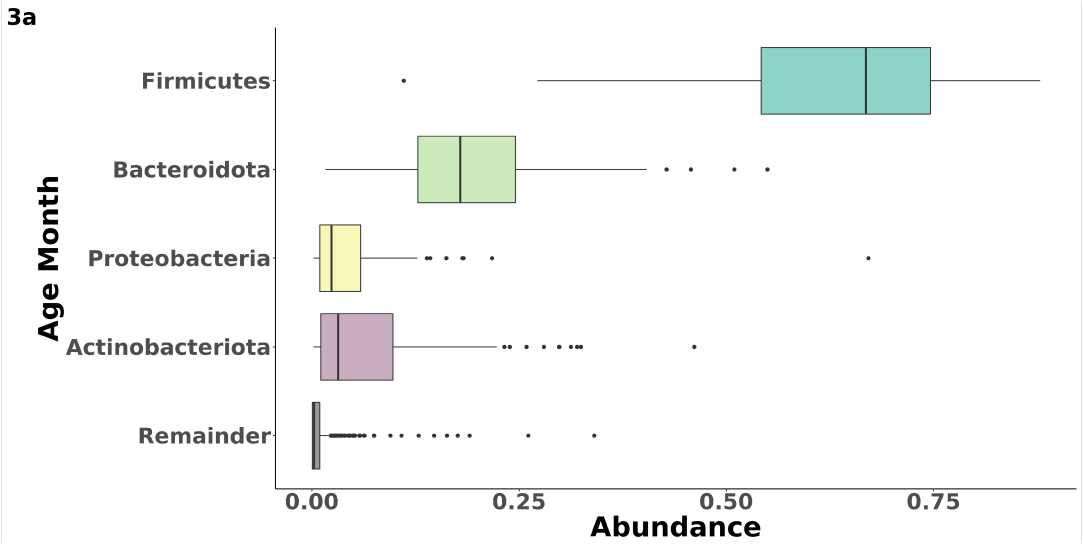
3a
Firmicutes
Bacteroidota
Proteobacteria
Actinobacteriota
Remainder
Age Month
0.00
0.25
0.50
0.75
Abundance

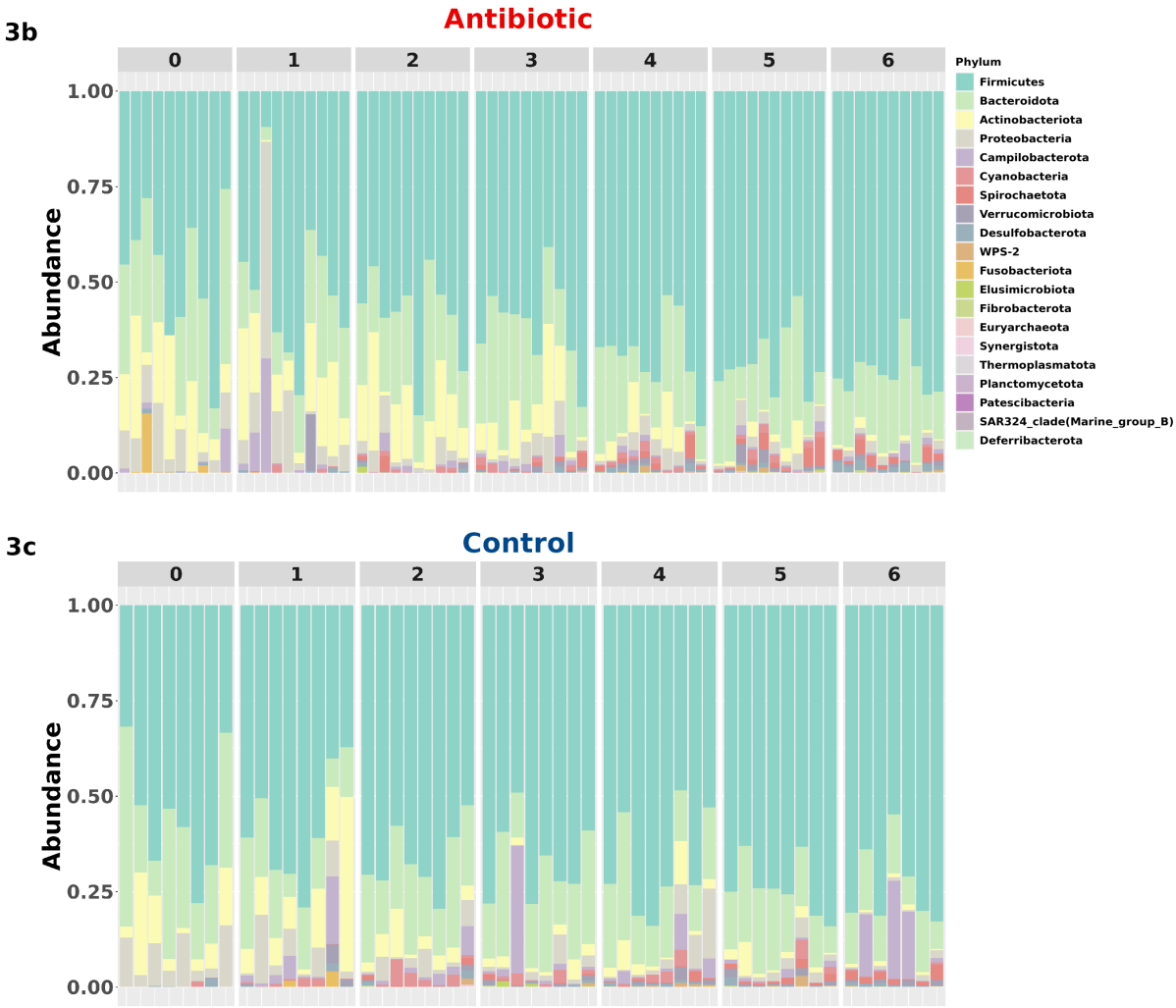

Figure 2.3: *Proteobacteria*, *Firmicutes*, *Bacteroidota*, and *Actinobacteria* make up the majority of developing fecal microbiota composition during the first 6 months of life. Percent abundance of all phyla >1% of total reads (Phyla representing <1% of the total reads were binned as "Remainder") (Fig. 3a) and total composition of antibiotic treated animals (top) and control animals (bottom) over 6-months (Fig. 3b).

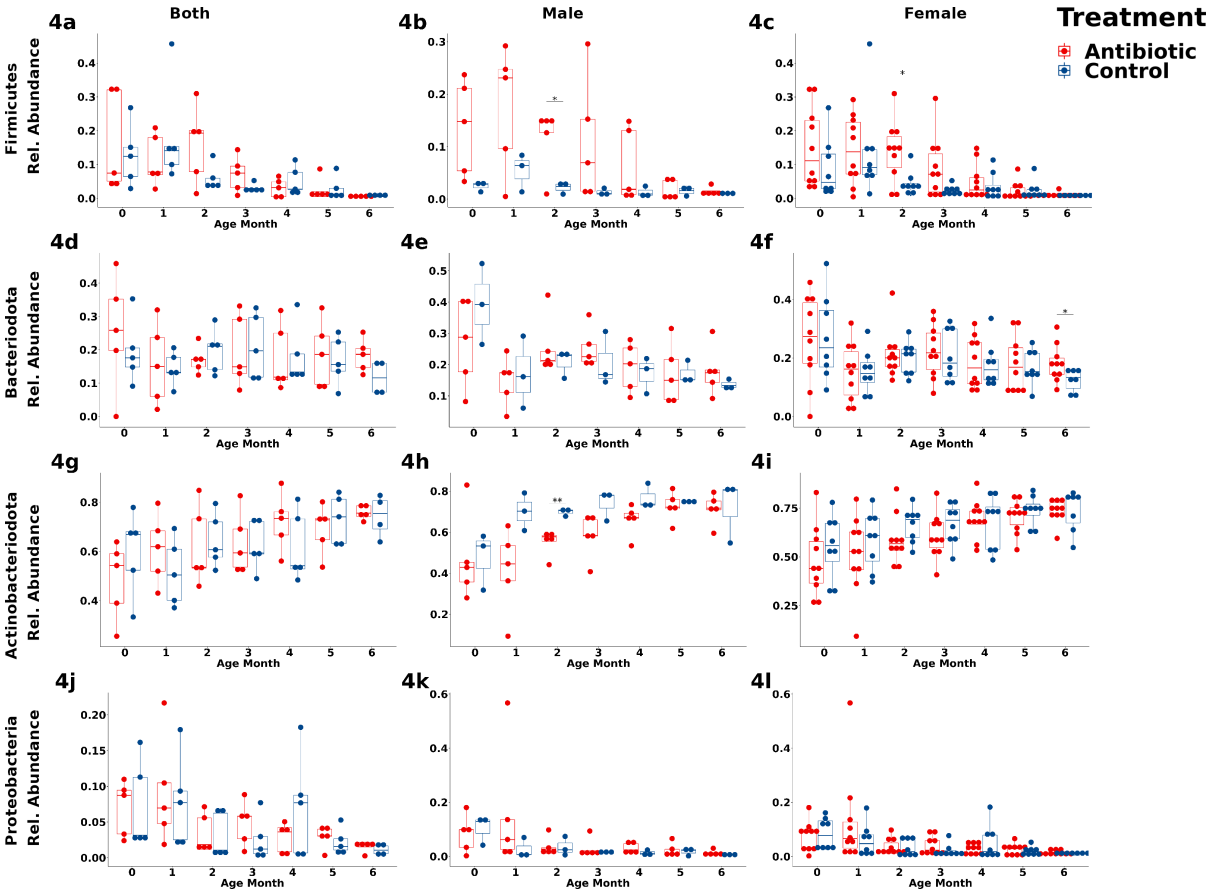

Figure 2.4: Early-life antibiotic exposure has both transient and lasting effects on the composition of the infant rhesus microbiome. Prominent changes are observed in males (Fig. 4a, 4e, 4h, 4k) relative to females (Fig. 4c, 4f, 4i, 4l). Abundance trajectories of *Firmicutes* (Fig. 4a, 4b, 4c), *Bacteroidota* (Fig. 4d, 4e, 4f), *Actinobacteria* (Fig. 4g, 4h, 4i) and *Proteobacteria* (Fig. 4j, 4k, 4l) were measured as the percent of read reads mapped to a given phyla for each sample. Sample sizes were as follows: Antibiotic exposed infants (n=10), Control infants (n=8), Antibiotic exposed males (n=5), antibiotic exposed females (n=5), control males (n=3), and control females (n=5). Due to a collection issue, one month-6 fecal swab is missing from the female control group. P <0.05 by ANOVA with paired samples t-test and Bonferroni correction. *, P <0.05; **, P <0.005.

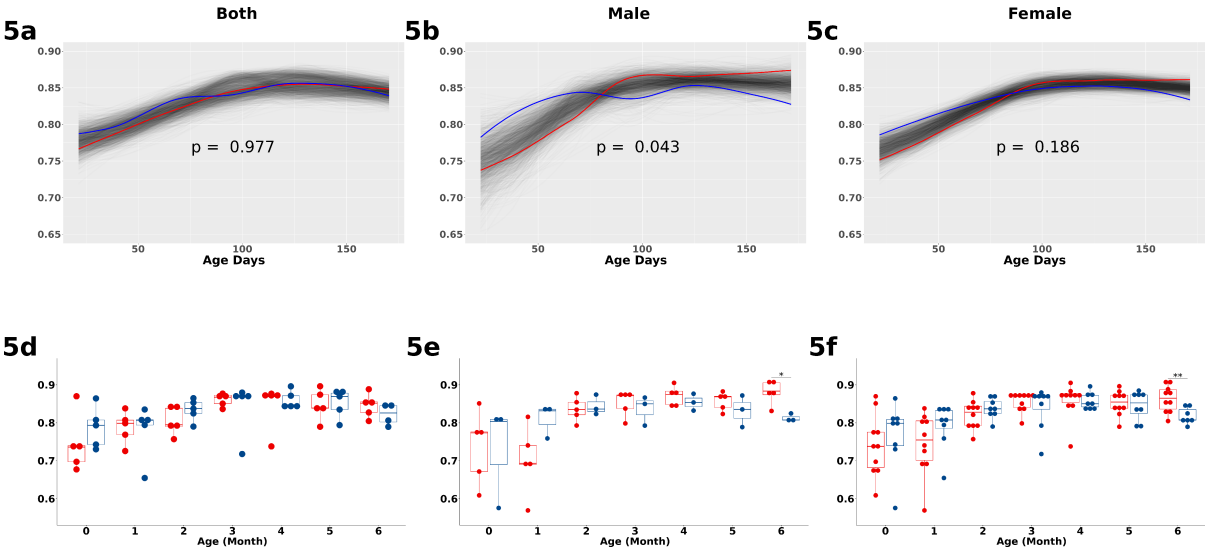

Figure 2.5: Persistent changes in alpha diversity are most pronounced at 6 months and in males. Changes in alpha diversity were more pronounced in males than females. Bacteria evenness of richness (Pielou's evenness) over time distinguishes from control (group spline in blue) and ABX (group spline in red) infants. Pielou's evenness between antibiotic treated and untreated males and females (1000 permutations, p=0.21) (Fig. 5a), evenness between antibiotic treated and untreated males (1000 permutations, p=0.02) (Fig. 5b), and evenness between antibiotic treated and untreated females (1000 permutations, p=0.98) (Fig. 5c). Pielou's evenness for both sexes (Fig. 5d), males (Fig. 5e), and females (Fig. 5f). Alpha diversity measured as Shannon index for box sexes (Fig. 5g), males (Fig. 5h), and females (Fig 5i). Sample sizes were as follows: Antibiotic exposed infants (n=10), Control infants (n=8), Antibiotic exposed males (n=5), antibiotic exposed females (n=5), control males (n=3), and control females (n=5). Due to a collection issue, one month-6 fecal swab is missing from the female control group. P <0.05 by ANOVA with paired samples t-test and Bonferroni correction. *, P <0.05; **, P <0.005.

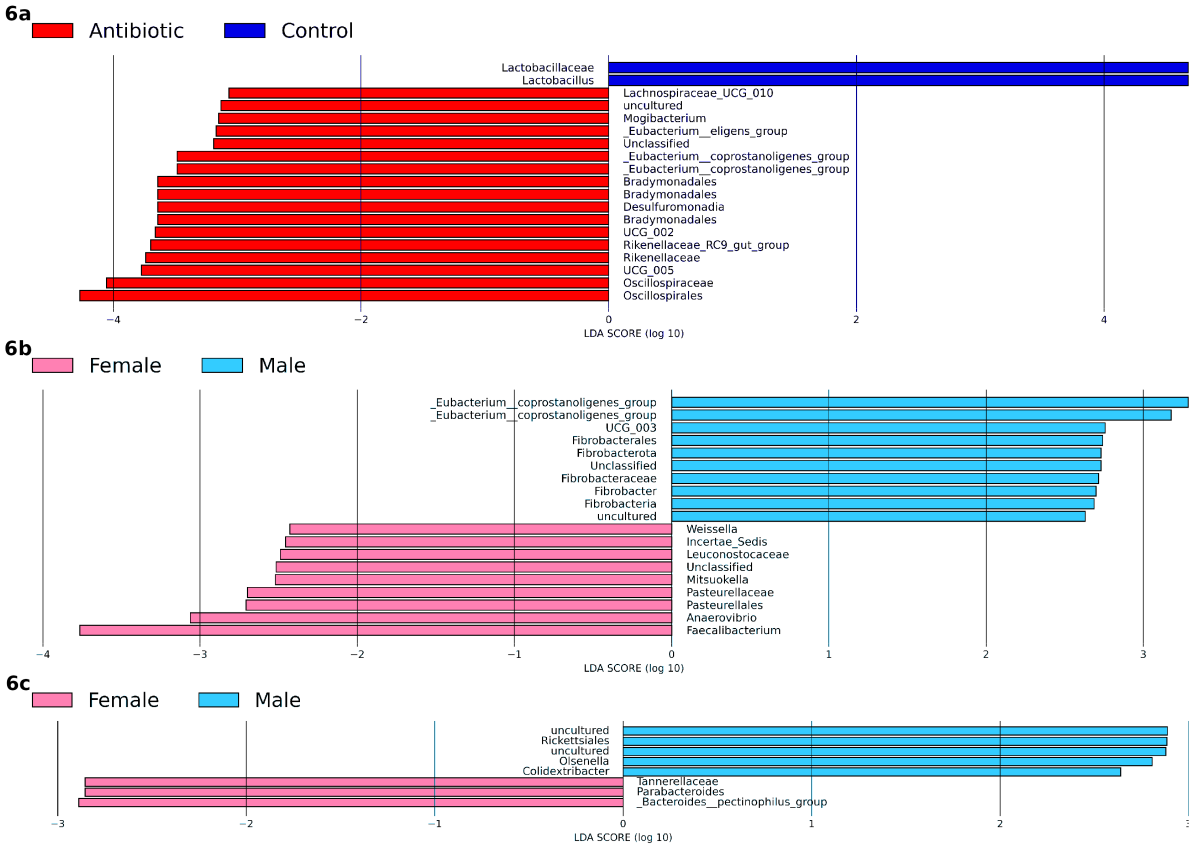

Figure 2.6: Early antibiotic exposure promotes differences in taxa abundances. Differential abundance was assessed using LEfSe to determine how different the microbiome of antibiotic-exposed and unexposed infants (Fig. 6a), antibiotic-exposed males and females (Fig. 6b), and control male and females (Fig. 6c), are at 6 months of age. Sample sizes were as follows: Antibiotic exposed infants (n=10), Control infants (n=8), Antibiotic exposed males (n=5), antibiotic exposed females (n=5), control males (n=3), and control females (n=5). Due to a collection issue, one month-6 fecal swab is missing from the female control group. (α= 0.05, logarithmic LDA score threshold = 2.0)

7a

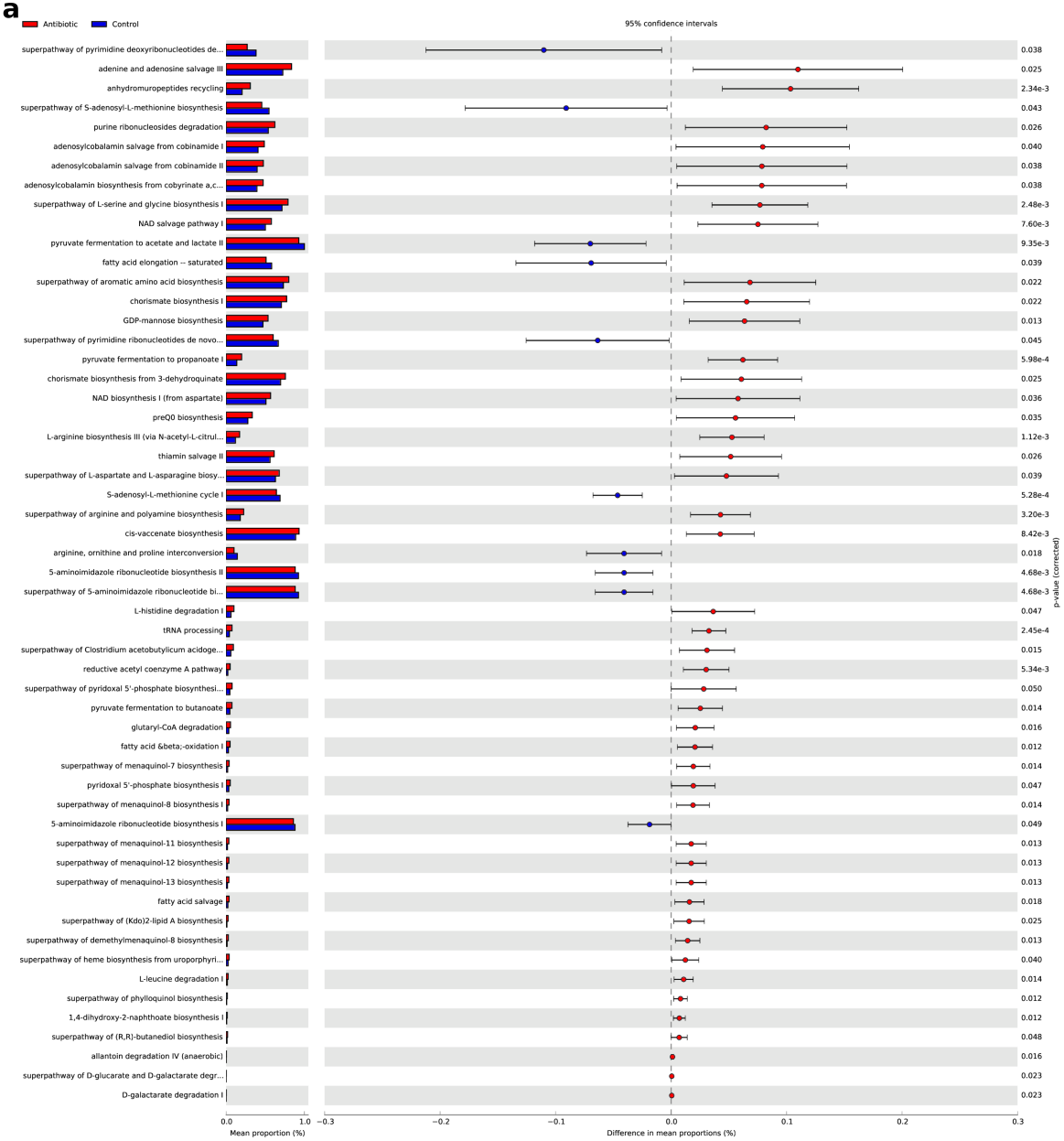
Antibiotic
Control
95% confidence intervals
superpathway of pyrimidine deoxyribonucleotides de...
adenine and adenosine salvage III
anhydromuropeptides recycling
superpathway of S-adenosyl-L-methionine biosynthesis
purine ribonucleosides degradation
adenosylcobalamin salvage from cobinamide I
adenosylcobalamin salvage from cobinamide II
adenosylcobalamin biosynthesis from cobyrinate a,c...
superpathway of L-serine and glycine biosynthesis I
NAD salvage pathway I
pyruvate fermentation to acetate and lactate II
fatty acid elongation -- saturated
superpathway of aromatic amino acid biosynthesis
chorismate biosynthesis I
GDP-mannose biosynthesis
superpathway of pyrimidine ribonucleotides de novo...
pyruvate fermentation to propanoate I
chorismate biosynthesis from 3-dehydroquinate
NAD biosynthesis I (from aspartate)
preQ0 biosynthesis
L-arginine biosynthesis III (via N-acetyl-L-citrul...
thiamin salvage II
superpathway of L-aspartate and L-asparagine biosy...
S-adenosyl-L-methionine cycle I
superpathway of arginine and polyamine biosynthesis
cis-vaccenate biosynthesis
arginine, ornithine and proline interconversion
5-aminoimidazole ribonucleotide biosynthesis II
superpathway of 5-aminoimidazole ribonucleotide bi...
L-histidine degradation I
tRNA processing
superpathway of Clostridium acetobutylicum acidoge...
reductive acetyl coenzyme A pathway
superpathway of pyridoxal 5'-phosphate biosynthesi...
pyruvate fermentation to butanoate
glutaryl-CoA degradation
fatty acid β-oxidation I
superpathway of menaquinol-7 biosynthesis
pyridoxal 5'-phosphate biosynthesis I
superpathway of menaquinol-8 biosynthesis I
5-aminoimidazole ribonucleotide biosynthesis I
superpathway of menaquinol-11 biosynthesis
superpathway of menaquinol-12 biosynthesis
superpathway of menaquinol-13 biosynthesis
fatty acid salvage
superpathway of (Kdo)2-lipid A biosynthesis
superpathway of demethylmenaquinol-8 biosynthesis
superpathway of heme biosynthesis from uroporphyri...
L-leucine degradation I
superpathway of phylloquinol biosynthesis
1,4-dihydroxy-2-naphthoate biosynthesis I
superpathway of (R,R)-butanediol biosynthesis
allantoin degradation IV (anaerobic)
superpathway of D-glucarate and D-galactarate degr...
D-galactarate degradation I
0.038
0.025
2.34e-3
0.043
0.026
0.040
0.038
0.038
2.48e-3
7.60e-3
9.35e-3
0.039
0.022
0.022
0.013
0.045
5.98e-4
0.025
0.036
0.035
1.12e-3
0.026
0.039
5.28e-4
3.20e-3
8.42e-3
0.018
4.68e-3
4.68e-3
0.047
2.45e-4
0.015
5.34e-3
0.050
0.014
0.016
0.012
0.014
0.047
0.014
0.049
0.013
0.013
0.013
0.018
0.025
0.013
0.040
0.014
0.012
0.012
0.048
0.016
0.023
0.023
p-value (corrected)
0.0
1.0
Mean proportion (%)
−0.3
−0.2
−0.1
0.0
0.1
0.2
0.3
Difference in mean proportions (%)

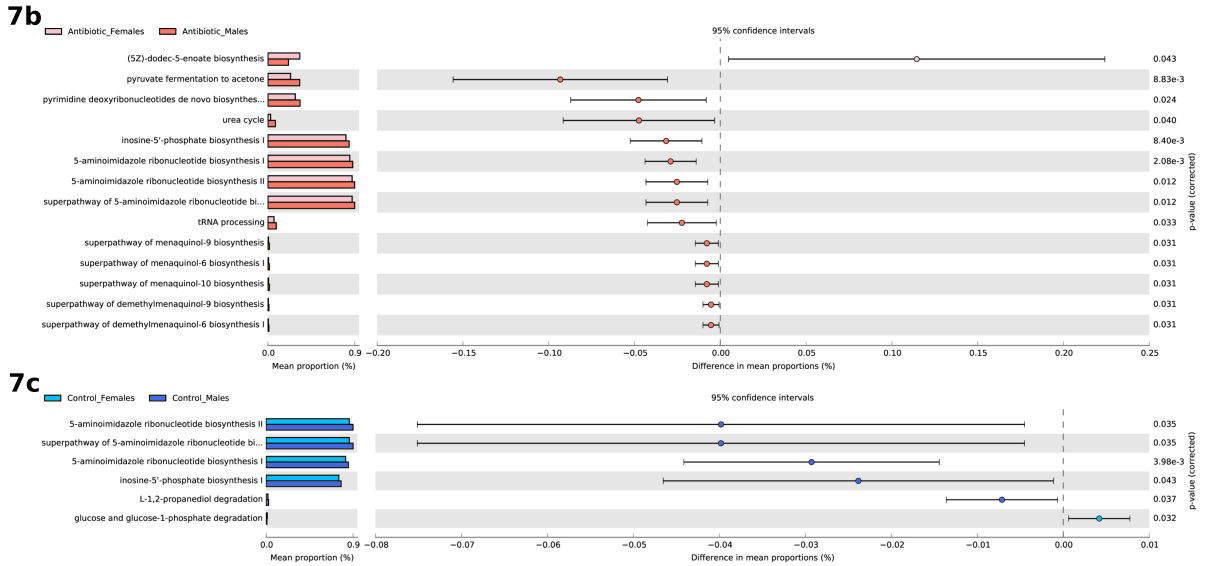

Figure 2.7: Metagenomic pathways are altered with early-life antibiotic treatment. Kegg biomarkers significantly different between antibiotic-treated (red) control (blue) infants (Fig. 7a). Kegg biomarkers significantly different between control (Fig. 7b) and antibiotic (Fig. 7c) exposed males (purple) and females (pink) at 6 months of age. Sample sizes were as follows: Antibiotic exposed infants (n=10), Control infants (n=8), Antibiotic exposed males (n=5), antibiotic exposed females (n=5), control males (n=3), and control females (n=5). Due to a collection issue, one month-6 fecal swab is missing from the female control group.

1sa

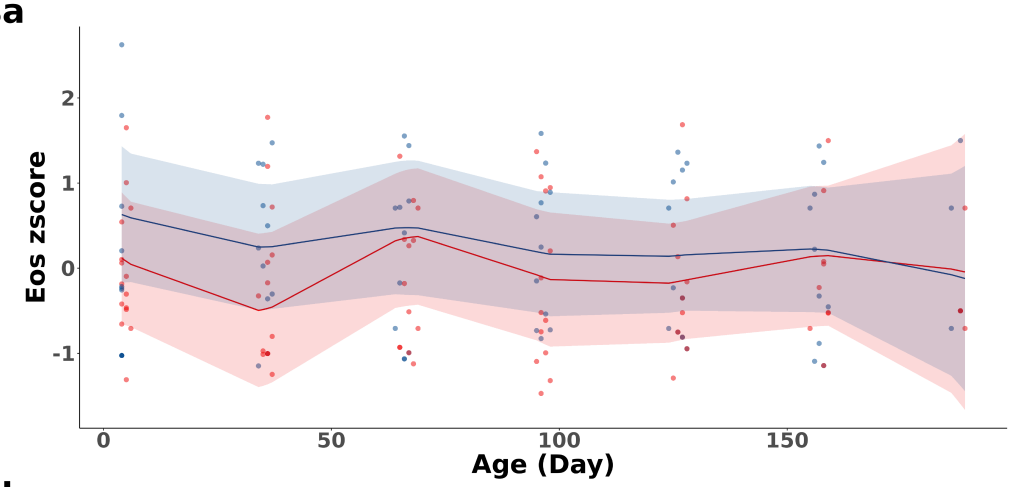
Eos zscore
2
1
0
-1
0
50
100
150
Age (Day)

1sb

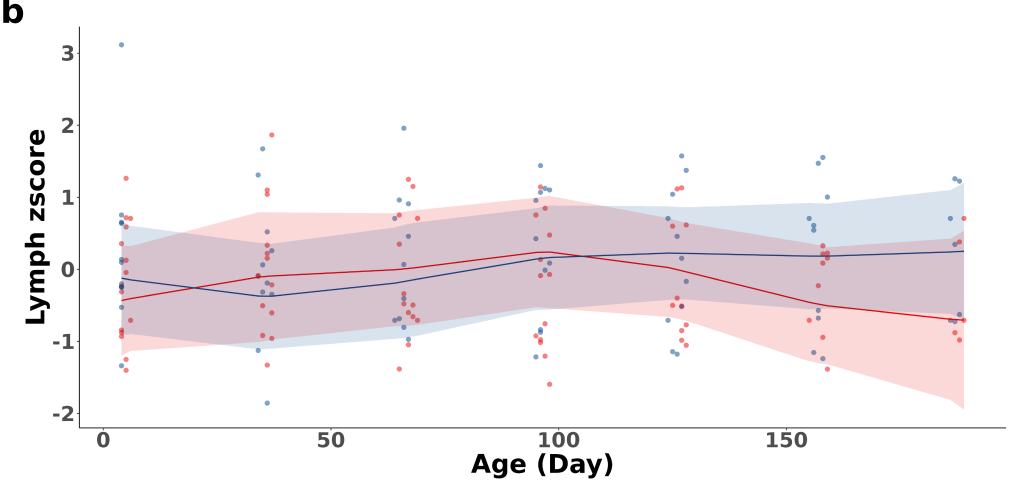
Lymph zscore
3
2
1
0
-1
-2
0
50
100
150
Age (Day)

1sc

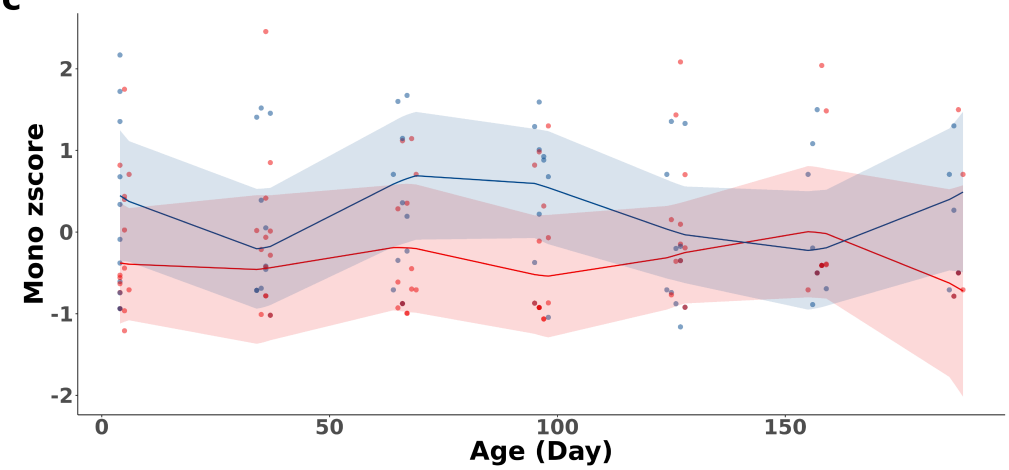
Mono zscore
2
1
0
-1
-2
0
50
100
150
Age (Day)

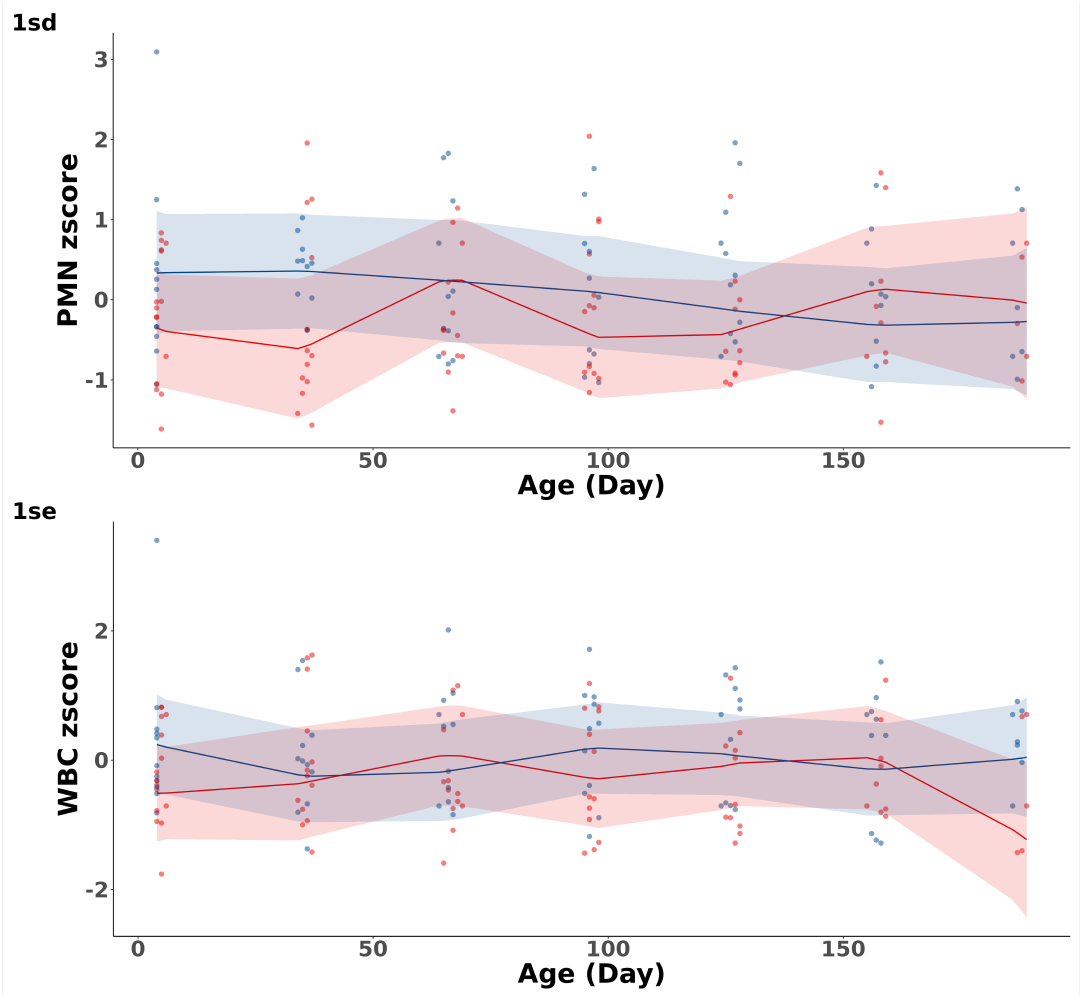

Supplementary Figure 2.1: Effect of early-life antibiotic exposure on clinical parameters. Mixed- effects models of eosinophil (Supp. 1a), total white blood cell (Supp. 1b), monocyte (Supp. 1c), and lymphocyte (Supp. 1d) concentration (cell/µl) z scores over the first 6 months of life. Loess splines were used to smooth data to account for the non-linear relationship between blood cell differential concentration and age. Age in days, sex, and antibiotic treatment status were used as covariates in the mixed-effects models.

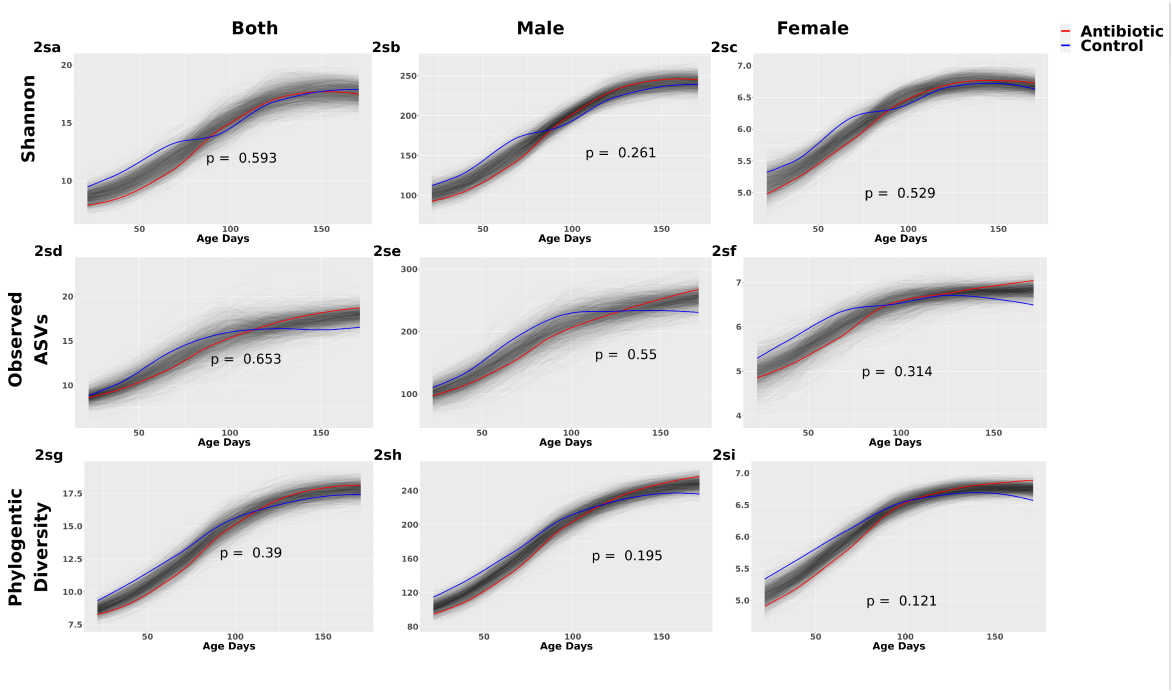

Supplementary Figure 2.2: Longitudinal effect of early antibiotic exposure on alpha diversity. Alpha diversity was measured as Shannon entropy (Supp. 2a-2c), observed ASVs (Supp. 2e-2f), and phylogenetic diversity (Supp. 2g-2i). Splines were permuted using the permuspliner function in the SplinectomeR to assess the longitudinal effect of antibiotics on infant's alpha diversity in the fecal microbiome.

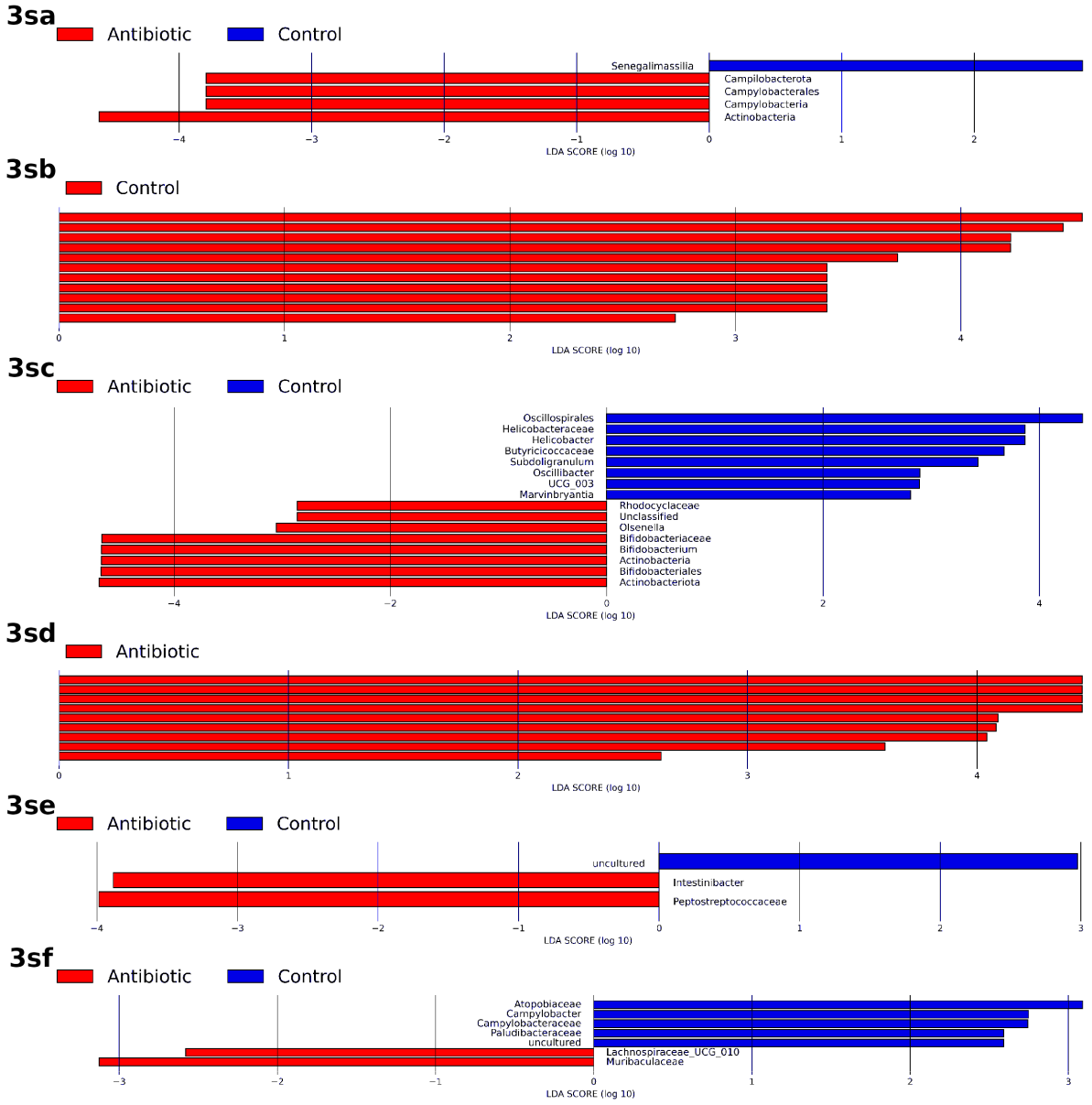

Supplementary Figure 2.3: LEfSe Differential abundance of taxa (antibiotic exposed and control). Differential abundance between antibiotic exposed and unexposed infants at month 0 (Supp. 3a), month 1 (Supp. 3b), month 2 (Supp. 3c), month 3 (Supp. 3d), month 4 (Supp. 3e), and month 5 (Supp. 3f). (α= 0.05, logarithmic LDA score threshold = 2.0)

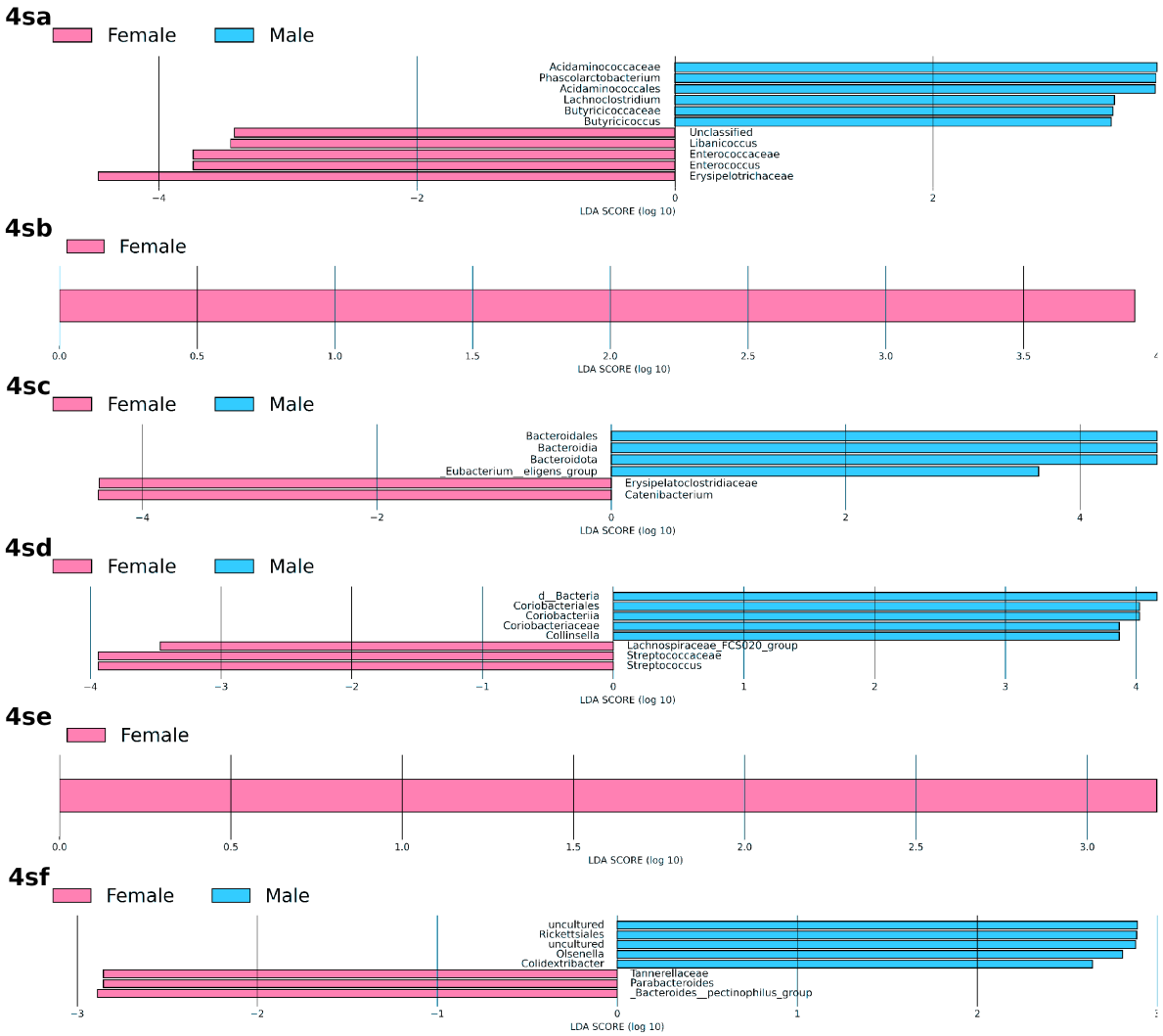

Supplementary Figure 2.4: LEfSe Differential abundance of taxa (antibiotic exposed males and females). Differential abundance between antibiotic treated males and females at month 0 (Supp. 4a), month 1 (Supp. 4b), month 2 (Supp. 4c), month 3 (Supp. 4d), month 4 (Supp. 4e), and month 5 (Supp. 4f). (α= 0.05, logarithmic LDA score threshold = 2.0)

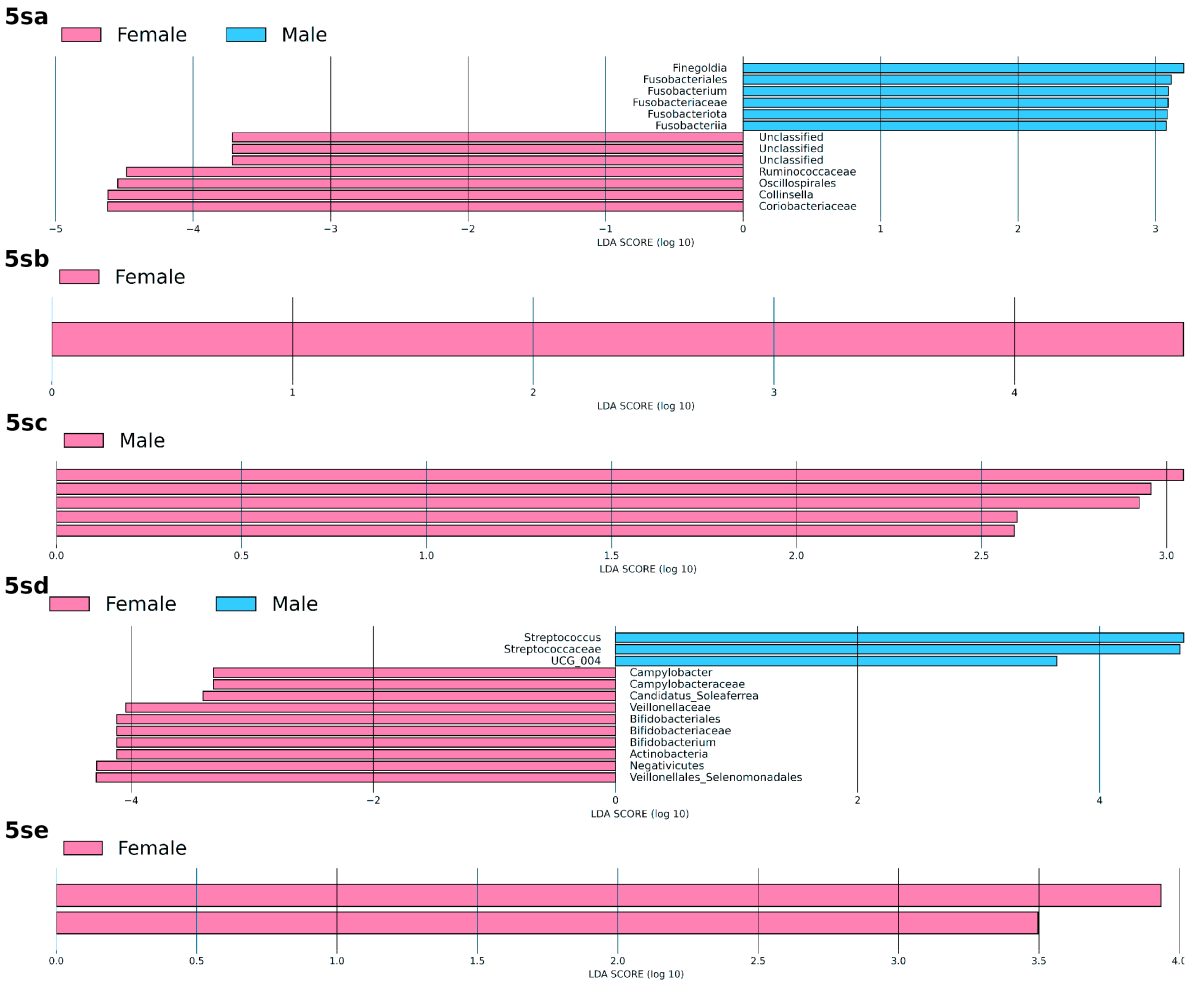

Supplementary Figure 2.5: LEfSe Differential abundance of taxa (control males and females). Differential abundance between control males and females at month 0 (Supp. 5a), month 2 (Supp. 5b), month 3 (Supp. 5c), month 4 (Supp. 5d), and month 5 (Supp. 5e). There were no differentially abundant taxa observed at 1 month between control males and females. (α= 0.05, logarithmic LDA score threshold = 2.0)

FIGURES

6sa

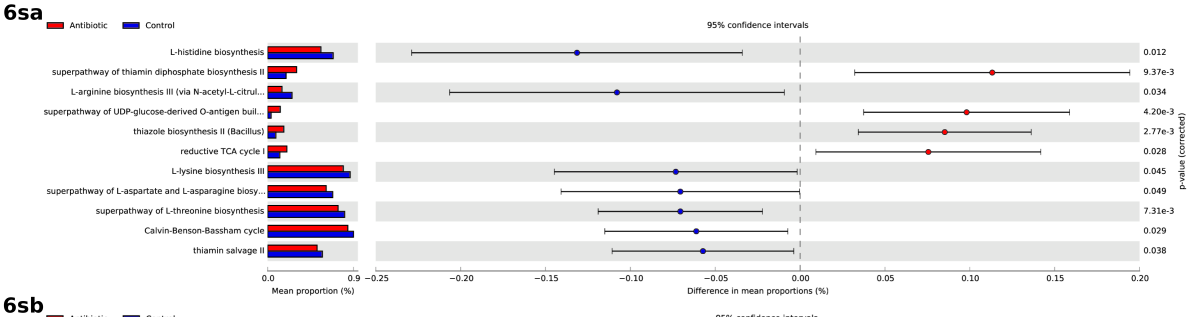

6sb

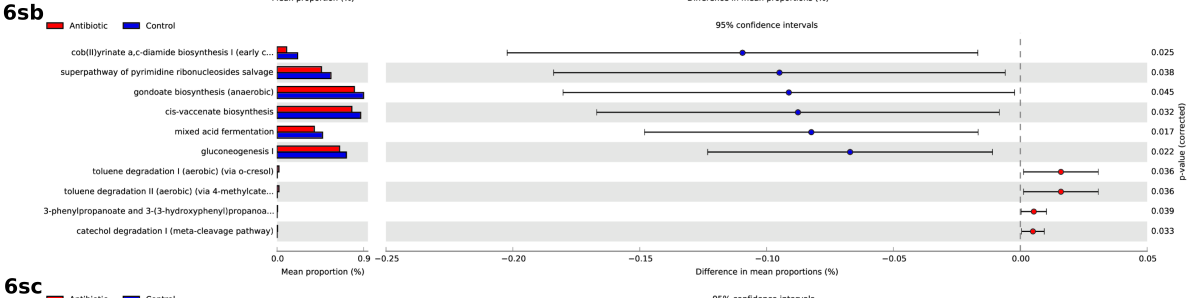

6sc

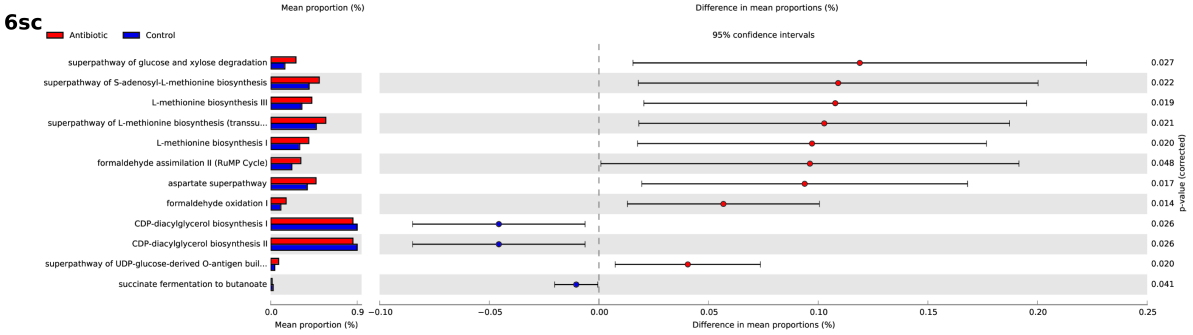

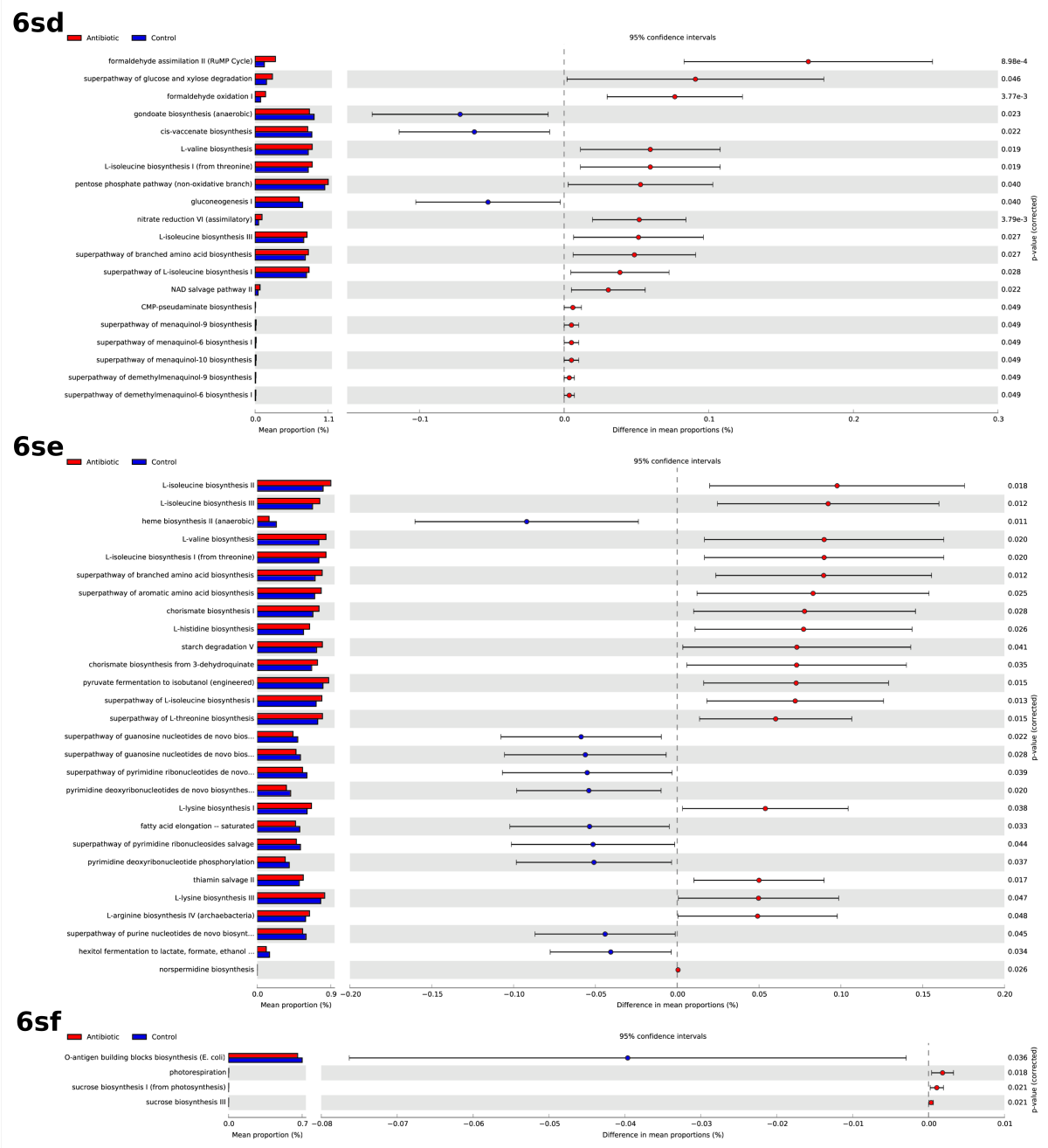

Supplementary Figure 2.6: The metagenomic function of the developing microbiome between antibiotic-exposed and control infants. Predicted KEGG biomarkers significantly different between antibiotic exposed (red) and control (blue) infants at 0 months (Supp. 6a), 1 month (Supp. 6b), 2 months (Supp. 6c), 3 months (Supp. 6d), 4 months (Supp. 6e), and 5 months (Supp. 6f).

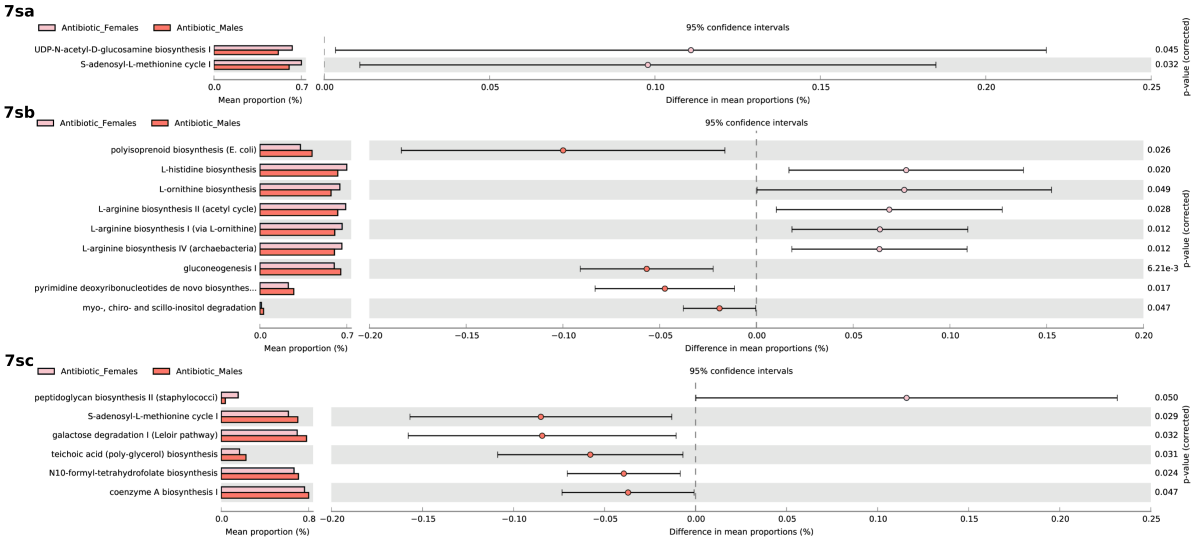

Supplementary Figure 2.7: The metagenomic function of the developing microbiome between antibiotic-exposed males and females. KEGG biomarkers significantly different between antibiotic exposed males (purple) and females (pink) at 1 month (Supp. 7a), 2 months (Supp. 7b), 3 months (Supp. 7c). There were not significantly different Kegg biomarkers observed at 0 months.

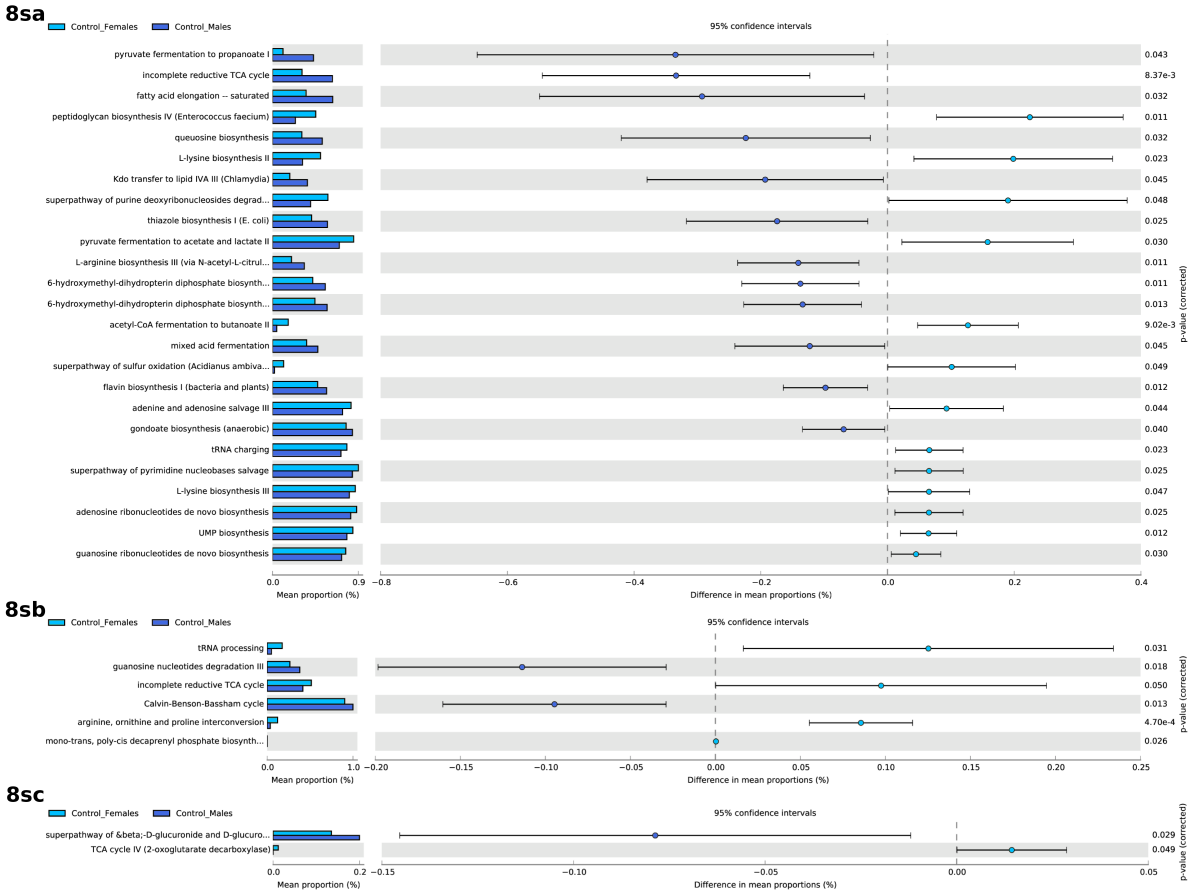
8sa
Control_Females
Control_Males
95% confidence intervals
pyruvate fermentation to propanoate I
incomplete reductive TCA cycle
fatty acid elongation -- saturated
peptidoglycan biosynthesis IV (Enterococcus faecium)
queuosine biosynthesis
L-lysine biosynthesis II
Kdo transfer to lipid IVA III (Chlamydia)
superpathway of purine deoxyribonucleosides degrad...
thiazole biosynthesis I (E. coli)
pyruvate fermentation to acetate and lactate II
L-arginine biosynthesis III (via N-acetyl-L-citrul...
6-hydroxymethyl-dihydropterin diphosphate biosynth...
6-hydroxymethyl-dihydropterin diphosphate biosynth...
acetyl-CoA fermentation to butanoate II
mixed acid fermentation
superpathway of sulfur oxidation (Acidianus ambiva...
flavin biosynthesis I (bacteria and plants)
adenine and adenosine salvage III
gondoate biosynthesis (anaerobic)
tRNA charging
superpathway of pyrimidine nucleobases salvage
L-lysine biosynthesis III
adenosine ribonucleotides de novo biosynthesis
UMP biosynthesis
guanosine ribonucleotides de novo biosynthesis
0.043
8.37e-3
0.032
0.011
0.032
0.023
0.045
0.048
0.025
0.030
0.011
0.011
0.013
9.02e-3
0.045
0.049
0.012
0.044
0.040
0.023
0.025
0.047
0.025
0.012
0.030
p-value (corrected)
0.0
0.9
Mean proportion (%)
−0.8
−0.6
−0.4
−0.2
0.0
0.2
0.4
Difference in mean proportions (%)
8sb
Control_Females
Control_Males
95% confidence intervals
tRNA processing
guanosine nucleotides degradation III
incomplete reductive TCA cycle
Calvin-Benson-Bassham cycle
arginine, ornithine and proline interconversion
mono-trans, poly-cis decaprenyl phosphate biosynth...
0.031
0.018
0.050
0.013
4.70e-4
0.026
p-value (corrected)
0.0
1.0
Mean proportion (%)
−0.20
−0.15
−0.10
−0.05
0.00
0.05
0.10
0.15
0.20
0.25
Difference in mean proportions (%)
8sc
Control_Females
Control_Males
95% confidence intervals
superpathway of β-D-glucuronide and D-glucuro...
TCA cycle IV (2-oxoglutarate decarboxylase)
0.029
0.049
p-value (corrected)
0.0
0.2
Mean proportion (%)
−0.15
−0.10
−0.05
0.00
0.05
Difference in mean proportions (%)

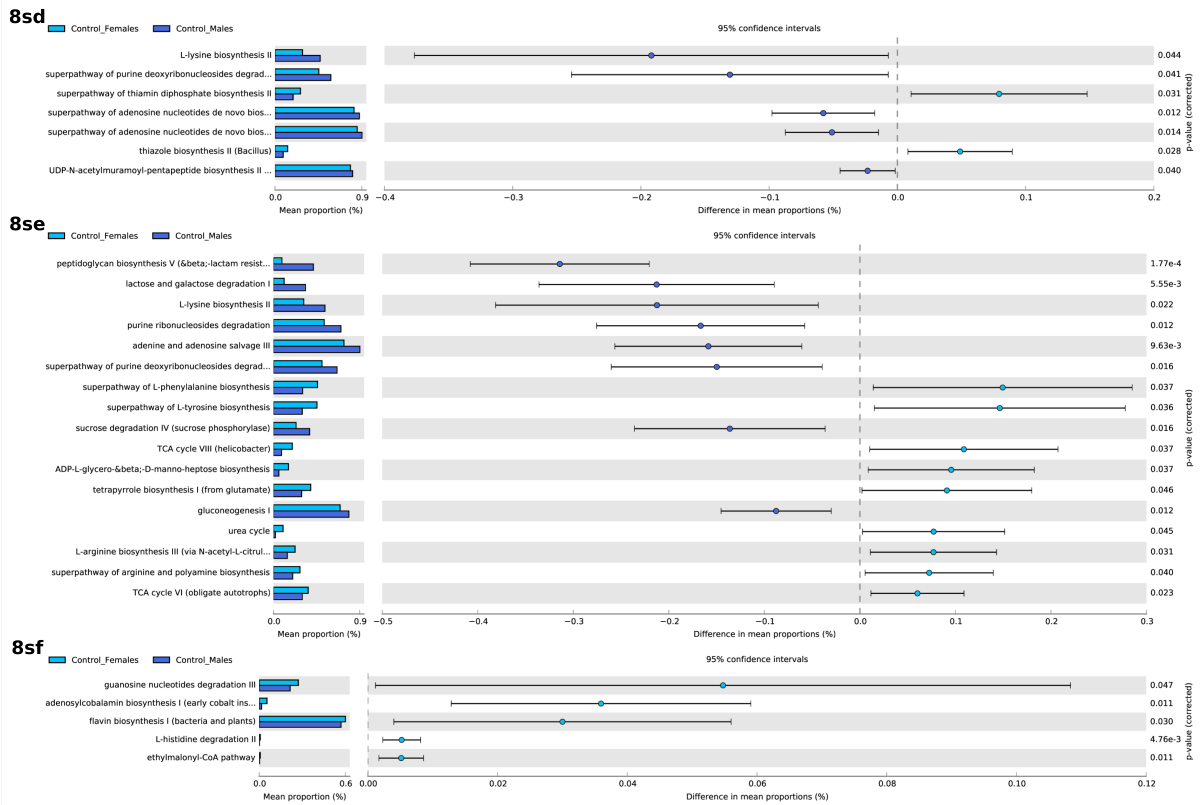

Supplementary Figure 2.8: The metagenomic function of the developing microbiome between control males and females. KEGG biomarkers significantly different between control males (purple) and females (pink) at 0 months (Supp. 8a), 1 month (Supp. 8b), 2 months (Supp. 8c), 3 months (Supp. 8d), 4 months (Supp. 8e), 5 months (Supp. 8f). There were not significantly different Kegg biomarkers observed at 5 months.

Tables

Table 2.1: Neutrophil to lymphocyte ratio z-score non-linear mixed-effects model. Variance of fixed effects were assessed through ANOVA.

Neutrophil to lymphocyte ratio z-score non-linear mixed-effects model.

$Variables$	$SumSq$	$MeanSq$	$NumDF$	$DenDF$	$Fvalue$	$Pr(>F)$
$ns(age\_days, df = 5)$	0.428	0.086	5	108.17	0.152	0.979
Sex	0.824	0.824	1	94.876	1.467	0.229
$Treatment$	0.242	0.242	1	94.876	0.431	0.513
$ns(age\_days, df = 5) : Sex$	5.301	1.06	5	108.17	1.889	0.102
$ns(age\_days, df = 5) : Treatment$	1.035	0.207	5	108.17	0.369	0.869
$Sex : Treatment$	1.017	1.017	1	94.876	1.811	0.182
$ns(age\_days, df = 5) : Sex : Treatment$	10.134	2.027	5	108.17	3.611	0.005

Table 2.2: Weight z-score linear mixed-effects model. Variance of fixed effects were assessed through ANOVA.

Weight z-score linear mixed-effects model.

$Variables$	$SumSq$	$MeanSq$	$NumDF$	$DenDF$	$Fvalue$	$Pr(>F)$
sex	0.021	0.021	1	26.984	0.62	0.438
$treatment$	0.004	0.004	1	26.984	0.119	0.733
age_days	150.164	150.164	1	159.231	4513.809	0
$sex : treatment$	0.022	0.022	1	26.984	0.667	0.421
$sex : age\_days$	0.165	0.165	1	159.231	4.955	0.027
$treatment : age\_days$	0.108	0.108	1	159.231	3.254	0.073
$sex : treatment : age\_days$	0.193	0.193	1	159.231	5.79	0.017

Chapter 3

Early Life Antibiotic Exposure affects the Nasopharyngeal Microbiota and Pulmonary Function in Rhesus Macaques

> The first scientific postulate is the objectivity of nature: nature does not have any intention or goal.
>
> Jacques Lucien Monod

Abstract

Background: Judicial use of antibiotics is essential for human health; however, overuse of antibiotics has been linked to allergy development and other maladies. Whether preventative or curative, use of antibiotics can persistently affect the architecture of the

ABSTRACT

developing respiratory microbiome is unknown. External factors such as tobacco smoke and infection have been implicated in the alteration of the gut and respiratory microbiomes of adults. Infants are susceptible to the effects of excessive antibiotic usage as disruption of microbiome maturation has been associated with persistent and pathological microbiome changes in rodent models. In addition to microbiome maturation, early development includes important lung developmental milestones necessary for proper lung function in adulthood. Here, we aimed to define the developing upper respiratory microbiome and assess whether antibiotic treatment would alter the microbiome of the upper respiratory tract in addition to altering pulmonary function. **Results:** Administration of a broad-spectrum antibiotic cocktail during the first week of life had transient effects on respiratory microbiome composition and function—alterations in microbiome composition were more pronounced when sex was considered. Lung function was reduced in antibiotic-treated male infants, and lung gene expression correlated with taxa abundances in the upper respiratory tract microbiome. Microbiome function was assessed using PiCrust, and metagenomic functional changes to the microbiome occurred in addition to microbiome changes in composition. Fewer bacteria pathway expression was observed in antibiotic-treated infants. **Conclusion:** Antibiotic treatment altered the respiratory microbiome, particularly in male infants. Changes in the composition of the respiratory microbiome occurred in parallel with physiological changes in lung function and expression of growth and development genes. Microbiome function was altered in conjunction with both microbiome and lung function changes.

Introduction

The lung serves is an important site for gas exchange in the body and is essential for respiration. In humans, the lung completes most of its growth during the first few years of life, and continued alveolarization and microvascular maturation commence into young adulthood (Schittny 2017). Recent findings demonstrate the interaction between the gut and lung in the complex interplay of the gut-lung axis (Gray et al. 2017). This interaction is partly due to bacteria and their bi-products, which can, directly and indirectly, interact with the immune system (Niu et al. 2023). Despite evidence of bi-directional crosstalk between the gut and lung, most studies focus on how the gut modulates the lung (Levan et al. 2019). However, researchers are increasingly studying lung and gut microbiome relationships (Segal et al. 2013, Dickson et al. 2014). Tobacco and some viral infections such as influenza and SARS-CoV-2 can alter the composition of the gut microbiome (Gu et al. 2020, Prakash et al. 2021, Zuo et al. 2021). Changes to the microbiome of the respiratory tract locally alter pulmonary physiology and immune function (Wang et al. 2013, Li et al. 2017).

We have previously demonstrated that early-life antibiotic treatment in infant rhesus monkeys leads to long-term alterations in microbiome diversity of the gut microbiome (unpublished). Additionally, we found that antibiotic treatment results in physiological changes, including reduced neutrophil-to-lymphocyte (NLR) ratio and elevated weight z-scores in antibiotic-treated infants. These findings suggested that antibiotics, when administered during an early window, can persistently alter the microbiome of rhesus monkeys. Acquiring a microbiome begins when an infant exits through the birth canal, and once born, the infant's microbiota is highly susceptible to change (Marques et al. 2010, Koenig et al. 2011, Natividad et al. 2022). Perturbation of the microbiome at this

early juncture is known to promote increased weight and asthma severity (Strömberg Celind et al. 2018, Uzan-Yulzari et al. 2021). Other researchers have made similar conclusions, primarily in murine models (Cox et al. 2014, Adami et al. 2018). However, whether antibiotics administered in early life can affect the microbiome in other mucosal sites, such as the upper respiratory tract, is unknown.

The respiratory microbiome is much less studied due to its low microbial density and transient nature than the gut microbiome. However, evidence suggests the lung microbiome affects lung function as both *Actinobacteria* and *Gemella* abundance in the respiratory tract is associated with decreasing Forced Vital Compacity (FCV) (Lee et al. 2019). We hypothesized that antibiotic treatment during the first week of life would be associated with nasopharyngeal microbiome alternations and physiological detriments in the respiratory tract.

To understand how early-life antibiotic treatment affects the developing microbiome and the lung, infant rhesus monkeys were given an antibiotic cocktail containing broad-spectrum antibiotics daily for 7 days. We define the developing rhesus monkey microbiome with 16s rRNA sequencing for 6 months and further investigate the effects of early antibiotic disruption on the developing nasopharyngeal microbiome.

Materials and Methods

Rhesus Macaques.

Infant colony-bred Indian rhesus macaques (Mucaca mulatta) born and housed at the California National Primate Research Center (CNPRC) were used in this study. The animals were negative for simian immunodeficiency virus (SIV), simian T lymphotropic

virus (STLV), and simian retrovirus (SRV), and they did not have a history of pharmacological or dietary intervention with known influences on the microbiome. All animals were healthy for the duration of the study. Animals were enrolled in the study on a tapered schedule, and although samples were collected once per month, the exact age in days of each animal may have differed slightly. Age in months and age in days are used to assess differences on continuous and discrete scales.

Diet, housing, and antibiotics.

All animals were housed indoors and breast-fed by their respective dams until weaning at 5 months. Infant monkeys were assigned to a control group (n=8; male n=3, female n=5) and an antibiotic (ABX) treatment group (n=10; male n=5, female n=5). Antibiotics or saline were administered to animals for 7 consecutive days. We previously found that intramuscular (I.M.) administration of a broad-spectrum antibiotic cocktail on postnatal days 1-7 results in an altered intestinal microbiome in rhesus monkeys (data not shown). Control animals were not administered antibiotics of any kind.

In contrast, the antibiotic-treated animals received an intramuscular (I.M.) broad-spectrum antibiotic cocktail containing Gentamicin (5 mg/kg), Ampicillin (50 mg/kg), and Vancomycin (15 mg/kg) daily at postnatal days 4 or 5 for 7 days. This cocktail was used because it is commonly administered to human infants suspected of having an infection, making the dosage and regimen in this study clinically relevant. Control animals were given a saline injection as a substitute for antibiotics via the same administration route, age, and antibiotic course duration.

RT-PCR.

Left cranial lobes were collected at necropsy, inflated with RNAlater, and micro-dissected into 3 sections: proximal, mid-level, and respiratory bronchioles. Tissue was frozen in RNAlater (Thermo Scientific) and stored at -80°C until RNA was ready to be collected. Tissue was thawed on ice with Trizol (Life Technologies). RNA was extracted using the manufacturer's instructions. RNA was treated using the Turbo DNA-free Kit (Invitrogen). RNA concentration was measured using the NanoDrop (ND-1000 Spectrophotometer). To generate cDNA, 500 ng of RNA was loaded into a 50 uL reaction with the MultiScribe Reverse Transcriptase (Applied Biosystems). 2μL of cDNA was loaded into the qPCR reaction with TaqMan Gene Expression Master Mix (Applied Biosystems). FAM TaqMan probes (Thermo Scientific) specific for rhesus FGF10 (Rh00610298_m1) and FGF7 (Rh02888111_m1) were used to amplify targets. Samples were run on the QuantStudio at the CNPRC in the PAL Core.

Microbiome Profiling.

DNA extraction.

The nasopharyngeal microbiota was assessed in total DNA from nasal swabs (Copan nasal swabs). Nasal swabs were collected monthly for 6 months and stored in Copan collection tubes at -80°. Swabs were thawed on ice and vortexed in Clary-Blair media until homogenous. Aliquots of approximately 200 µl were used for total bacterial DNA extraction. DNA was isolated using the Qiagen DNeasy PowerSoil kit (Qiagen) with the following modifications. After adding buffer C1, samples were incubated at 65° for 10 min and then subjected to homogenization using a Qiagen TissueLyser (Qiagen) for 10

min at 20 cycles per second. The samples were then turned 180 degrees and subjected to further homogenization for an additional 10 min at 20 cycles per second, per the manufacturer's recommendation. Samples were eluted in 60 µl of buffer C6.

PCR amplification.

Amplification of the V3-V4 domain of the 16S rRNA gene was performed using a DNA template and primers 319F (F stands for forward) [TCGTCGGCAGCGTCAGATGTG-TATAAGAGACAG(spacer)GTAC TCCTACGGGAGGCAGCAGT] and 806R (R stands for reverse) [GTCTCGTGGGCTCGGAGATGTGTATAAGAGACAG(spacer)CCGGA CTACNVGGGTWTCTAAT] using a two-step PCR procedure. In step one of the amplification procedure, both forward and reverse primers contained an Illumina tag sequence, a variable length spacer to increase diversity and improve the quality of the sequencing run, a linker sequence, and the 16S target sequence. Each PCR contained 1 U Kapa2G Robust Hot Start Polymerase (Kapa Biosystems), 1.5 mM MgCl2, 0.2 mM final concentration of deoxynucleotide triphosphate (dNTP) mix, 0.2µL final concentration of each primer, and 1µL of DNA for each sample. PCR conditions were as follows: an initial incubation of 95° for 45 s, 50° for 30 s, 72° for 30 s and a final extension of 72° for 3 min. In step two, each sample was barcoded with a unique forward and reverse barcode combination using forward and reverse primers with an Illumina P5 adaptor sequence, a unique 8-nucleotide (nt) barcode, a partial matching sequence of the forward adaptor used in step one and reverse primers with an Illumina P7 adaptor, unique 8-nt barcode, and a partial matching sequence of the reverse adaptor used in step 1. The PCR in step two contained 1U Kapa2G Robust Hot Start polymerase (Kapa Biosystems). 1.5 mM MgCl2, 0.2 mM final concentration dNTP mix, 0.2 µM final concentration of each uniquely barcoded primer, and 1µL of the product from the PCR in step one diluted at

7:1 ratio in water. PCR conditions were as follows: (i) an initial incubation at 95° for 3 min; (ii) 8 cycles, with 1 cycle consisting of 95° for 30 s, 58° for 30 s, and 72° for 30 s; and (iii) a final extension step of 72° for 3 min. The final product was quantified on a Qubit instrument using the Qubit Broad Range DNA kit (Invitrogen), and individual amplicons were pooled in equal concentrations. The pooled library was cleaned utilizing Ampure XP beads (Beckman Coulter). The library was quantified via qPCR followed by 300-bp paired-end sequencing using an Illumina Miseq instrument in the Genome DNA Technologies Core, University of California, Davis.

Bioinformatics.

All samples were sequenced on an Illumina MiSeq platform at the Genome DNA Technology Core at the University of California, Davis. Analysis began with demultiplexing sequence reads. Demultiplexing of the raw FASTQ files and adapter trimming of sequences were performed using dbcAmplicons version 0.8.5. (https://github.com/msettles/dbcAmplicons). The unmerged forward and reverse reads were imported into QIIME2 version 2020.8 (https://docs.qiime2.org/2020.8/), and amplicon sequencing variants (ASVs) were determined following the DADA2 analysis pipeline (Callahan et al. 2016). Snakemake (Köster and Rahmann 2012) was used as a workflow manager to manage the QIIME2 environment (https://github.com/nasiegel88/tagseq-qiime2-snakemake-1). Each sequence was assigned to its given samples based on the given barcode. Reads that did not match any barcode were discarded (failed to meet minimum quality thresholds). Barcoded forward and reverse sequencing reads were quality-filtered and merged. Sequences that were only observed one time or only in a single sample were also discarded. Chimeras were detected and filtered from paired-end reads. Comparison of clustered sequences

was performed against SILVA 138. All data generated in this study utilize the same Data processing, filtering and trimming of reads, instrumentation, technician reference database, packages, and pipeline.

The data were filtered as follows: ambiguous phyla were removed and phyla with a mean prevalence of less than 10 were removed. Taxa were agglomerated at the genus level if possible and all taxa without genus-level taxonomic assignments were retained. Samples with less than 5000 reads were removed.

Statistical analysis.

All R packages involved in analyses were installed in R 4.0.3 and managed by the package manager, mamba, unless otherwise stated. Linear correlations were done using the `stat_cor` function from the ggpubr (version 0.4.0) R package. Statistical analysis of microbial communities was performed primarily using the Bioconductor package Phyloseq (version 1.34.0). Differential abundance analyses were performed using Linear discriminant analysis effect size (LEfSe) as described in the literature (Segata et al. 2011). Alpha diversity indices were computed in Qiime2 and measured as Shannon index, Pielou's evenness, observed ASVs, and phylogenetic diversity. This method is less sensitive to the limitations of using aggregate data over time. We performed 1000 permutations. Metagenomic analysis of Picrust2 predicted Kegg pathways was analyzed in Statistical Analysis of Metagenomic Profiles (STAMP, version 2.1.3). Differences in bacterial pathway % mean proportions were assessed with Welch's t-test and significance was taken at $p < 0.05$.

Data availability.

Raw reads were deposited to the Sequence Read Archive (insert project number) and are available on Open Science Framework (https://osf.io/87gsx/). The figures and code present in this study can be found on GitHub (https://github.com/lmillergrp/siegel_et_al_2021).

Results

Microbiome composition

The developing infant rhesus monkey microbiome was measured to be predominantly composed of the phyla *Firmicutes*, *Actinobacteriodota*, *Fusobacteriota*, and *Proteobacteria*. These four phyla accounted for 99% of the detectable microbes in the nasal microbiome. In contrast, the remaining phyla accounted for 1% (Fig. 3.1a). Of the predominant phyla of the upper respiratory microbiome, significant differences in taxa abundance were only observed between antibiotic-treated and control monkeys in *Firmicutes*, *Fusobacteriota*, and *Proteobacteria*. A significant increase in *Firmicutes* abundance was observed at 6-months. When sex was considered it was observed that the difference in *Firmicutes* abundance was primarily driven by males and not females (Fig. 3.7a-3.7c). Antibiotic-treated females demonstrated elevated *Fusobacteriota* at months 0 and 2. Additionally, *Proteobacteria* abundance was elevated on month 4 for antibiotic-treated females (Fig. 3.7i). Lastly, although the phylum *Actinobacteriodota* was the most highly abundant phylum in the nasal microbiome, no significance of early-life antibiotic treatment was observed with or without taking sex into account.

Pulmonary function

Pulmonary function testing was conducted on all animals at 6 months of age. Our results demonstrated a sexually dimorphic reduction in vital compacity, a measure of lung function, in antibiotic-treated males compared to control males. At the same time, no significant difference was observed in females (Fig. 3.1b). We suspected that the respiratory microbiome may have a role in the changes observed in pulmonary function. Thus, the composition of the nasopharyngeal microbiome was assessed using 16S sequencing. Diversity is a standard marker of microbiome health, with changes marking a change in health status (Lloyd-Price et al. 2016, Jackson et al. 2018). We first correlated measures of lung function to both nasal microbiome diversity and bacterial abundance of the nasal microbiome. The only microbe that correlated with pulmonary function was *g_[Eubacterium]_coprostanoligenes_group* (LDA=3.88) (Fig. 3.5d). However, measures of microbiome diversity correlated with multiple measures for pulmonary function, including Total Lung Volume, and Vital and Inspiratory Capacity (Fig. 3.5a-3.5c).

Lefse was used to identify differentially abundant taxa between antibiotic and control animals each month (Segata et al. 2011). To determine if changes in gene expression could be associated with reduced lung function, we then focused on genes related to growth and development (data not shown). Micro-dissected airways from rhesus monkeys were separated into 3 components: proximal, middle-level, and respiratory bronchioles. Next, correlations were conducted to determine whether the microbiome abundance of specific taxa at 6 months of age correlated with lung gene expression. Fibroblast Growth Factor 10 and 7 (FGF10 and FGF7) expression in the proximal airways were 2 of the only genes investigated that showed a prominent relationship between taxa abundance in the upper respiratory tract (Fig. 3.2, Fig. 3.3). Except for *p_Actinobacteriota* (LDA=5.13)

which negatively correlated with FGF10 expression, taxa positively correlated with increasing FGF10 expression included: *c_Clostridia* (LDA=4.75), *f_Eggerthellaceae* (LDA=4.37), *f_Ruminococcaceae* (LDA=4.65), *g_Ruminococcaceae* (LDA=4.65), *g_Slackia* (LDA=4.37), *o_Oscillospirales* (LDA=4.67), *p_Firmicutes* (LDA=4.87) (Fig. 3.2). Of these taxa, *f_Eggerthellaceae*, and *g_Slackia* positively correlated with FGF10 expression in control animals; conversely *c_Clostridia*, *f_Ruminococcaceae*, *g_Ruminococcaceae*, and *p_Firmicutes* positively correlated with the growth factor's expression antibiotic-treated animals. For FGF7 *f_Eggerthelaceae* (LDA=4.37), *f_Ruminococcaceae* (LDA=4.65), *g_Helicobacter* (LDA=4.32), *g_Slackia* (LDA=4.37), *p_Campilobacterota* (LDA=4.32) posively correlated with increasing gene expression. *f_Eggerthellaceae*, *g_Helicobacter*, *g_Slackia*, and *p_Campilobacterota* positively correlated with FGF7 expression control animals while only *f_Ruminococcaceae* positively correlated with FGF7 expression following antibiotic treatment (Fig. 3.3).

Most of our correlations showed the most robust relationships when comparing lung gene expression in the proximal airways to bacteria abundances in the upper respiratory tract. However, the mid-level lung region also demonstrated relationships between gene expression in the lung and bacteria abundance in the upper respiratory tract. We report that *g_[Eubacterium]_coprostanoligenes_group* positively correlated with increasing SFTPA1 expression in antibiotic-treated animals while *o_Coriobacteriales* negatively correlated with MMP16 expression (Fig. 3.6).

Differential abundance

We wanted to see the significantly different taxa abundances between antibiotic-exposed and unexposed infant rhesus monkeys. To accomplish this, LefSe was used to assess the differential abundances of bacteria between treatment groups for each month. In all

months save for months 1 and 6, the upper respiratory microbiome of antibiotic-treated monkeys had more differentially abundant taxa than controls (Fig. 3.4). *c_Clostridia* was enriched in the respiratory microbiome of antibiotic-exposed infants each month, while control animals were consistently enriched for *g_Corynebacterium*, a known commensal of the respiratory microbiome (De Steenhuijsen Piters et al. 2020, Andrade et al. 2022).

Because we have reported sex differences in gut microbiome composition following early-life antibiotic treatment, we also assessed whether sex drove changes in respiratory microbiome abundance. We next compared respiratory microbiomes of antibiotic-treated males to females. Months 1 and 3 only showed enrichment of microbes in the respiratory microbiome of antibiotic females (Supp. Fig. 3.2). Conversely, there was no time-point where antibiotic-exposed males exclusively demonstrated differentially abundant bacteria (Supp. Fig. 3.2). At months 1 and 5, antibiotic-exposed males had significantly more differentially abundant taxa than females. Lastly, months 4 and 6 favored control animals with more differentially abundant taxa than antibiotic-exposed animals during these time points (Supp. Fig 3.1, 3.2).

To better understand how the developing respiratory microbiome differs between males and females at baseline, we next used LefSe to see how the abundances of key taxa differed by sex. At baseline control male monkeys had more differentially abundant taxa than females for months 0, 2, 3, and 4 (Supp. Fig. 3.1). Conversely, females have more significantly enriched microbes at months 1, 5, and 6 (Supp. Fig. 3.1). Surprisingly, no microbes were consistently enriched in the respiratory microbiome of males or females during the 6-month study. This finding supports the transient nature of the respiratory microbiome (Pérez-Cobas et al. 2023).

Bacteria metagenomic function

Since bacteria metabolism bi-products have been documented to alter host physiology (Ma et al. 2022), we also wanted to see if any predicted bacteria products could be driving the lung function changes we observed. Picrust, a tool used to infer bacteria metagenomic function based on 16S sequencing data, was used for each month of the study (Douglas et al. 2020). Tricarboxylic acid cycle (TCA) related pathways such as TCA cycle IV (2-oxoglutarate decarboxylase), incomplete reductive TCA cycle, and reductive TCA cycle 1, were only elevated in control animals during the first 2 months (Fig. 3.8a-3.8c). Conversely, for antibiotic-treated animals in months 5 and 6 TCA cycle I (prokaryotic), TCA cycle V (2-oxoglutarate:ferredoxin oxidoreductase), TCA cycle VIII (Helicobacter), and TCA cycle VII (acetate-producers) (Fig. 3.8f, 3.8g) were elevated. Additionally, antibiotic-treated animals had more enriched metagenomic pathways than control animals except for months 4 and 6 (Fig. 3.8e, 3.8h).

We then considered the effect of sex on bacteria metagenomic function in the upper respiratory microbiome. Upon faceting by sex, it was found that metagenomic function could not be inferred at most time points except for months 0 and 6, suggesting the antibiotic treatment affects bacteria colonization of the upper respiratory tract (Supp. Fig. 3.3). None of the pathways identified when comparing antibiotic-treated males to females were involved in the TCA cycle, further suggesting a marked reduction in microbial function in the respiratory microbiome following antibiotic treatment. Our suspicion was confirmed when assessing the metagenomic function of control animals where function could be inferred at all time points (Supp. Fig. 3.3-3.4). The sex that contained the most enriched pathway expression varied from month to month, and a TCA-related pathway occurred only in control females at month 3 for TCA cycle VIII (Helicobacter) (Supp. Fig. 3.4).

Discussion

Our earlier study defined the healthy rhesus gut microbiome and demonstrated early-life antibiotic treatment's physiological and microbiome effects. In this study, we aimed to characterize the rhesus monkey upper respiratory microbiome at baseline and after early-life antibiotic treatment. Utilizing a rhesus monkey model enabled us to investigate the microbiome and lung changes in a controlled manner while using a highly translatable model of human infant development (Asgharian et al. 2012, Phillips et al. n.d.).

This study defined the composition of the upper respiratory microbiome in healthy infant rhesus monkeys and assessed the impact of early-life antibiotic treatment on lung development. We found that the upper respiratory microbiome of infant rhesus monkeys is sparse in microbial density. The transient nature of this microbial site is clear from the fact that it did not achieve a stable abundance within a 6-month period. Our results indicated the developing upper respiratory microbiome is predominantly composed of the phyla *Actinobacteriota*, which accounted for an average of 75% of the total microbiome for any given sample or time point. The respiratory microbiome also had a substantial proportion of *Firmcutes* and *Proteobacteria*. Together these 3 populations account for 99% of the total microbiome. The most abundant genera were *g_Corynebacterium*, *g_Staphylococcus*, and *g_Streptococcus*. These genera are known commensals of the upper respiratory tract (De Steenhuijsen Piters et al. 2020, Andrade et al. 2022). This study partially concurs with a similar one that characterized the nasopharyngeal microbiota in children aged 18 months. This study found that the nasopharyngeal microbiome was dominated by *Proteobacteria*, *Firmicutes*, *Bacteroidetes*, *Actinobacteria* and *Fusobacteria*, and made note of the high variability between samples. Out of the 5 most dominant taxa in the previous study, 4 were consistent with our results, differing only in the abun-

dance of *Bacteroidetes*, which was absent in our study. This difference could be due to the age of the subjects as the study by Bogaert et al. was conducted on children 18 months of age (Bogaert et al. 2011).

Pulmonary function analysis has been shown to correlate with bacteria abundance in the microbiome(Lee et al. 2019). Indeed, when comparing young and elderly patients, researchers demonstrated that lung function decline, specifically in elderly patients, negatively correlated with *Firmicutes* and *Fusobacteria* abundance, while positively correlating with *Actinobacteria* abundance. Although we did not see a correlation with the same taxa and lung function testing parameters, we did observe a correlation between *g_[Eubacterium]_coprostanoligenes_group*, a member of the *Firmicutes* phylum, abundance, and lung function. This correlation was seen in the vital capacity of the lung, which is a measure of the maximum amount of air a person can expel from the lungs after a maximum inhalation. This result is consistent with previous studies that have shown that *Firmicutes* abundance is negatively correlated with lung function (Takahashi et al. 2018, Albedewi et al. 2022).

Currently, the invasive nature of sampling the lungs makes it difficult to study the lung microbiome in pediatric populations. Furthermore, interrogating the lung transcriptome is also challenging due to the difficulty in obtaining lung tissue samples. Researchers working with human patients will use blood as a substitute for lung tissue when making a connection between the lung microbiome and the host transcriptome. Such techniques supply data that suggest that interactions between RSV and nasopharyngeal microbiota can modulate the host immune response, potentially affecting clinical disease severity (de Steenhuijsen Piters et al. 2016). However, the use of blood as a proxy for lung tissue is not without its limitations. For example, the blood transcriptome is not a direct representation of the lung transcriptome, and the blood microbiome is not a direct

representation of the lung microbiome. Using the non-human primate model, we were able to obtain lung tissue samples from infant rhesus monkeys. With discordance in gene function or expression as a plausible reason behind by reduced vital compacity that was observed in antibiotic-treated males, we assessed the expression of growth and development genes in the lung. We selected genes based on literature searches for those with prominent expression in the lung and with known involvement in lung development and maturation. We then correlated the expression of these genes with the abundance of bacteria in the upper respiratory tract. This was conducted by micro-dissecting the lungs of euthanized rhesus monkeys into 3 components: proximal, mid-level, and respiratory bronchioles. The components are 3 major divisions of the lung including the large airways, the mid-level branches, and respiratory bronchioles where gas exchange occurs. The expression of genes related to growth and development was assessed in each of these regions and we showed that gene expression in different lung regions correlated with the nearby microbiomes. The gene expression of growth and development genes from the proximal airways correlated with the greatest number of taxa abundances. We suspect this is because the proximal airways are physically closer to the nasopharynx than the mid-level or respiratory bronchioles.

Sex differences in the gut microbiome, sparse as they are, have been reported in humans more often than sex differences in the respiratory microbiome (Gomez et al. 2015, Baars et al. 2018, Gao et al. 2019, Zhang et al. 2021). To the best of our knowledge this the first study highlight sex differences in the respiratory microbiome of rhesus macaques. Our data suggest that early-life antibiotic treatment affects the developing microbiome past the juncture when antibiotics are administered. Although we did not see longitudinal effects of antibiotics on the developing microbiome, we report sexually dimorphic changes in the *Firmicutes* abundance at 6 months of age, with control males having increased

abundance (Fig. 3.4b). This result agrees with published literature which asserts that the upper respiratory microbiome is sparse in microbial density and transient (Bogaert et al. 2011, Claassen-Weitz et al. 2020).

Due to the substantial genetic variation associated with non-human primate studies, our study was not without limitations (Vallender and Miller 2013). Outbred animals are more prone to higher variability due to differences in genetic factors for example, MHC genotype significantly influences antibody responses against commensal microbes in the gut, and these responses have been proven to correlate with the establishment of distinct microbial communities (Kubinak et al. 2015). Furthermore, the microbiome is known to be influenced by environmental factors such as diet, and housing conditions (Kuthyar et al. 2022). Although we controlled for these factors in our study, we cannot rule out the possibility that these factors influenced our results. Microbial density is always an issue when dealing with microbiomes of the respiratory tract and our study is no exception. Due to issue issues obtaining enough microbial DNA to sequence at early time points, we were unable to sequence the microbiome of all animals at all time points. Additionally, our sample size was small as most of our treatment groups had a sample size of 5, and the control male group only had a sample size of 3.

FGF10 is the primary morphogen promoting lung branching morphogenesis in mouse models and the absence of Fgf10 or its receptor FGFR2b results in incomplete lung agenesis in mice (Moerlooze et al. 2000). Similarly, FGF7, along with FGF10 important for patterning and growth of the lung bud in early pulmonary development (Lebeche et al. 1999). Although we looked at various lung growth and development genes, only FGF7 and FGF10 demonstrated significant correlations with the microbiome. This result does not prove that the reduced vital compacity observed in antibiotic-treated male infants was caused by changes in FGF expression in response to changes in the microbiome.

A more thorough study needs to be conducted to understand the effects of antibiotic treatment on FGF expression, and changes in their expression could result in reduced lung function.

The tricarboxylic acid (TCA) cycle is a series of chemical reactions used by all aerobic organisms to release stored energy through the oxidation of acetyl-CoA derived from carbohydrates, fats, and proteins into carbon dioxide and chemical energy in the form of adenosine triphosphate (ATP). TCA cycle intermediates have been observed to correlate with host cardiometabolic risk factors among underweight, normal-weight, and overweight adults in the gut microbiome [wanOverweightUnderweightStatus2020]. Furthermore, TCA cycle intermediates are altered in the gut microbiome of patients with inflammatory bowel disease (Aldars-García et al. 2021). Detecting TCA cycle pathways in the upper respiratory microbiome suggests the presence of active and functional microbes. However, figuring out their activity in the upper respiratory microbiome is challenging because Picrust infers metagenomic function from 16s sequencing data, even though TCA cycle pathways were enriched in path antibiotic and control animals. Thus, future studies will need to measure the metabolism of the respiratory tract microbiome using techniques such as GC-MS. 16S is suitable for explorative studies where the composition of the microbial site is not well known; however, to obtain a holistic understanding of the microbes present, such as function, whole genome sequencing should be conducted (Sulaiman et al. 2021).

In summary, our study defines the developing rhesus monkey nasal microbiome and assesses the impact of early-life antibiotic treatment in normal lung development. These observations suggest an active upper respiratory microbiome; however, our current study could not confirm whether the nasopharynx microbiomes are alive and functional. Still, our results show an interaction between the microbes of the upper respiratory tract and

lung development and function. Ours is the first study to characterize the developing rhesus monkey nasopharyngeal microbiome in health and after early-life antibiotic treatment.

Acknowledgments

This publication was made possible by an NIEHS-funded diversity supplement awarded to Noah Siegel (P51OD011107). Its contents are solely the responsibility of the authors and do not necessarily represent the official views of the NIEHS or NIH.

Disclosure

The authors have no relevant affiliations or financial involvement with any organization or entity with a financial interest in or financial conflict with the subject matter or materials discussed in the manuscript.

Figures

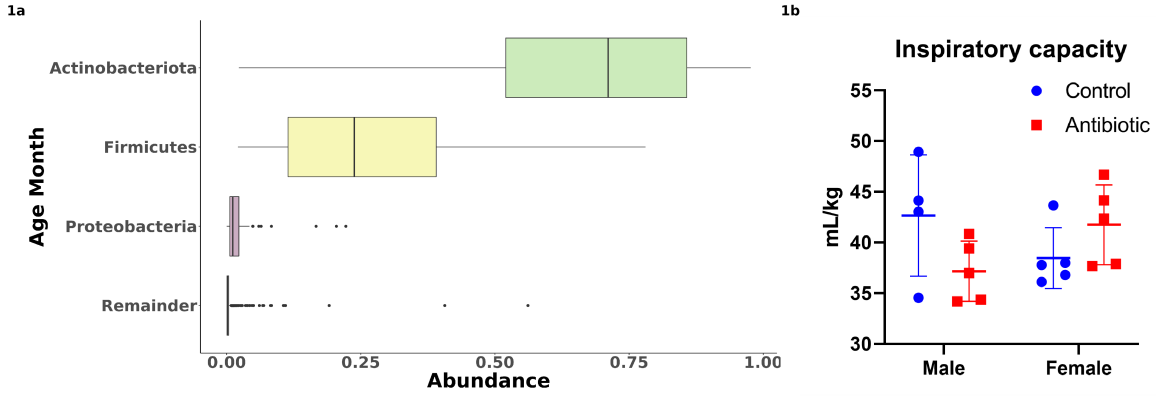

Supplementary Figure 3.1: Nasal microbiome composition and lung function. Percent abundance of all phyla >1% of total reads (Phyla representing <1% of the total reads were binned as "Remainder") (Fig. 1a). Inspiratory capacity for antibiotic-treated and control animals separated by sex (P <0.05) (Fig. 1b).

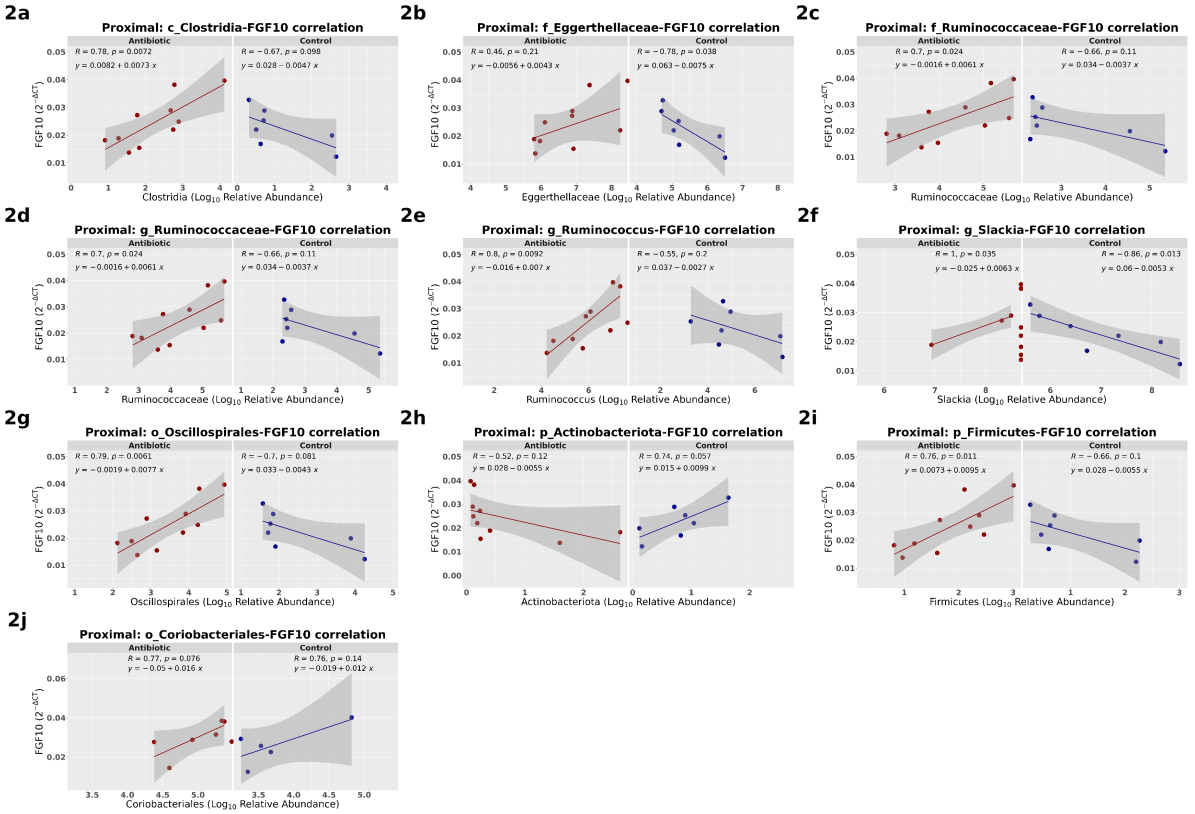

Supplementary Figure 3.2: Proximal lung expression of FGF10 positively correlates with nasal microbiome abundance. Linear correlations were constructed to correlate FGF10 expression to bacteria relative abundance in the nasopharynx.

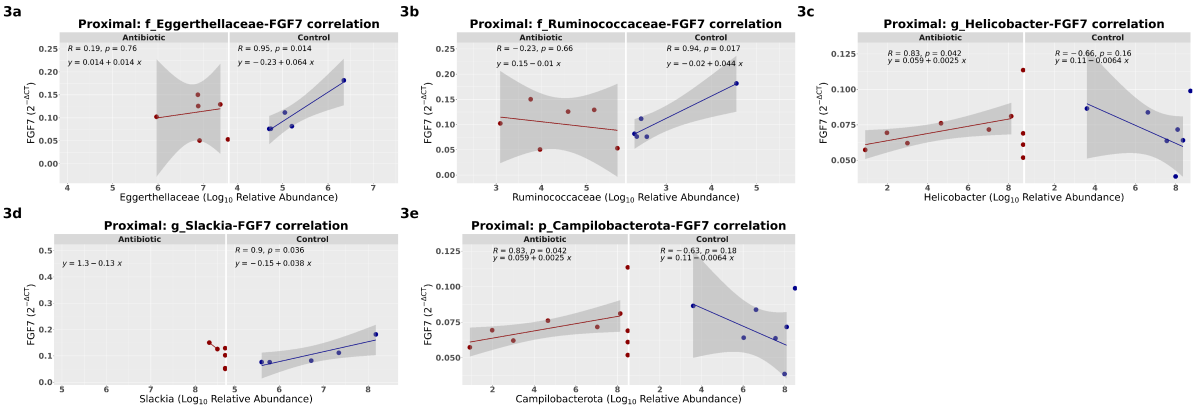

Supplementary Figure 3.3: Proximal lung expression of FGF7 positively correlates with nasal microbiome abundance. Linear correlations were constructed to correlate FGF7 expression to bacteria relative abundance in the nasopharynx.

4a

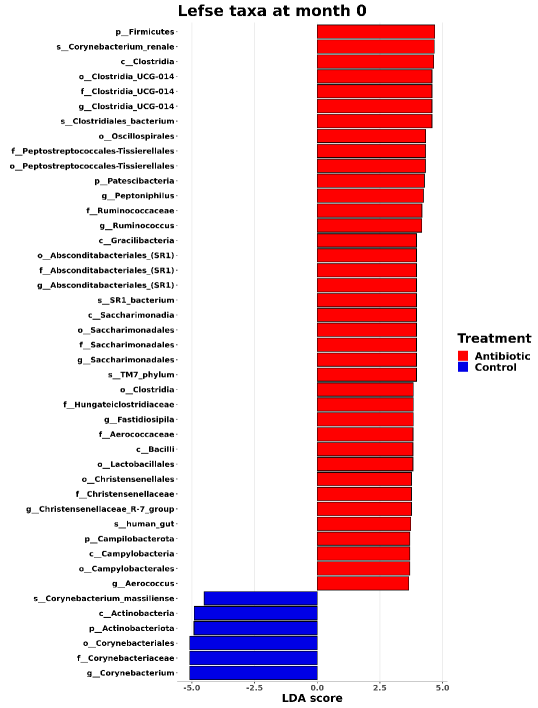
Lefse taxa at month 0
p__Firmicutes
s__Corynebacterium_renale
c__Clostridia
o__Clostridia_UCG-014
f__Clostridia_UCG-014
g__Clostridia_UCG-014
s__Clostridiales_bacterium
o__Oscillospirales
f__Peptostreptococcales-Tissierellales
o__Peptostreptococcales-Tissierellales
p__Patescibacteria
g__Peptoniphilus
f__Ruminococcaceae
g__Ruminococcus
c__Gracilibacteria
o__Absconditabacteriales_(SR1)
f__Absconditabacteriales_(SR1)
g__Absconditabacteriales_(SR1)
s__SR1_bacterium
c__Saccharimonadia
o__Saccharimonadales
f__Saccharimonadales
g__Saccharimonadales
s__TM7_phylum
o__Clostridia
f__Hungateiclostridiaceae
g__Fastidiosipila
f__Aerococcaceae
c__Bacilli
o__Lactobacillales
o__Christensenellales
f__Christensenellaceae
g__Christenseneliaceae_R-7_group
s__human_gut
p__Campilobacterota
c__Campylobacteria
o__Campylobacterales
g__Aerococcus
s__Corynebacterium_massiliense
c__Actinobacteria
p__Actinobacteriota
o__Corynebacteriales
f__Corynebacteriaceae
g__Corynebacterium
-5.0
-2.5
0.0
2.5
5.0
LDA score
Treatment
Antibiotic
Control

4b

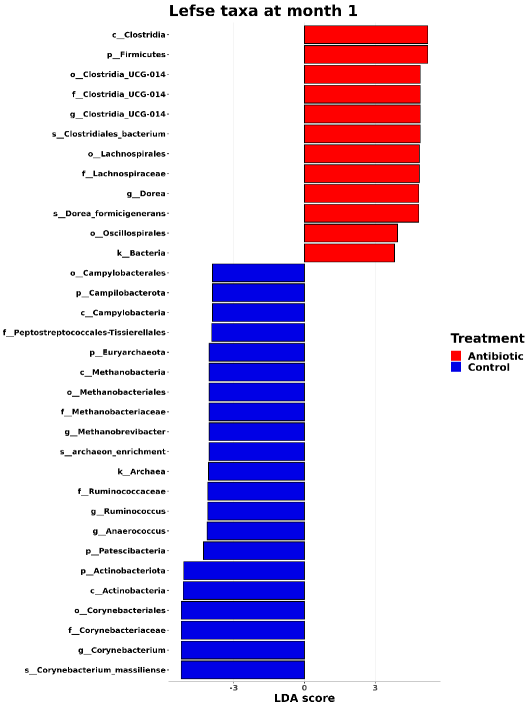
Lefse taxa at month 1
c__Clostridia
p__Firmicutes
o__Clostridia_UCG-014
f__Clostridia_UCG-014
g__Clostridia_UCG-014
s__Clostridiales_bacterium
o__Lachnospirales
f__Lachnospiraceae
g__Dorea
s__Dorea_formicigenerans
o__Oscillospirales
k__Bacteria
o__Campylobacterales
p__Campilobacterota
c__Campylobacteria
f__Peptostreptococcales-Tissierellales
p__Euryarchaeota
c__Methanobacteria
o__Methanobacteriales
f__Methanobacteriaceae
g__Methanobrevibacter
s__archaeon_enrichment
k__Archaea
f__Ruminococcaceae
g__Ruminococcus
g__Anaerococcus
p__Patescibacteria
p__Actinobacteriota
c__Actinobacteria
o__Corynebacteriales
f__Corynebacteriaceae
g__Corynebacterium
s__Corynebacterium_massiliense
-3
0
3
LDA score
Treatment
Antibiotic
Control

4c

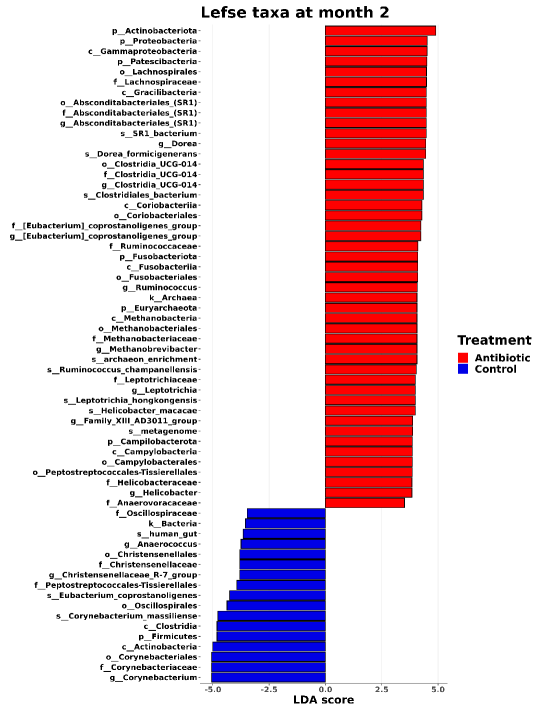
Lefse taxa at month 2
p__Actinobacteriota
p__Proteobacteria
c__Gammaproteobacteria
p__Patescibacteria
o__Lachnospirales
f__Lachnospiraceae
c__Gracilibacteria
o__Absconditabacteriales_(SR1)
f__Absconditabacteriales_(SR1)
g__Absconditabacteriales_(SR1)
s__SR1_bacterium
g__Dorea
s__Dorea_formicigenerans
o__Clostridia_UCG-014
f__Clostridia_UCG-014
g__Clostridia_UCG-014
s__Clostridiales_bacterium
c__Coriobacteriia
o__Coriobacteriales
f__[Eubacterium]_coprostanoligenes_group
g__[Eubacterium]_coprostanoligenes_group
f__Ruminococcaceae
p__Fusobacteriota
c__Fusobacteriia
o__Fusobacteriales
g__Ruminococcus
k__Archaea
p__Euryarchaeota
c__Methanobacteria
o__Methanobacteriales
f__Methanobacteriaceae
g__Methanobrevibacter
s__archaeon_enrichment
s__Ruminococcus_champanellensis
f__Leptotrichiaceae
g__Leptotrichia
s__Leptotrichia_hongkongensis
s__Helicobacter_macacae
g__Family_XIII_AD3011_group
s__metagenome
p__Campilobacterota
c__Campylobacteria
o__Campylobacterales
o__Peptostreptococcales-Tissierellales
f__Helicobacteraceae
g__Helicobacter
f__Anaerovoracaceae
f__Oscillospiraceae
k__Bacteria
s__human_gut
g__Anaerococcus
o__Christensenellales
f__Christensenellaceae
g__Christensenellaceae_R-7_group
f__Peptostreptococcales-Tissierellales
s__Eubacterium_coprostanoligenes
o__Oscillospirales
s__Corynebacterium_massiliense
c__Clostridia
p__Firmicutes
c__Actinobacteria
o__Corynebacteriales
f__Corynebacteriaceae
g__Corynebacterium
-5.0
-2.5
0.0
2.5
5.0
LDA score
Treatment
Antibiotic
Control

4d

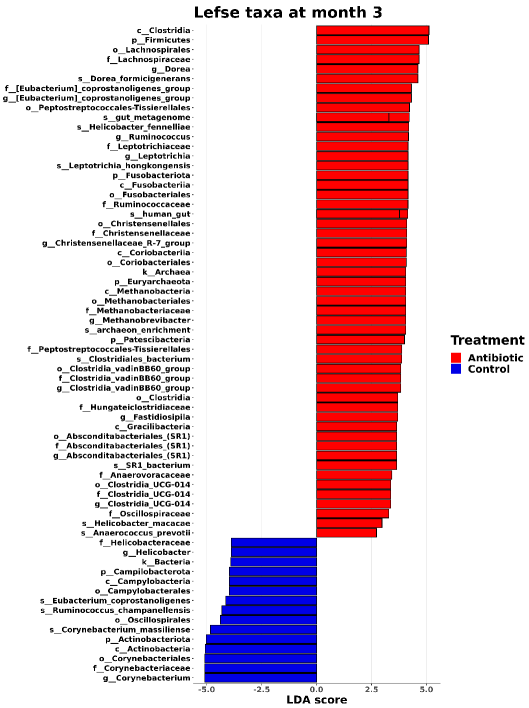
Lefse taxa at month 3
c__Clostridia
p__Firmicutes
o__Lachnospirales
f__Lachnospiraceae
g__Dorea
s__Dorea_formicigenerans
f__[Eubacterium]_coprostanoligenes_group
g__[Eubacterium]_coprostanoligenes_group
o__Peptostreptococcales-Tissierellales
s__gut_metagenome
s__Helicobacter_fennelliae
g__Ruminococcus
f__Leptotrichiaceae
g__Leptotrichia
s__Leptotrichia_hongkongensis
p__Fusobacteriota
c__Fusobacteriia
o__Fusobacteriales
f__Ruminococcaceae
s__human_gut
o__Christensenellales
f__Christensenellaceae
g__Christensenellaceae_R-7_group
c__Coriobacteriia
o__Coriobacteriales
k__Archaea
p__Euryarchaeota
c__Methanobacteria
o__Methanobacteriales
f__Methanobacteriaceae
g__Methanobrevibacter
s__archaeon_enrichment
p__Patescibacteria
f__Peptostreptococcales-Tissierellales
s__Clostridiales_bacterium
o__Clostridia_vadinBB60_group
f__Clostridia_vadinBB60_group
g__Clostridia_vadinBB60_group
o__Clostridia
f__Hungateiclostridiaceae
g__Fastidiosipila
c__Gracilibacteria
o__Absconditabacteriales_(SR1)
f__Absconditabacteriales_(SR1)
g__Absconditabacteriales_(SR1)
s__SR1_bacterium
f__Anaerovoracaceae
o__Clostridia_UCG-014
f__Clostridia_UCG-014
g__Clostridia_UCG-014
f__Oscillospiraceae
s__Helicobacter_macacae
s__Anaerococcus_prevotii
f__Helicobacteraceae
g__Helicobacter
k__Bacteria
p__Campilobacterota
c__Campylobacteria
o__Campylobacterales
s__Eubacterium_coprostanoligenes
s__Ruminococcus_champanellensis
o__Oscillospirales
s__Corynebacterium_massiliense
p__Actinobacteriota
c__Actinobacteria
o__Corynebacteriales
f__Corynebacteriaceae
g__Corynebacterium
-5.0
-2.5
0.0
2.5
5.0
LDA score
Treatment
Antibiotic
Control

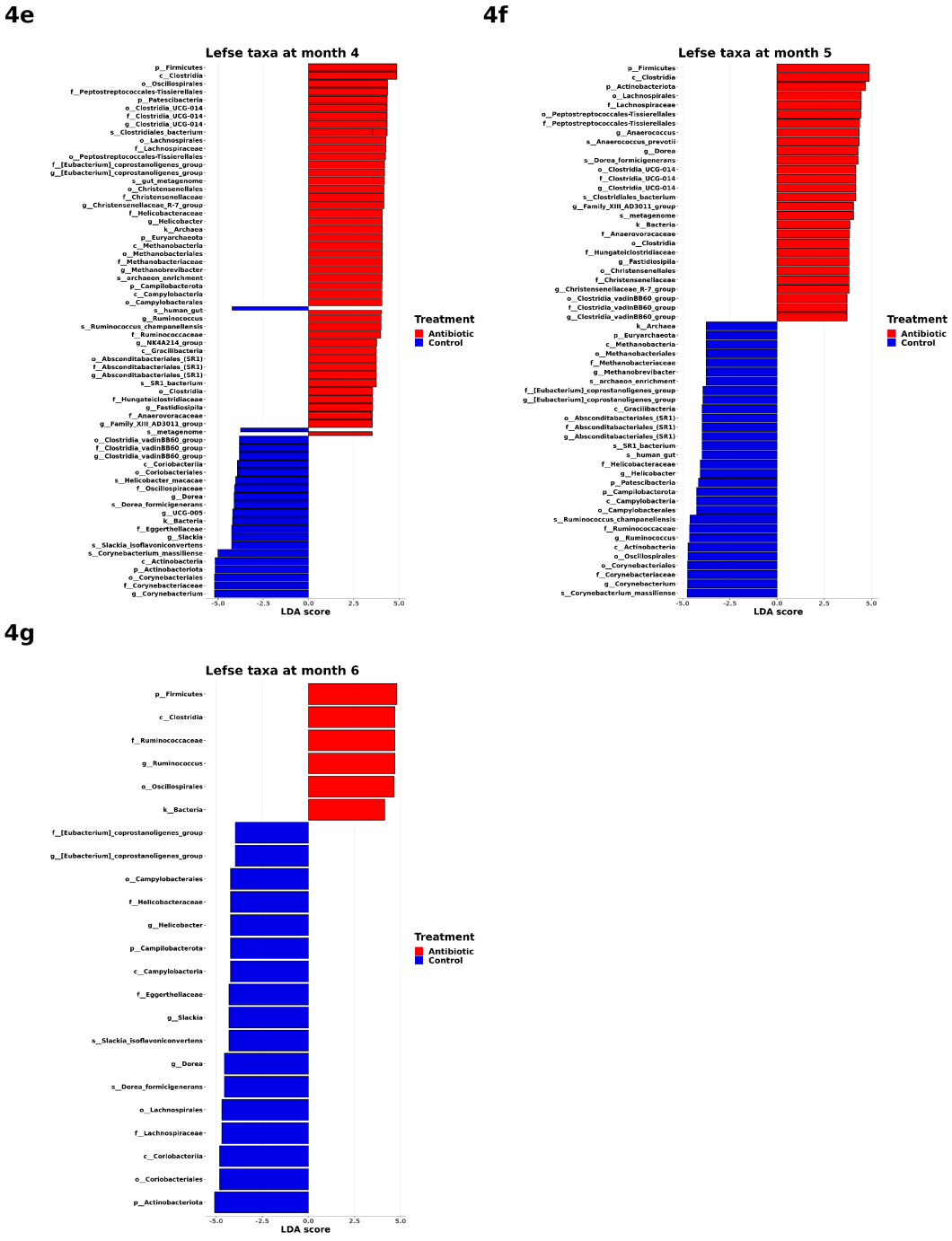

Supplementary Figure 3.4: Early-life antibiotic treatment alters bacteria relative abundance. Differential abundance was assessed using LEfSe to determine how different the microbiome of antibiotic-exposed and unexposed infants. Lefse was done for each month compared antibiotic-treated (red) and control (blue) at month 0 (4a), month 1 (4b), month 2 (4c), month 3 (4d), month 4 (4e), month 5, (4f), month 6 (4g).

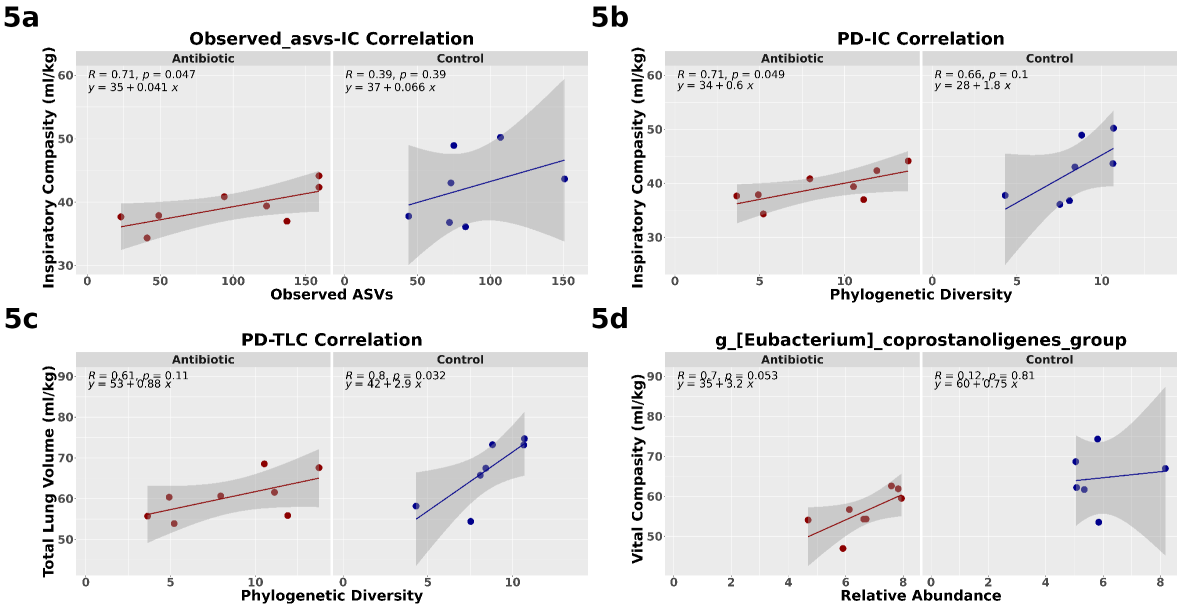

Supplementary Figure 3.5: Lung function correlates with alpha diversity and bacteria relative abundance. Linear correlations were constructed to relate lung function to alpha diversity and bacteria abundance.

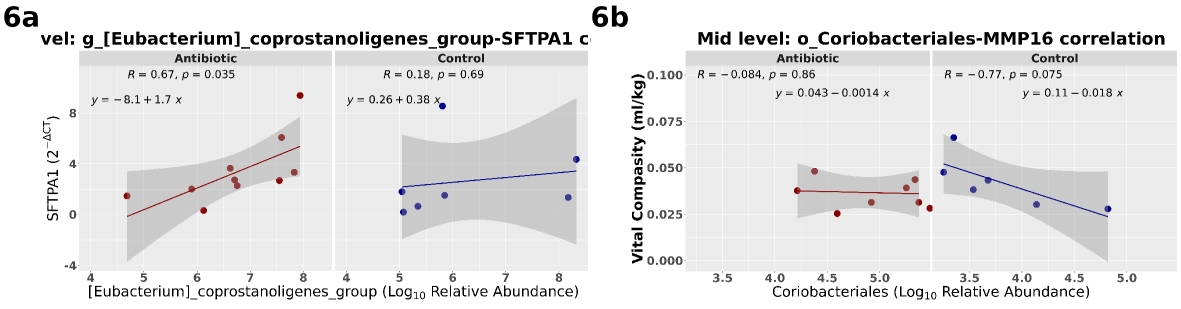

Supplementary Figure 3.6: Mid-level lung gene expression and lung function correlate with bacteria relative abundance. Linear correlations were made between bacteria abundance and lung function or lung gene expression.

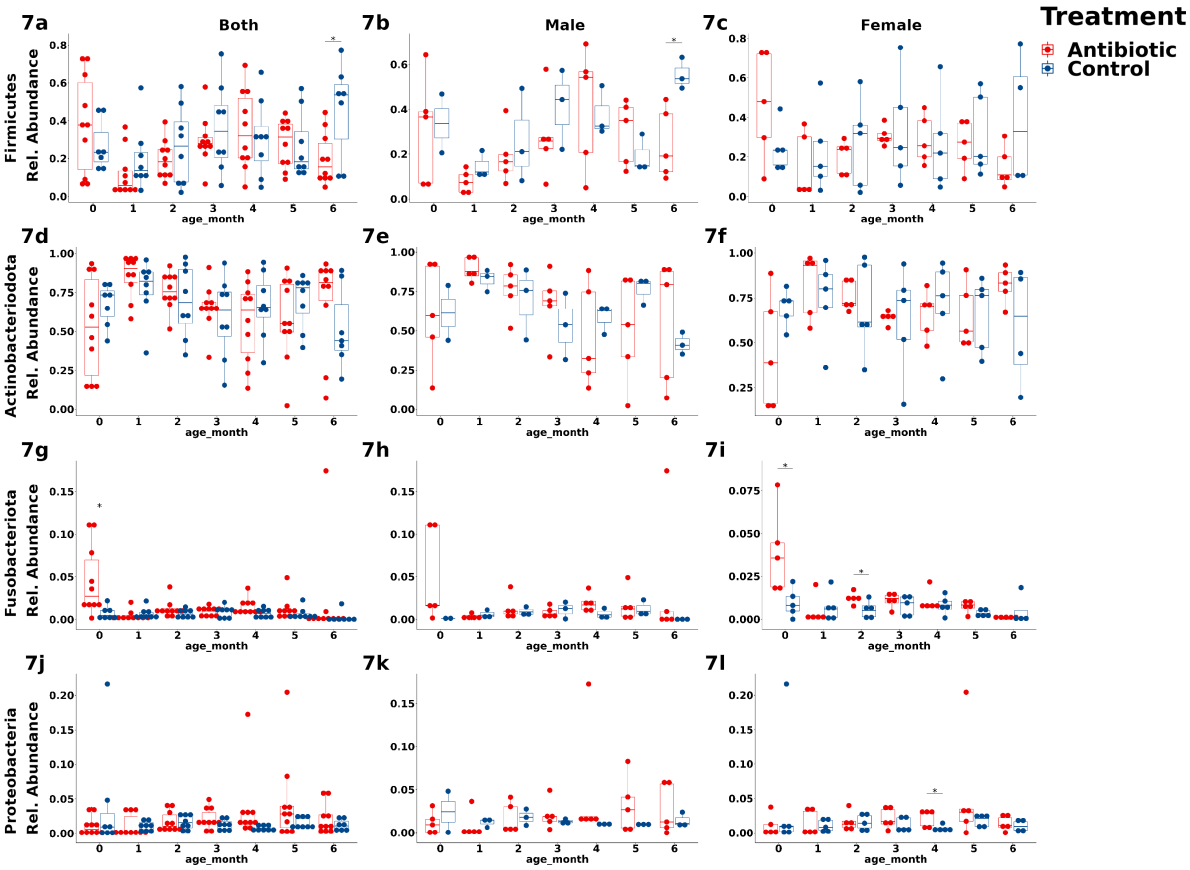

Supplementary Figure 3.7: Early-life antibiotic exposure has transient on the composition of the infant rhesus microbiome. Prominent changes are observed in males (Fig. 7a, 7e, 7h, 7k) relative to females (Fig. 7c, 7f, 7i, 7l). Abundance trajectories of *Firmicutes* (Fig. 7a, 7b, 7c), *Actinobacteriodota* (Fig. 7d, 7e, 7f), *Actinobacteria* (Fig. 7g, 7h, 7i) and *Proteobacteria* (Fig. 7j, 7k, 7l) were measured as the relative abundnace. ($P < 0.05$) by ANOVA with paired samples t-test and Bonferroni correction. *, ($P < 0.05$)

8a

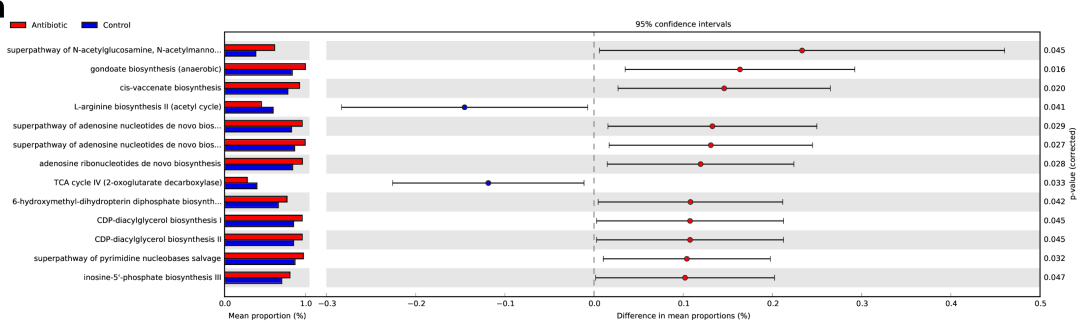
Antibiotic
Control
95% confidence intervals
superpathway of N-acetylglucosamine, N-acetylmanno...
gondoate biosynthesis (anaerobic)
cis-vaccenate biosynthesis
L-arginine biosynthesis II (acetyl cycle)
superpathway of adenosine nucleotides de novo bios...
superpathway of adenosine nucleotides de novo bios...
adenosine ribonucleotides de novo biosynthesis
TCA cycle IV (2-oxoglutarate decarboxylase)
6-hydroxymethyl-dihydropterin diphosphate biosynth...
CDP-diacylglycerol biosynthesis I
CDP-diacylglycerol biosynthesis II
superpathway of pyrimidine nucleobases salvage
inosine-5'-phosphate biosynthesis III
0.045
0.016
0.020
0.041
0.029
0.027
0.028
0.033
0.042
0.045
0.045
0.032
0.047
p-value (corrected)
Mean proportion (%)
Difference in mean proportions (%)

8b

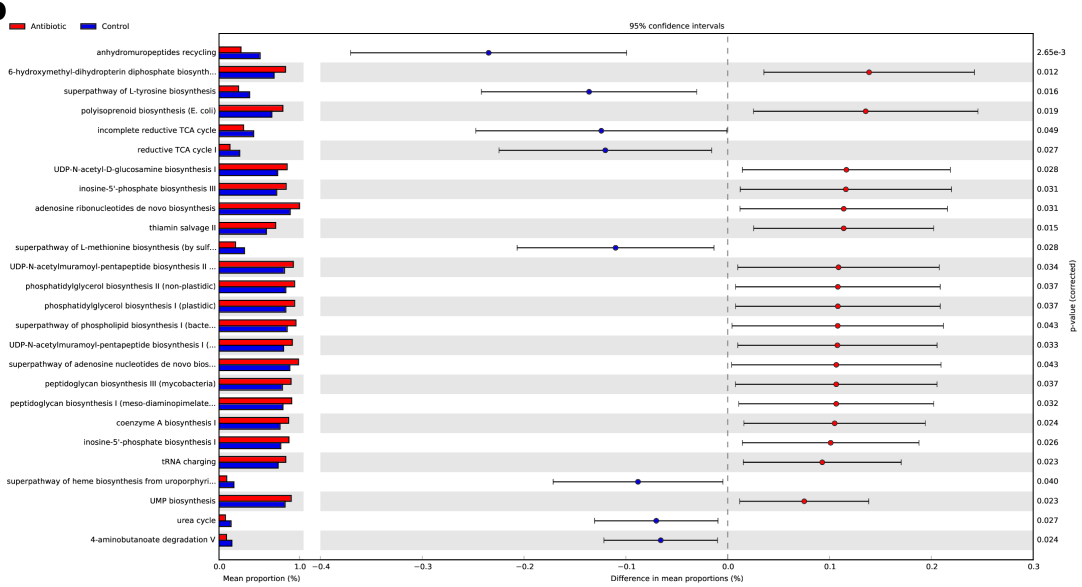
Antibiotic
Control
95% confidence intervals
anhydromuropeptides recycling
6-hydroxymethyl-dihydropterin diphosphate biosynth...
superpathway of L-tyrosine biosynthesis
polyisoprenoid biosynthesis (E. coli)
incomplete reductive TCA cycle
reductive TCA cycle I
UDP-N-acetyl-D-glucosamine biosynthesis I
inosine-5'-phosphate biosynthesis III
adenosine ribonucleotides de novo biosynthesis
thiamin salvage II
superpathway of L-methionine biosynthesis (by sulf...
UDP-N-acetylmuramoyl-pentapeptide biosynthesis II ...
phosphatidylglycerol biosynthesis II (non-plastidic)
phosphatidylglycerol biosynthesis I (plastidic)
superpathway of phospholipid biosynthesis I (bacte...
UDP-N-acetylmuramoyl-pentapeptide biosynthesis I (...
superpathway of adenosine nucleotides de novo bios...
peptidoglycan biosynthesis III (mycobacteria)
peptidoglycan biosynthesis I (meso-diaminopimelate...
coenzyme A biosynthesis I
inosine-5'-phosphate biosynthesis I
tRNA charging
superpathway of heme biosynthesis from uroporphyri...
UMP biosynthesis
urea cycle
4-aminobutanoate degradation V
2.65e-3
0.012
0.016
0.019
0.049
0.027
0.028
0.031
0.031
0.015
0.028
0.034
0.037
0.037
0.043
0.033
0.043
0.037
0.032
0.024
0.026
0.023
0.040
0.023
0.027
0.024
p-value (corrected)
Mean proportion (%)
Difference in mean proportions (%)

8c

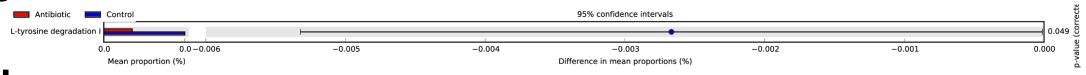
Antibiotic
Control
95% confidence intervals
L-tyrosine degradation I
0.049
p-value (correcte
Mean proportion (%)
Difference in mean proportions (%)

8d

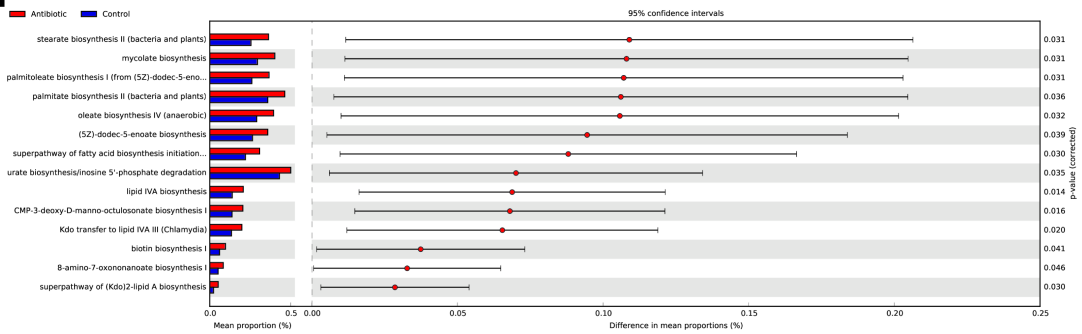
Antibiotic
Control
95% confidence intervals
stearate biosynthesis II (bacteria and plants)
mycolate biosynthesis
palmitoleate biosynthesis I (from (5Z)-dodec-5-eno...
palmitate biosynthesis II (bacteria and plants)
oleate biosynthesis IV (anaerobic)
(5Z)-dodec-5-enoate biosynthesis
superpathway of fatty acid biosynthesis initiation...
urate biosynthesis/inosine 5'-phosphate degradation
lipid IVA biosynthesis
CMP-3-deoxy-D-manno-octulosonate biosynthesis I
Kdo transfer to lipid IVA III (Chlamydia)
biotin biosynthesis I
8-amino-7-oxononanoate biosynthesis I
superpathway of (Kdo)2-lipid A biosynthesis
0.031
0.031
0.031
0.036
0.032
0.039
0.030
0.035
0.014
0.016
0.020
0.041
0.046
0.030
p-value (corrected)
Mean proportion (%)
Difference in mean proportions (%)

8e

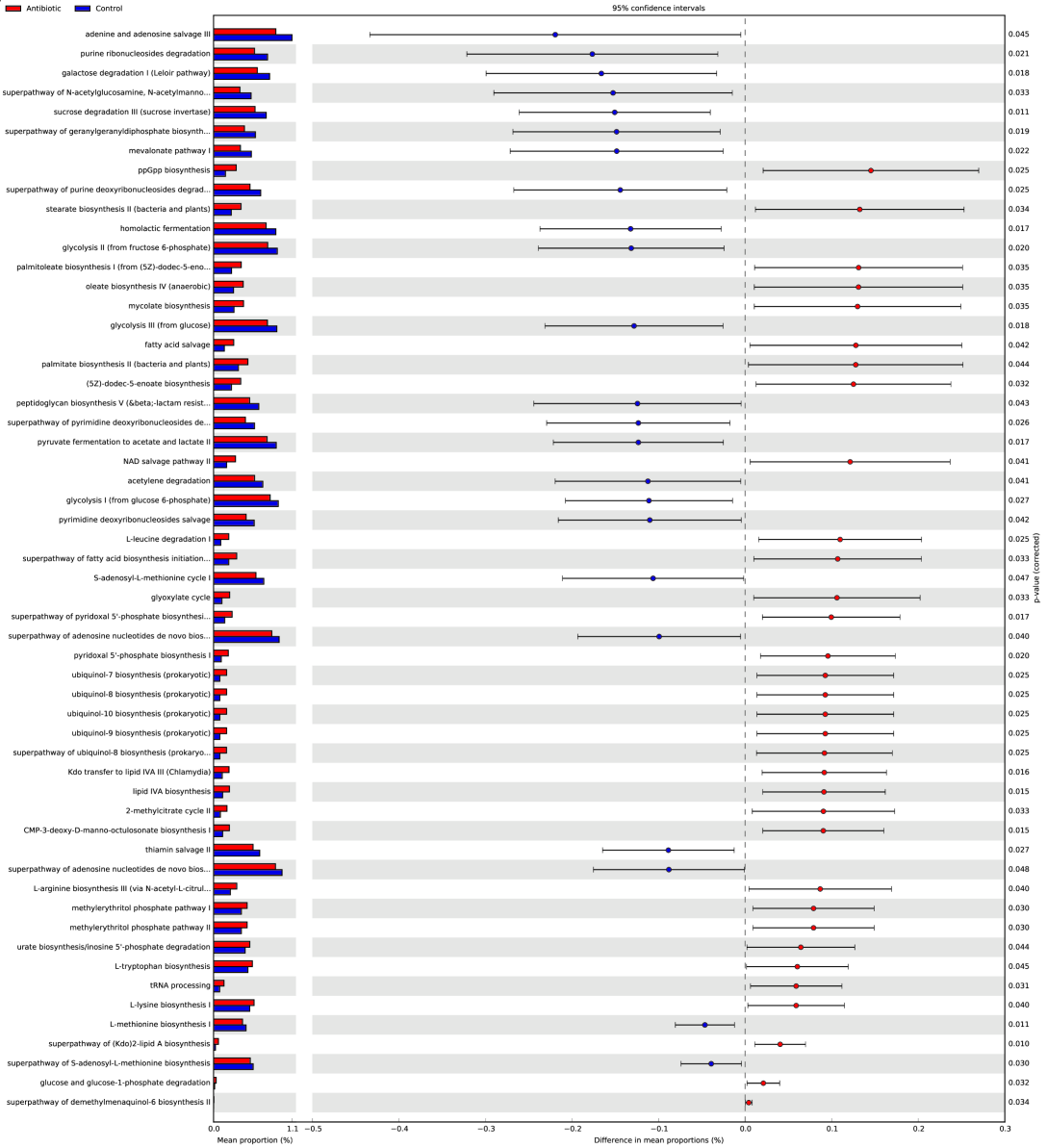
Antibiotic
Control
95% confidence intervals
adenine and adenosine salvage III
purine ribonucleosides degradation
galactose degradation I (Leloir pathway)
superpathway of N-acetylglucosamine, N-acetylmanno...
sucrose degradation III (sucrose invertase)
superpathway of geranylgeranyldiphosphate biosynth...
mevalonate pathway I
ppGpp biosynthesis
superpathway of purine deoxyribonucleosides degrad...
stearate biosynthesis II (bacteria and plants)
homolactic fermentation
glycolysis II (from fructose 6-phosphate)
palmitoleate biosynthesis I (from (5Z)-dodec-5-eno...
oleate biosynthesis IV (anaerobic)
mycolate biosynthesis
glycolysis III (from glucose)
fatty acid salvage
palmitate biosynthesis II (bacteria and plants)
(5Z)-dodec-5-enoate biosynthesis
peptidoglycan biosynthesis V (β-lactam resist...
superpathway of pyrimidine deoxyribonucleosides de...
pyruvate fermentation to acetate and lactate II
NAD salvage pathway II
acetylene degradation
glycolysis I (from glucose 6-phosphate)
pyrimidine deoxyribonucleosides salvage
L-leucine degradation I
superpathway of fatty acid biosynthesis initiation...
S-adenosyl-L-methionine cycle I
glyoxylate cycle
superpathway of pyridoxal 5'-phosphate biosynthesi...
superpathway of adenosine nucleotides de novo bios...
pyridoxal 5'-phosphate biosynthesis I
ubiquinol-7 biosynthesis (prokaryotic)
ubiquinol-8 biosynthesis (prokaryotic)
ubiquinol-10 biosynthesis (prokaryotic)
ubiquinol-9 biosynthesis (prokaryotic)
superpathway of ubiquinol-8 biosynthesis (prokaryo...
Kdo transfer to lipid IVA III (Chlamydia)
lipid IVA biosynthesis
2-methylcitrate cycle II
CMP-3-deoxy-D-manno-octulosonate biosynthesis I
thiamin salvage II
superpathway of adenosine nucleotides de novo bios...
L-arginine biosynthesis III (via N-acetyl-L-citrul...
methylerythritol phosphate pathway I
methylerythritol phosphate pathway II
urate biosynthesis/inosine 5'-phosphate degradation
L-tryptophan biosynthesis
tRNA processing
L-lysine biosynthesis I
L-methionine biosynthesis I
superpathway of (Kdo)2-lipid A biosynthesis
superpathway of S-adenosyl-L-methionine biosynthesis
glucose and glucose-1-phosphate degradation
superpathway of demethylmenaquinol-6 biosynthesis II
0.045
0.021
0.018
0.033
0.011
0.019
0.022
0.025
0.025
0.034
0.017
0.020
0.035
0.035
0.035
0.018
0.042
0.044
0.032
0.043
0.026
0.017
0.041
0.041
0.027
0.042
0.025
0.033
0.047
0.033
0.017
0.040
0.020
0.025
0.025
0.025
0.025
0.025
0.016
0.015
0.033
0.015
0.027
0.048
0.040
0.030
0.030
0.044
0.045
0.031
0.040
0.011
0.010
0.030
0.032
0.034
p-value (corrected)
0.0
1.1
−0.5
−0.4
−0.3
−0.2
−0.1
0.0
0.1
0.2
0.3
Mean proportion (%)
Difference in mean proportions (%)

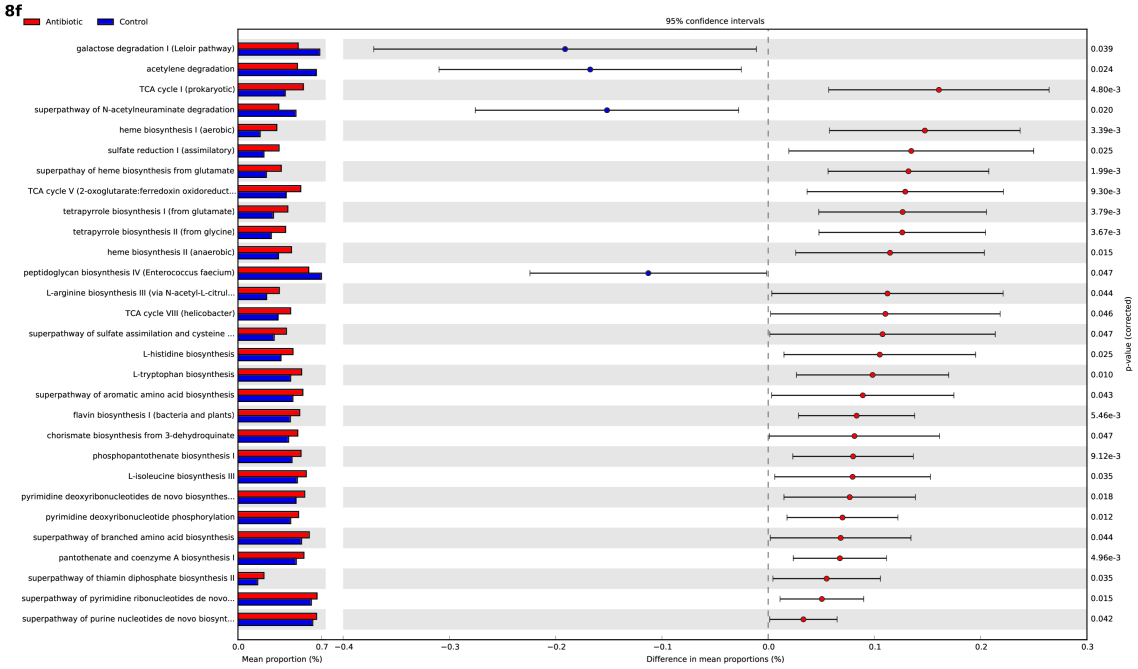
8f
Antibiotic
Control
95% confidence intervals
galactose degradation I (Leloir pathway)
acetylene degradation
TCA cycle I (prokaryotic)
superpathway of N-acetylneuraminate degradation
heme biosynthesis I (aerobic)
sulfate reduction I (assimilatory)
superpathay of heme biosynthesis from glutamate
TCA cycle V (2-oxoglutarate:ferredoxin oxidoreduct...
tetrapyrrole biosynthesis I (from glutamate)
tetrapyrrole biosynthesis II (from glycine)
heme biosynthesis II (anaerobic)
peptidoglycan biosynthesis IV (Enterococcus faecium)
L-arginine biosynthesis III (via N-acetyl-L-citrul...
TCA cycle VIII (helicobacter)
superpathway of sulfate assimilation and cysteine ...
L-histidine biosynthesis
L-tryptophan biosynthesis
superpathway of aromatic amino acid biosynthesis
flavin biosynthesis I (bacteria and plants)
chorismate biosynthesis from 3-dehydroquinate
phosphopantothenate biosynthesis I
L-isoleucine biosynthesis III
pyrimidine deoxyribonucleotides de novo biosynthes...
pyrimidine deoxyribonucleotide phosphorylation
superpathway of branched amino acid biosynthesis
pantothenate and coenzyme A biosynthesis I
superpathway of thiamin diphosphate biosynthesis II
superpathway of pyrimidine ribonucleotides de novo...
superpathway of purine nucleotides de novo biosynt...
0.039
0.024
4.80e-3
0.020
3.39e-3
0.025
1.99e-3
9.30e-3
3.79e-3
3.67e-3
0.015
0.047
0.044
0.046
0.047
0.025
0.010
0.043
5.46e-3
0.047
9.12e-3
0.035
0.018
0.012
0.044
4.96e-3
0.035
0.015
0.042
p-value (corrected)
0.0
0.7
Mean proportion (%)
−0.4
−0.3
−0.2
−0.1
0.0
0.1
0.2
0.3
Difference in mean proportions (%)

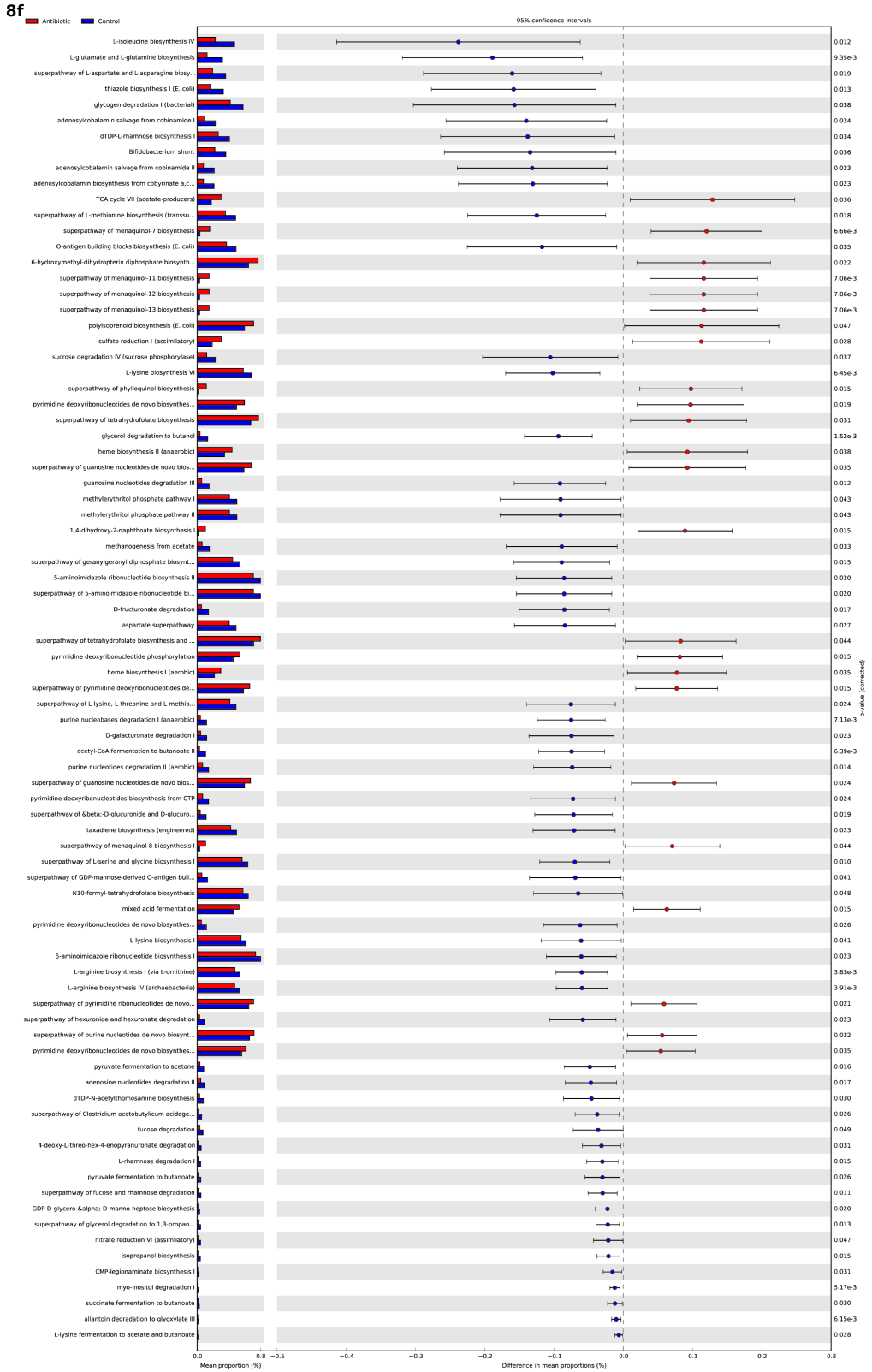
8f
Antibiotic
Control
95% confidence intervals
L-isoleucine biosynthesis IV
L-glutamate and L-glutamine biosynthesis
superpathway of L-aspartate and L-asparagine biosy...
thiazole biosynthesis I (E. coli)
glycogen degradation I (bacterial)
adenosylcobalamin salvage from cobinamide I
dTDP-L-rhamnose biosynthesis I
Bifidobacterium shunt
adenosylcobalamin salvage from cobinamide II
adenosylcobalamin biosynthesis from cobyrinate a,c...
TCA cycle VII (acetate-producers)
superpathway of L-methionine biosynthesis (transsu...
superpathway of menaquinol-7 biosynthesis
O-antigen building blocks biosynthesis (E. coli)
6-hydroxymethyl-dihydropterin diphosphate biosynth...
superpathway of menaquinol-11 biosynthesis
superpathway of menaquinol-12 biosynthesis
superpathway of menaquinol-13 biosynthesis
polyisoprenoid biosynthesis (E. coli)
sulfate reduction I (assimilatory)
sucrose degradation IV (sucrose phosphorylase)
L-lysine biosynthesis VI
superpathway of phylloquinol biosynthesis
pyrimidine deoxyribonucleotides de novo biosynthes...
superpathway of tetrahydrofolate biosynthesis
glycerol degradation to butanol
heme biosynthesis II (anaerobic)
superpathway of guanosine nucleotides de novo bios...
guanosine nucleotides degradation III
methylerythritol phosphate pathway I
methylerythritol phosphate pathway II
1,4-dihydroxy-2-naphthoate biosynthesis I
methanogenesis from acetate
superpathway of geranylgeranyl diphosphate biosynt...
5-aminoimidazole ribonucleotide biosynthesis II
superpathway of 5-aminoimidazole ribonucleotide bi...
D-fructuronate degradation
aspartate superpathway
superpathway of tetrahydrofolate biosynthesis and ...
pyrimidine deoxyribonucleotide phosphorylation
heme biosynthesis I (aerobic)
superpathway of pyrimidine deoxyribonucleotides de...
superpathway of L-lysine, L-threonine and L-methio...
purine nucleobases degradation I (anaerobic)
D-galacturonate degradation I
acetyl-CoA fermentation to butanoate II
purine nucleotides degradation II (aerobic)
superpathway of guanosine nucleotides de novo bios...
pyrimidine deoxyribonucleotides biosynthesis from CTP
superpathway of β-D-glucuronide and D-glucuro...
taxadiene biosynthesis (engineered)
superpathway of menaquinol-8 biosynthesis I
superpathway of L-serine and glycine biosynthesis I
superpathway of GDP-mannose-derived O-antigen buil...
N10-formyl-tetrahydrofolate biosynthesis
mixed acid fermentation
pyrimidine deoxyribonucleotides de novo biosynthes...
L-lysine biosynthesis I
5-aminoimidazole ribonucleotide biosynthesis I
L-arginine biosynthesis I (via L-ornithine)
L-arginine biosynthesis IV (archaebacteria)
superpathway of pyrimidine ribonucleotides de novo...
superpathway of hexuronide and hexuronate degradation
superpathway of purine nucleotides de novo biosynt...
pyrimidine deoxyribonucleotides de novo biosynthes...
pyruvate fermentation to acetone
adenosine nucleotides degradation II
dTDP-N-acetylthomosamine biosynthesis
superpathway of Clostridium acetobutylicum acidoge...
fucose degradation
4-deoxy-L-threo-hex-4-enopyranuronate degradation
L-rhamnose degradation I
pyruvate fermentation to butanoate
superpathway of fucose and rhamnose degradation
GDP-D-glycero-α-D-manno-heptose biosynthesis
superpathway of glycerol degradation to 1,3-propan...
nitrate reduction VI (assimilatory)
isopropanol biosynthesis
CMP-legionaminate biosynthesis I
myo-inositol degradation I
succinate fermentation to butanoate
allantoin degradation to glyoxylate III
L-lysine fermentation to acetate and butanoate
0.012
9.35e-3
0.019
0.013
0.038
0.024
0.034
0.036
0.023
0.023
0.036
0.018
6.66e-3
0.035
0.022
7.06e-3
7.06e-3
7.06e-3
0.047
0.028
0.037
6.45e-3
0.015
0.019
0.031
1.52e-3
0.038
0.035
0.012
0.043
0.043
0.015
0.033
0.015
0.020
0.020
0.017
0.027
0.044
0.015
0.035
0.015
0.024
7.13e-3
0.023
6.39e-3
0.014
0.024
0.024
0.019
0.023
0.044
0.010
0.041
0.048
0.015
0.026
0.041
0.023
3.83e-3
3.91e-3
0.021
0.023
0.032
0.035
0.016
0.017
0.030
0.026
0.049
0.031
0.015
0.026
0.011
0.020
0.013
0.047
0.015
0.031
5.17e-3
0.030
6.15e-3
0.028
p-value (corrected)
0.0
0.8
−0.5
−0.4
−0.3
−0.2
−0.1
0.0
0.1
0.2
0.3
Mean proportion (%)
Difference in mean proportions (%)

Supplementary Figure 3.8: Metagenomic pathways are altered with early-life antibiotic treatment. Kegg biomarkers significantly different between antibiotic-treated (red) and control (blue) infants at month 0 (8a), month 1 (8b), month 2 (8c), month 3 (8d), month 4 (8e), month 5, (8f), month 6 (8g).

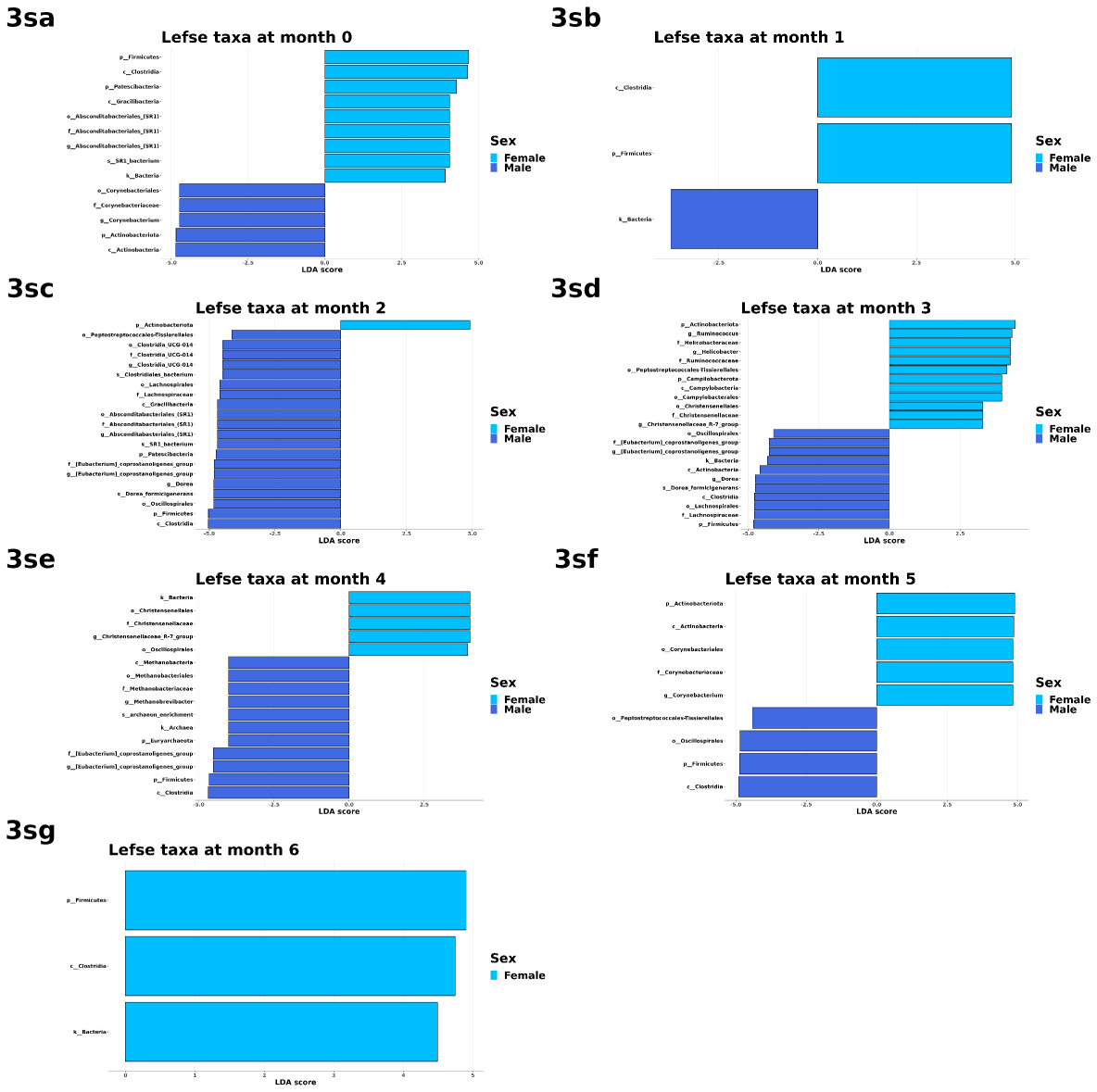

Supplementary Figure 3.1: Baseline sex differences in bacteria relative abundance. Differential abundance was assessed using LEfSe to determine how different the microbiome of antibiotic-exposed and unexposed infants. Lefse was done for each month compared to control male (dark blue) and control (teal) at month 0 (3a), month 1 (3b), month 2 (3c), month 3 (3d), month 4 (3e), month 5, (3f), month 6 (3g).

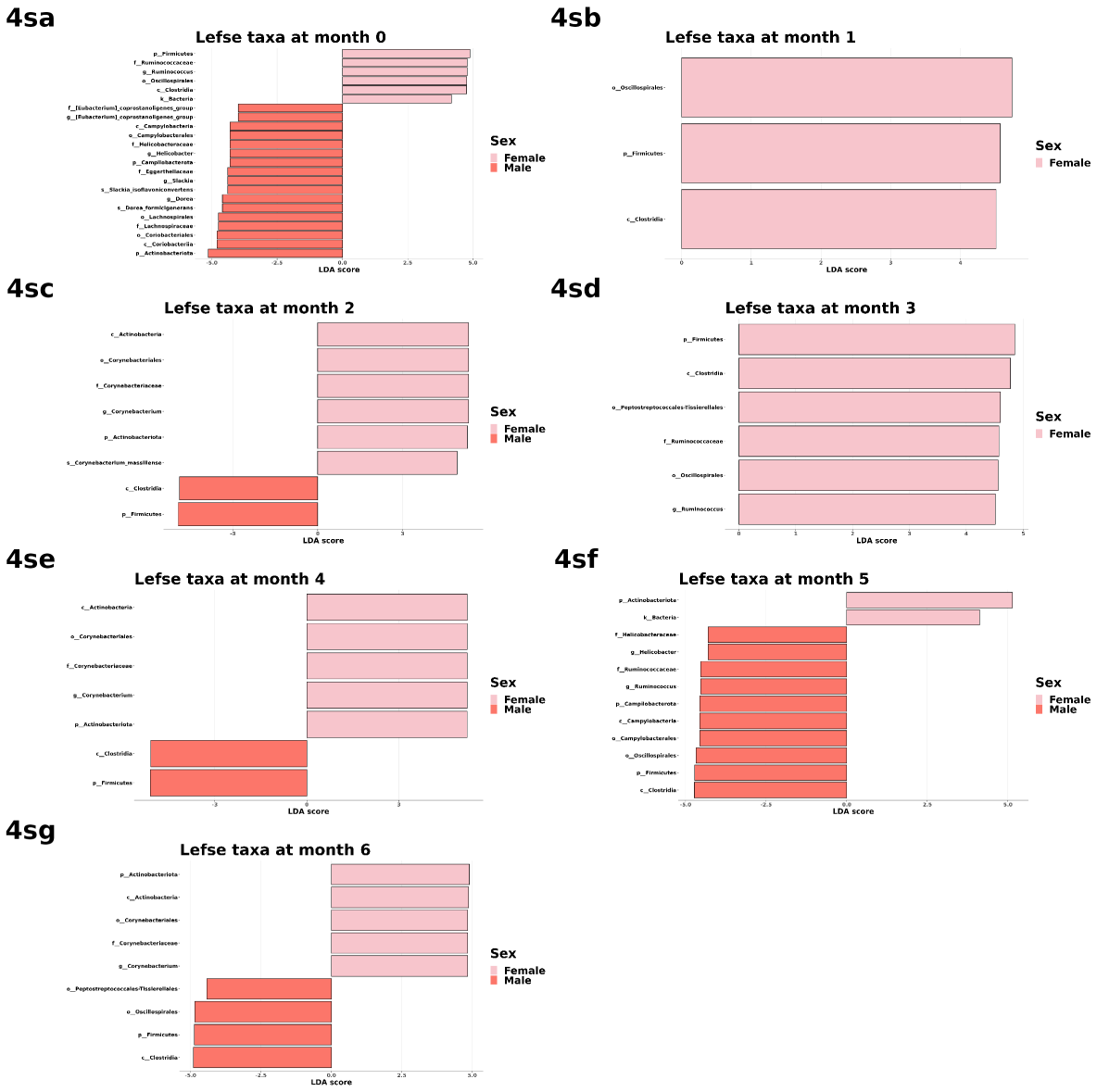

Supplementary Figure 3.2: Sex differences following early-life antibiotic treatment on bacteria relative abundance. Differential abundance was assessed using LEfSe to determine how different the microbiome of antibiotic-exposed and unexposed infants. Lefse was done for each month compared antibiotic-treated male (orange) and control (pink) at month 0 (4a), month 1 (4b), month 2 (4c), month 3 (4d), month 4 (4e), month 5, (4f), month 6 (4g).

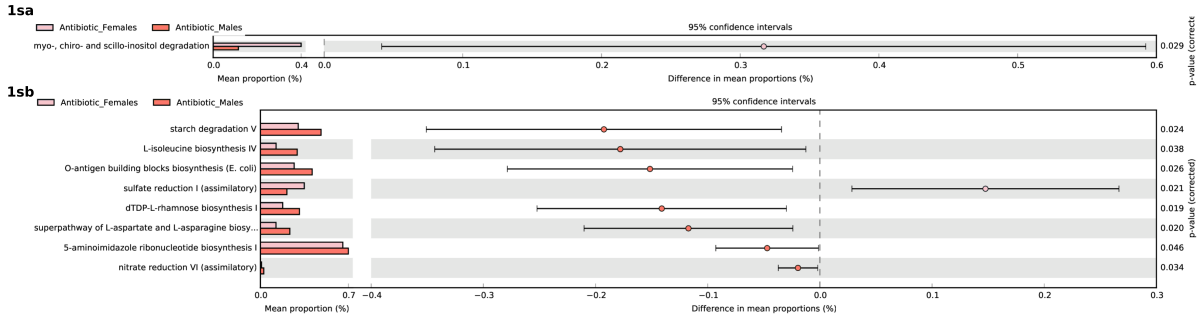

Supplementary Figure 3.3: Metagenomic pathways are altered with early-life antibiotic treatment. Kegg biomarkers significantly different between antibiotic-treated male (orange) and female (pink) infants at month 0 (2a) and month 6 (2g).

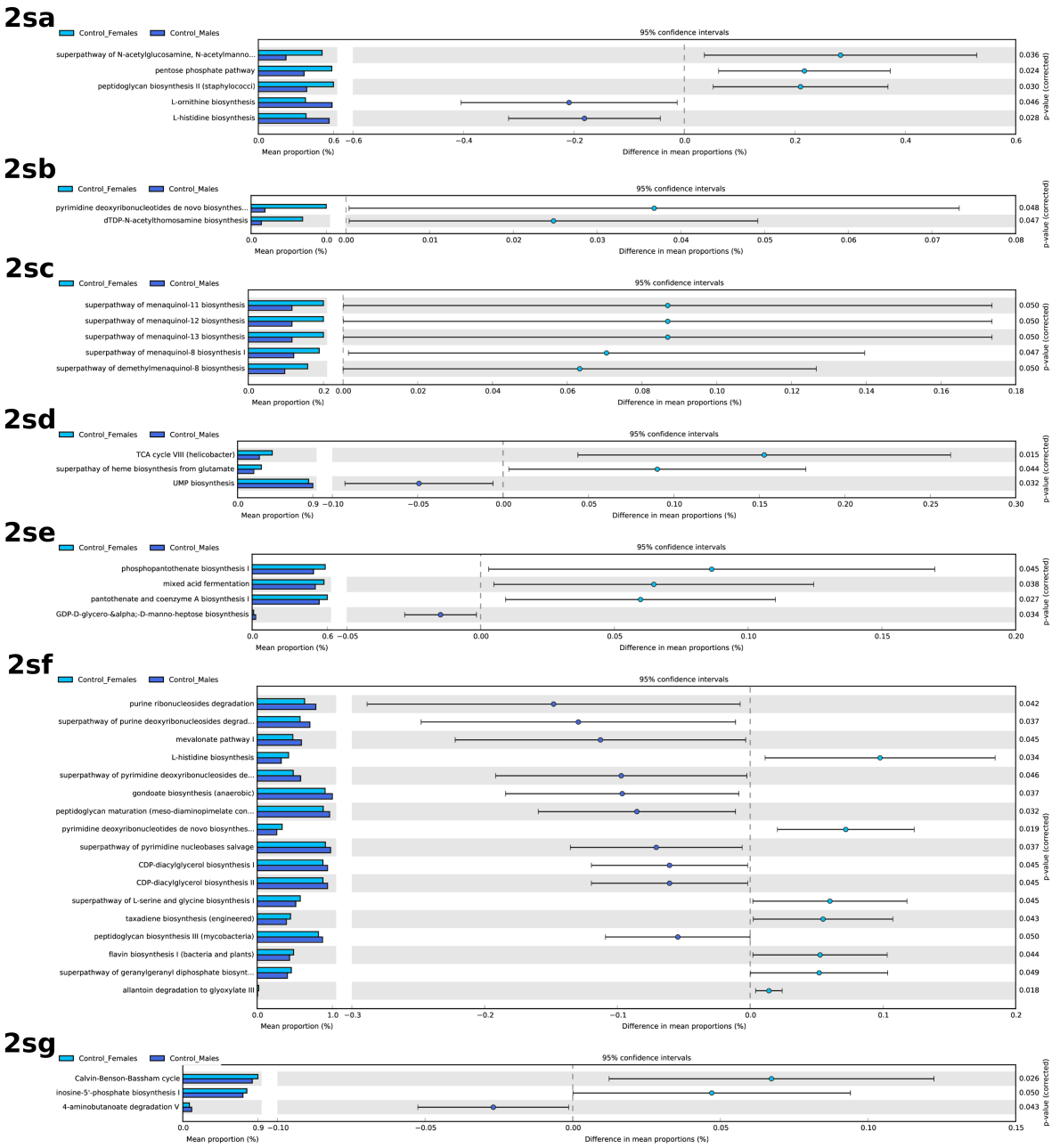

Supplementary Figure 3.4: Metagenomic pathways are altered with early-life antibiotic treatment. Kegg biomarkers significantly different between control male (dark blue) and female (teal) infants at month 0 (2a), month 1 (2b), month 2 (2c), month 3 (2d), month 4 (2e), month 5, (2f), month 6 (2g).

Conclusion

> There is no real ending. It's just the place where you stop the story.
>
> Frank Herbert

The use of culture-independent techniques to understand the microbiome has come a long way since it was first introduced in the 1980s. The development of high-throughput sequencing technologies has enabled researchers to study the microbiome in various contexts, including the human microbiome. The human microbiome is a complex ecosystem that is shaped by a variety of factors, including host genetics, diet, and environment. The microbiome plays a critical role in human health and disease, and understanding the factors that shape the microbiome is essential for developing novel therapeutics.

We first explored the current field of microbiome research, acknowledging the contribution of sex on its development and function. What is known about the gut and respiratory microbiomes was introduced, as well as how that information was ascertained, such as the models used to understand the microbiome. Murine models give us flexibility in understanding the microbiome, but they are not without their limitations. The use of non-human primates, such as the rhesus macaque, allows us to better understand the microbiome in a model that is more similar to humans. However, studies on the rhesus microbiome are sparse in comparison to murine models. Therefore, the primary goal of

this project was to better understand the developing rhesus monkey microbiome and how it is impacted by early-life antibiotic exposure.

As the use of antibiotics continues to remain prevalent, it is important to understand the impact they have on the developing microbiome. This dissertation has explored the development of the gut, lung, and upper respiratory microbiome in rhesus macaques. In utilizing the rhesus monkey model, we can better understand how perturbations of my microbiome in early translate to humans. The second chapter explored the effects of early-life antibiotic exposure on the gut microbiome.

The third chapter explored the effects of early-life antibiotic exposure on the lung microbiome. It is now evident that the lung microbiome is not sterile and that it plays a critical role in lung health and disease. The lung microbiome is shaped by a variety of factors, including the gut microbiome. This is due to the gut-lung axis, a bi-directional form of communication between the gut microbiome and the lung. The lower lung microbiome is also shaped by the upper respiratory microbiome. The upper respiratory microbiome is the first point of contact for microbes entering the lung.

The field of microbiome research is still in its infancy. There is still much to be learned about the microbiome and how it impacts human health and disease. The use of non-human primate models, such as the rhesus macaque, will continue to be an important tool in understanding the microbiome. The use of non-human primate models will allow us to better understand the microbiome in a model that is more similar to humans. Using non-human primate models also allows us to better understand the impact of early-life antibiotic exposure on the microbiome.

This dissertation primarily uses 16S amplicon sequencing to inter microbial populations based on slight variations in the 16S rRNA gene. However, 16S amplicon sequencing is limited in its ability to identify microbes at the species level. The use of shotgun

metagenomic sequencing will allow us to better understand the microbiome at the species level. Shotgun metagenomic sequencing will also allow us to better understand the functional capacity of the microbiome. Shotgun metagenomic sequencing can provide insight into early-life antibiotic exposure effects on the microbiome. Additionally, the use of shotgun metagenomic sequencing will allow us to better understand the impact of early-life antibiotic exposure on the functional capacity of the microbiome.

Exploring the potential ramifications of a respiratory virus infection in infants who have previously been administered antibiotics represents an alternative avenue for this research project. The concept of early life commensal colonization is new, but it is becoming increasingly evident that it plays a critical role in immune development.

Colophon

This document is set in EB Garamond, Source Code Pro and Lato. The body text is set at 11pt with cmr.

It was written in R Markdown and LaTeX, and rendered into PDF using aggiedown and bookdown.

This document was typeset using the XeTeX typesetting system, and the University of California Thesis class. Under the hood, the elements of the document formatting source code have been taken from the Latex, Knitr, and RMarkdown templates for UC Berkeley's graduate thesis, and Dissertate: a LaTeX dissertation template to support the production and typesetting of a PhD dissertation at Harvard, Princeton, and NYU

The source files for this thesis, along with all the data files, have been organised into a Github repository, 2023-disseration, which is available at `https://github.com/nasiegel88/2023-dissertation`. A hard copy of the thesis can be found in the University of California, Davis library.

This version of the thesis was generated on 2023-11-30 01:37:38. The repository is currently at this commit:

```
[c5b8f2d] 2023-11-30: test revview
```

The computational environment that was used to generate this version is as follows:

```
- Session info
   ---------------------------------------------------------------
 setting value
 version R version 4.0.5 (2021-03-31)
 os Ubuntu 20.04.6 LTS
 system x86_64, linux-gnu
 ui X11
 language (EN)
 collate C.UTF-8
 ctype C.UTF-8
 tz Etc/UTC
 date 2023-11-30
 pandoc 2.19.2 @ /home/runner/micromamba/envs/environment/bin/ (via
    rmarkdown)

- Packages
   -------------------------------------------------------------------
 package * version date (UTC) lib source
 aggiedown 1.0 2023-11-30 [1] Github (ryanpeek/aggiedown@ae99300)
 bookdown 0.29 2022-09-12 [1] CRAN (R 4.0.5)
 cachem 1.0.6 2021-08-19 [1] CRAN (R 4.0.5)
 callr 3.7.2 2022-08-22 [1] CRAN (R 4.0.5)
 cli 3.4.1 2022-09-23 [1] CRAN (R 4.0.5)
 colorspace 2.0-3 2022-02-21 [1] CRAN (R 4.0.5)
 crayon 1.5.1 2022-03-26 [1] CRAN (R 4.0.5)
```

```
devtools 2.4.4 2022-07-20 [1] CRAN (R 4.0.5)
digest 0.6.29 2021-12-01 [1] CRAN (R 4.0.5)
dplyr 1.0.10 2022-09-01 [1] CRAN (R 4.0.5)
ellipsis 0.3.2 2021-04-29 [1] CRAN (R 4.0.3)
evaluate 0.16 2022-08-09 [1] CRAN (R 4.0.5)
fansi 1.0.3 2022-03-24 [1] CRAN (R 4.0.5)
fastmap 1.1.0 2021-01-25 [1] CRAN (R 4.0.3)
fs 1.5.2 2021-12-08 [1] CRAN (R 4.0.5)
generics 0.1.3 2022-07-05 [1] CRAN (R 4.0.5)
ggplot2 3.3.6 2022-05-03 [1] CRAN (R 4.0.5)
git2r * 0.27.1 2020-05-03 [1] CRAN (R 4.0.0)
glue 1.6.2 2022-02-24 [1] CRAN (R 4.0.5)
gtable 0.3.1 2022-09-01 [1] CRAN (R 4.0.5)
htmltools 0.5.3 2022-07-18 [1] CRAN (R 4.0.5)
htmlwidgets 1.5.4 2021-09-08 [1] CRAN (R 4.0.5)
httpuv 1.6.6 2022-09-08 [1] CRAN (R 4.0.5)
knitr * 1.40 2022-08-24 [1] CRAN (R 4.0.5)
later 1.2.0 2021-04-23 [1] CRAN (R 4.0.3)
lifecycle 1.0.4 2023-11-07 [1] CRAN (R 4.0.5)
magrittr 2.0.3 2022-03-30 [1] CRAN (R 4.0.5)
memoise 2.0.1 2021-11-26 [1] CRAN (R 4.0.5)
mime 0.12 2021-09-28 [1] CRAN (R 4.0.5)
miniUI 0.1.1.1 2018-05-18 [1] CRAN (R 4.0.5)
munsell 0.5.0 2018-06-12 [1] CRAN (R 4.0.5)
pillar 1.8.1 2022-08-19 [1] CRAN (R 4.0.5)
```

```
pkgbuild 1.3.1 2021-12-20 [1] CRAN (R 4.0.5)
pkgconfig 2.0.3 2019-09-22 [1] CRAN (R 4.0.5)
pkgload 1.3.0 2022-06-27 [1] CRAN (R 4.0.5)
prettyunits 1.1.1 2020-01-24 [1] CRAN (R 4.0.5)
processx 3.7.0 2022-07-07 [1] CRAN (R 4.0.5)
profvis 0.3.7 2020-11-02 [1] CRAN (R 4.0.3)
promises 1.2.0.1 2021-02-11 [1] CRAN (R 4.0.3)
ps 1.7.1 2022-06-18 [1] CRAN (R 4.0.5)
purrr 0.3.4 2020-04-17 [1] CRAN (R 4.0.3)
R6 2.5.1 2021-08-19 [1] CRAN (R 4.0.5)
Rcpp 1.0.9 2022-07-08 [1] CRAN (R 4.0.5)
remotes 2.4.2 2021-11-30 [1] CRAN (R 4.0.5)
rlang 1.1.2 2023-11-04 [1] CRAN (R 4.0.5)
rmarkdown 2.16 2022-08-24 [1] CRAN (R 4.0.5)
rstudioapi 0.14 2022-08-22 [1] CRAN (R 4.0.5)
scales 1.2.1 2022-08-20 [1] CRAN (R 4.0.5)
sessioninfo 1.2.2 2021-12-06 [1] CRAN (R 4.0.5)
shiny 1.7.2 2022-07-19 [1] CRAN (R 4.0.5)
stringi 1.7.8 2022-07-11 [1] CRAN (R 4.0.5)
stringr 1.4.1 2022-08-20 [1] CRAN (R 4.0.5)
tibble 3.1.8 2022-07-22 [1] CRAN (R 4.0.5)
tidyselect 1.1.2 2022-02-21 [1] CRAN (R 4.0.5)
urlchecker 1.0.1 2021-11-30 [1] CRAN (R 4.0.5)
usethis 2.1.6 2022-05-25 [1] CRAN (R 4.0.5)
utf8 1.2.2 2021-07-24 [1] CRAN (R 4.0.5)
```

```
vctrs 0.6.4 2023-10-12 [1] CRAN (R 4.0.5)

xfun 0.33 2022-09-12 [1] CRAN (R 4.0.5)

xtable 1.8-4 2019-04-21 [1] CRAN (R 4.0.5)

yaml 2.3.5 2022-02-21 [1] CRAN (R 4.0.5)


[1] /home/runner/micromamba/envs/environment/lib/R/library
```

References

10 Adami, A. J., S. J. Bracken, L. A. Guernsey, E. Rafti, K. R. Maas, J. Graf, A. P. Matson, R. S. Thrall, and C. M. Schramm. 2018. Early-Life Antibiotics Attenuate Regulatory T Cell Generation and Increase the Severity of Murine House Dust Mite-Induced Asthma. Pediatric research 84:426–434.

Adriansjach, J., S. T. Baum, E. J. Lefkowitz, W. J. Van Der Pol, T. W. Buford, and R. J. Colman. 2020. Age-Related Differences in the Gut Microbiome of Rhesus Macaques. The Journals of Gerontology Series A: Biological Sciences and Medical Sciences 75:1293–1298.

Albedewi, H., I. Bindayel, A. Albarrag, and H. Banjar. 2022. Correlation of Gut Microbiota, Vitamin D Status, and Pulmonary Function Tests in Children With Cystic Fibrosis. Frontiers in Nutrition 9:884104.

Aldars-García, L., J. P. Gisbert, and M. Chaparro. 2021. Metabolomics Insights into Inflammatory Bowel Disease: A Comprehensive Review. Pharmaceuticals 14:1190.

Anahtar, M. N., E. H. Byrne, K. E. Doherty, B. A. Bowman, H. S. Yamamoto, M. Soumillon, N. Padavattan, N. Ismail, A. Moodley, M. E. Sabatini, M. S. Ghebremichael, C. Nusbaum, C. Huttenhower, H. W. Virgin, T. Ndung'u, K. L. Dong, B. D. Walker, R. N. Fichorova, and D. S. Kwon. 2015. Cervicovaginal Bacteria

Are a Major Modulator of Host Inflammatory Responses in the Female Genital Tract. Immunity 42:965–976.

Andrade, B. G. N., R. R. C. Cuadrat, F. R. Tonetti, H. Kitazawa, and J. Villena. 2022. The role of respiratory microbiota in the protection against viral diseases: Respiratory commensal bacteria as next-generation probiotics for COVID-19. Bioscience of Microbiota, Food and Health 41:94–102.

Asgharian, B., O. Price, G. McClellan, R. Corley, D. R. Einstein, R. E. Jacob, J. Harkema, S. A. Carey, E. Schelegle, D. Hyde, J. S. Kimbell, and F. J. Miller. 2012. Development of a rhesus monkey lung geometry model and application to particle deposition in comparison to humans. Inhalation Toxicology 24:869–899.

Axelrad, J. E., O. Olén, J. Askling, B. Lebwohl, H. Khalili, M. C. Sachs, and J. F. Ludvigsson. 2019. Gastrointestinal Infection Increases Odds of Inflammatory Bowel Disease in a Nationwide Case–Control Study. Clinical Gastroenterology and Hepatology 17:1311–1322.e7.

Baars, A., A. Oosting, M. Lohuis, M. Koehorst, S. El Aidy, F. Hugenholtz, H. Smidt, M. Mischke, M. V. Boekschoten, H. J. Verkade, J. Garssen, E. M. van der Beek, J. Knol, P. de Vos, J. van Bergenhenegouwen, and F. Fransen. 2018. Sex differences in lipid metabolism are affected by presence of the gut microbiota. Scientific Reports 8:13426.

Bailey, L. C., C. B. Forrest, P. Zhang, T. M. Richards, A. Livshits, and P. A. DeRusso. 2014. Association of antibiotics in infancy with early childhood obesity. JAMA Pediatrics 168:1063–1069.

Bassis, C. M., J. R. Erb-Downward, R. P. Dickson, C. M. Freeman, T. M. Schmidt, V. B. Young, J. M. Beck, J. L. Curtis, G. B. Huffnagle, and J. Ravel. 2015. Analysis

of the Upper Respiratory Tract Microbiotas as the Source of the Lung and Gastric Microbiotas in Healthy Individuals.

Baughman, R. P., J. E. Thorpe, J. Staneck, M. Rashkin, and P. T. Frame. 1987. Use of the Protected Specimen Brush in Patients with Endotracheal or Tracheostomy Tubes. Chest 91:233–236.

Biagi, E., C. Franceschi, S. Rampelli, M. Severgnini, R. Ostan, S. Turroni, C. Consolandi, S. Quercia, M. Scurti, D. Monti, M. Capri, P. Brigidi, and M. Candela. 2016. Gut Microbiota and Extreme Longevity. Current Biology 26:1480–1485.

Biesbroek, G., E. Tsivtsivadze, E. A. M Sanders, R. Montijn, R. H. Veenhoven, B. J. F Keijser, and D. Bogaert. 2014a. Early Respiratory Microbiota Composition Determines Bacterial Succession Patterns and Respiratory Health in Children. Am J Respir Crit Care Med 190:1283–1292.

Biesbroek, B. AA, W. X, K. BJ, V. RH, S. EA, and B. D. 2014b. The impact of breastfeeding on nasopharyngeal microbial communities in infants. American journal of respiratory and critical care medicine 190:298–308.

Blaser, M. J. 2016. Antibiotic use and its consequences for the normal microbiome. Science 352:544–545.

Bogaert, D., B. Keijser, S. Huse, J. Rossen, and R. Veenhoven. 2011. Variability and Diversity of Nasopharyngeal Microbiota in Children: A Metagenomic Analysis. PLoS ONE 6:17035.

Bokulich, N. A., J. Chung, T. Battaglia, N. Henderson, M. Jay, H. Li, A. D. Lieber, F. Wu, G. I. Perez-Perez, Y. Chen, W. Schweizer, X. Zheng, M. Contreras, M. G. Dominguez-Bello, and M. J. Blaser. 2016. Antibiotics, birth mode, and diet

shape microbiome maturation during early life. Science Translational Medicine 8:343ra82.

Bolnick, D. I., L. K. Snowberg, P. E. Hirsch, C. L. Lauber, E. Org, B. Parks, A. J. Lusis, R. Knight, J. G. Caporaso, and R. Svanbäck. 2014. Individual diet has sex-dependent effects on vertebrate gut microbiota. Nature Communications 5.

Bosch, A. A. T. M., E. Levin, M. A. van Houten, R. Hasrat, G. Kalkman, G. Biesbroek, W. A. A. de Steenhuijsen Piters, P.-K. C. M. de Groot, P. Pernet, B. J. F. Keijser, E. A. M. Sanders, and D. Bogaert. 2016. Development of Upper Respiratory Tract Microbiota in Infancy is Affected by Mode of Delivery. EBioMedicine 9:336–345.

Callahan, B. J., P. J. Mcmurdie, M. J. Rosen, A. W. Han, A. J. A. Johnson, and S. P. Holmes. 2016. Dada2: High-resolution sample inference from illumina amplicon data 13.

Cantey, J. B., P. S. Wozniak, and P. J. Sánchez. 2015. Prospective surveillance of antibiotic use in the neonatal intensive care unit: Results from the SCOUT study. Pediatric Infectious Disease Journal 34:267–272.

Chen, R., L. Wang, T. Koch, V. Curtis, H. Yin-DeClue, S. A. Handley, L. Shan, M. J. Holtzman, M. Castro, and L. Wang. 2020. Sex effects in the association between airway microbiome and asthma. Annals of allergy, asthma & immunology : official publication of the American College of Allergy, Asthma, & Immunology 125:652–657.e3.

Chen, Y.-L., C.-H. Wang, F.-C. Yang, W. Ismail, P.-H. Wang, C.-J. Shih, Y.-C. Wu, and Y.-R. Chiang. 2016. Identification of Comamonas testosteroni as an androgen degrader in sewage. Scientific Reports 6:35386.

References

Cho, I., S. Yamanishi, L. Cox, B. A. Methé, J. Zavadil, K. Li, Z. Gao, D. Mahana, K. Raju, I. Teitler, H. Li, A. V. Alekseyenko, and M. J. Blaser. 2012. Antibiotics in early life alter the murine colonic microbiome and adiposity. Nature 488:621–626.

Claassen-Weitz, S., S. Gardner-Lubbe, K. S. Mwaikono, E. du Toit, H. J. Zar, and M. P. Nicol. 2020. Optimizing 16S rRNA gene profile analysis from low biomass nasopharyngeal and induced sputum specimens. BMC Microbiology 20:113.

Collie, D., L. Glendinning, J. Govan, S. Wright, E. Thornton, P. Tennant, C. Doherty, and G. McLachlan. 2015. Lung Microbiota Changes Associated with Chronic Pseudomonas aeruginosa Lung Infection and the Impact of Intravenous Colistimethate Sodium. PloS One 10:e0142097.

Cong, X., W. Xu, S. Janton, W. A. Henderson, A. Matson, J. M. McGrath, K. Maas, and J. Graf. 2016. Gut microbiome developmental patterns in early life of preterm infants: Impacts of feeding and gender. PLoS ONE 11:1–19.

Cox, L. M., and M. J. Blaser. 2015. Antibiotics in early life and obesity. Nature Reviews Endocrinology 11:182–190.

Cox, L. M., S. Yamanishi, J. Sohn, A. V. Alekseyenko, J. M. Leung, I. Cho, S. G. Kim, H. Li, Z. Gao, D. Mahana, J. G. Zárate Rodriguez, A. B. Rogers, N. Robine, P. Loke, and M. J. Blaser. 2014. Altering the intestinal microbiota during a critical developmental window has lasting metabolic consequences. Cell 158:705–721.

Daly, C. M., J. Saxena, J. Singh, M. R. Bullard, E. O. Bondy, A. Saxena, R. E. Buffalino, M. F. Melville, and L. R. Freeman. 2022. Sex differences in response to a high fat, high sucrose diet in both the gut microbiome and hypothalamic astrocytes and microglia. Nutritional Neuroscience 25:321–335.

de Goffau, M. C., S. Lager, U. Sovio, F. Gaccioli, E. Cook, S. J. Peacock, J. Parkhill, D. S. Charnock-Jones, and G. C. S. Smith. 2019. Human placenta has no microbiome but can contain potential pathogens. Nature 572:329–334.

De Steenhuijsen Piters, W. A. A., J. Binkowska, and D. Bogaert. 2020. Early Life Microbiota and Respiratory Tract Infections. Cell Host & Microbe 28:223–232.

de Steenhuijsen Piters, W. A. A., S. Heinonen, R. Hasrat, E. Bunsow, B. Smith, M.-C. Suarez-Arrabal, D. Chaussabel, D. M. Cohen, E. A. M. Sanders, O. Ramilo, D. Bogaert, and A. Mejias. 2016. Nasopharyngeal Microbiota, Host Transcriptome, and Disease Severity in Children with Respiratory Syncytial Virus Infection. American Journal of Respiratory and Critical Care Medicine 194:1104–1115.

Dickson, R. P., J. R. Erb-Downward, N. R. Falkowski, E. M. Hunter, S. L. Ashley, and G. B. Huffnagle. 2018. The Lung Microbiota of Healthy Mice Are Highly Variable, Cluster by Environment, and Reflect Variation in Baseline Lung Innate Immunity. American Journal of Respiratory and Critical Care Medicine 198:497–508.

Dickson, R. P., J. R. Erb-Downward, C. M. Freeman, L. McCloskey, N. R. Falkowski, G. B. Huffnagle, and J. L. Curtis. 2017. Bacterial topography of the healthy human lower respiratory tract. mBio 8.

Dickson, R. P., F. J. Martinez, and G. B. Huffnagle. 2014. The role of the microbiome in exacerbations of chronic lung diseases. Lancet (London, England) 384:691–702.

DiGiulio, D. B., B. J. Callahan, P. J. McMurdie, E. K. Costello, D. J. Lyell, A. Robaczewska, C. L. Sun, D. S. A. Goltsman, R. J. Wong, G. Shawa, D. K. Stevenson, S. P. Holmes, and D. A. Relman. 2015. Temporal and spatial variation of the human microbiota during pregnancy. Proceedings of the National Academy of Sciences of the United States of America 112:11060–11065.

References

Ding, T., and P. D. Schloss. 2014. Dynamics and associations of microbial community types across the human body. Nature 509:357–360.

Douglas, G. M., V. J. Maffei, J. R. Zaneveld, S. N. Yurgel, J. R. Brown, C. M. Taylor, C. Huttenhower, and M. G. I. Langille. 2020. PICRUSt2 for prediction of metagenome functions. Nature Biotechnology 38:685–688.

Feleszko, W., J. Jaworska, R.-D. Rha, S. Steinhausen, A. Avagyan, A. Jaudszus, B. Ahrens, D. A. Groneberg, U. Wahn, and E. Hamelmann. 2007. Probiotic-induced suppression of allergic sensitization and airway inflammation is associated with an increase of T regulatory-dependent mechanisms in a murine model of asthma. Clinical & Experimental Allergy 37:498–505.

Fernandez, K. R., L. M. Hansen, P. Vandamme, B. L. Beaman, and J. V. Solnick. 2002. Captive rhesus monkeys (Macaca mulatta) are commonly infected with helicobacter cinaedi. Journal of Clinical Microbiology 40:1908–1912.

Flores, R., J. Shi, B. Fuhrman, X. Xu, T. D. Veenstra, M. H. Gail, P. Gajer, J. Ravel, and J. J. Goedert. 2012. Fecal microbial determinants of fecal and systemic estrogens and estrogen metabolites: A cross-sectional study. Journal of Translational Medicine 10:253.

Fouladi, F., M. J. Bailey, W. B. Patterson, M. Sioda, I. C. Blakley, A. A. Fodor, R. B. Jones, Z. Chen, J. S. Kim, F. Lurmann, C. Martino, R. Knight, F. D. Gilliland, and T. L. Alderete. 2020. Air pollution exposure is associated with the gut microbiome as revealed by shotgun metagenomic sequencing. Environment International 138.

Gao, B., L. Chi, R. Mahbub, X. Bian, P. Tu, H. Ru, and K. Lu. 2017. Multi-Omics Reveals that Lead Exposure Disturbs Gut Microbiome Development, Key Metabolites, and Metabolic Pathways. Chemical Research in Toxicology 30:996–

1005.

Gao, H., Q. Shu, J. Chen, K. Fan, P. Xu, Q. Zhou, C. Li, and H. Zheng. 2019. Antibiotic Exposure Has Sex-Dependent Effects on the Gut Microbiota and Metabolism of Short-Chain Fatty Acids and Amino Acids in Mice. mSystems 4:e00048–19.

Gisler, A., I. Korten, K. de Hoogh, D. Vienneau, U. Frey, F. Decrue, O. Gorlanova, A. Soti, M. Hilty, P. Latzin, and J. Usemann. 2021. Associations of air pollution and greenness with the nasal microbiota of healthy infants: A longitudinal study. Environmental Research 202:111633.

Gleeson, K., S. L. Maxwell, and D. F. Eggli. 1997. Quantitative Aspiration During Sleep in Normal Subjects. Chest 111:1266–1272.

Gomez, A., D. Luckey, and V. Taneja. 2015. The gut microbiome in autoimmunity: Sex matters. Clinical Immunology 159:154–162.

Gray, J., K. Oehrle, G. Worthen, T. Alenghat, J. Whitsett, H. Deshmukh, S. Transl, and M. Author. 2017. Intestinal Commensal Bacteria Mediate Lung Mucosal Immunity and Promote Resistance of Newborn Mice to Infection Graphical abstract HHS Public Access Author manuscript. Sci Transl Med 9.

Grimaldi, C. M., J. Cleary, A. S. Dagtas, D. Moussai, and B. Diamond. 2002. Estrogen alters thresholds for B cell apoptosis and activation. The Journal of Clinical Investigation 109:1625–1633.

Groves, H. T., L. Cuthbertson, P. James, M. F. Moffatt, M. J. Cox, and J. S. Tregoning. 2018. Respiratory Disease following Viral Lung Infection Alters the Murine Gut Microbiota. Frontiers in Immunology 9:182.

References

Gu, S., Y. Chen, Z. Wu, Y. Chen, H. Gao, L. Lv, F. Guo, X. Zhang, R. Luo, C. Huang, H. Lu, B. Zheng, J. Zhang, R. Yan, H. Zhang, H. Jiang, Q. Xu, J. Guo, Y. Gong, L. Tang, and L. Li. 2020. Alterations of the Gut Microbiota in Patients With Coronavirus Disease 2019 or H1N1 Influenza. Clinical Infectious Diseases 71:2669–2678.

Harmsen, H. J. M., A. C. M. Wildeboer-Veloo, G. C. Raangs, A. A. Wagendorp, N. Klijn, J. G. Bindels, and G. W. Welling. 2000. Analysis of Intestinal Flora Development in Breast-Fed and Formula-Fed Infants by Using Molecular Identification and Detection Methods. Journal of Pediatric Gastroenterology and Nutrition 30:61.

Haro, C., O. A. Rangel-Zúñiga, J. F. Alcalá-Díaz, F. Gómez-Delgado, P. Pérez-Martínez, J. Delgado-Lista, G. M. Quintana-Navarro, B. B. Landa, J. A. Navas-Cortés, M. Tena-Sempere, J. C. Clemente, J. López-Miranda, F. Pérez-Jiménez, and A. Camargo. 2016. Intestinal microbiota is influenced by gender and body mass index. PLoS ONE 11:1–16.

Hasegawa, Y., B. Curtis, V. Yutuc, M. Rulien, K. Morrisroe, K. Watkins, C. Ferrier, C. English, L. Hewitson, and C. M. Slupsky. 2018. Microbial structure and function in infant and juvenile rhesus macaques are primarily affected by age, not vaccination status. Scientific Reports 8:15867.

He, Y., Q. Wen, F. Yao, D. Xu, Y. Huang, and J. Wang. 2017. Gut-lung axis: The microbial contributions and clinical implications. Critical Reviews in Microbiology 43:81–95.

Hewitt, R. J., and C. M. Lloyd. 2021. Regulation of immune responses by the airway epithelial cell landscape. Nature Reviews Immunology 21:347–362.

Hilty, M., C. Burke, H. Pedro, P. Cardenas, A. Bush, C. Bossley, J. Davies, A. Ervine, L. Poulter, L. Pachter, M. F. Moffatt, and W. O. C. Cookson. 2010. Disordered Microbial Communities in Asthmatic Airways. PLOS ONE 5:e8578.

Huang, Y. J., S. Nariya, J. M. Harris, S. V. Lynch, D. F. Choy, J. R. Arron, and H. Boushey. 2015. The airway microbiome in patients with severe asthma: Associations with disease features and severity. The Journal of Allergy and Clinical Immunology 136:874–884.

Huffnagle, G. B., R. P. Dickson, and N. W. Lukacs. 2017. The respiratory tract microbiome and lung inflammation: A two-way street. Mucosal Immunology 10:299–306.

Huttenhower, C., D. Gevers, R. Knight, S. Abubucker, J. H. Badger, A. T. Chinwalla, H. H. Creasy, A. M. Earl, M. G. FitzGerald, R. S. Fulton, M. G. Giglio, K. Hallsworth-Pepin, E. A. Lobos, R. Madupu, V. Magrini, J. C. Martin, M. Mitreva, D. M. Muzny, E. J. Sodergren, J. Versalovic, A. M. Wollam, K. C. Worley, J. R. Wortman, S. K. Young, Q. Zeng, K. M. Aagaard, O. O. Abolude, E. Allen-Vercoe, E. J. Alm, L. Alvarado, G. L. Andersen, S. Anderson, E. Appelbaum, H. M. Arachchi, G. Armitage, C. A. Arze, T. Ayvaz, C. C. Baker, L. Begg, T. Belachew, V. Bhonagiri, M. Bihan, M. J. Blaser, T. Bloom, V. Bonazzi, J. Paul Brooks, G. A. Buck, C. J. Buhay, D. A. Busam, J. L. Campbell, S. R. Canon, B. L. Cantarel, P. S. G. Chain, I.-M. A. Chen, L. Chen, S. Chhibba, K. Chu, D. M. Ciulla, J. C. Clemente, S. W. Clifton, S. Conlan, J. Crabtree, M. A. Cutting, N. J. Davidovics, C. C. Davis, T. Z. DeSantis, C. Deal, K. D. Delehaunty, F. E. Dewhirst, E. Deych, Y. Ding, D. J. Dooling, S. P. Dugan, W. Michael Dunne, A. Scott Durkin, R. C. Edgar, R. L. Erlich, C. N. Farmer, R. M. Farrell, K. Faust, M. Feldgarden, V. M. Felix, S. Fisher, A. A. Fodor, L. J. Forney, L. Foster, V. Di Francesco, J. Friedman, D. C. Friedrich, C. C. Fronick, L. L. Fulton, H. Gao, N.

Garcia, G. Giannoukos, C. Giblin, M. Y. Giovanni, J. M. Goldberg, J. Goll, A. Gonzalez, A. Griggs, S. Gujja, S. Kinder Haake, B. J. Haas, H. A. Hamilton, E. L. Harris, T. A. Hepburn, B. Herter, D. E. Hoffmann, M. E. Holder, C. Howarth, K. H. Huang, S. M. Huse, J. Izard, J. K. Jansson, H. Jiang, C. Jordan, V. Joshi, J. A. Katancik, W. A. Keitel, S. T. Kelley, C. Kells, N. B. King, D. Knights, H. H. Kong, O. Koren, S. Koren, K. C. Kota, C. L. Kovar, N. C. Kyrpides, P. S. La Rosa, S. L. Lee, K. P. Lemon, N. Lennon, C. M. Lewis, L. Lewis, R. E. Ley, K. Li, K. Liolios, B. Liu, Y. Liu, C.-C. Lo, C. A. Lozupone, R. Dwayne Lunsford, T. Madden, A. A. Mahurkar, P. J. Mannon, E. R. Mardis, V. M. Markowitz, K. Mavromatis, J. M. McCorrison, D. McDonald, J. McEwen, A. L. McGuire, P. McInnes, T. Mehta, K. A. Mihindukulasuriya, J. R. Miller, P. J. Minx, I. Newsham, C. Nusbaum, M. O'Laughlin, J. Orvis, I. Pagani, K. Palaniappan, S. M. Patel, M. Pearson, J. Peterson, M. Podar, C. Pohl, K. S. Pollard, M. Pop, M. E. Priest, L. M. Proctor, X. Qin, J. Raes, J. Ravel, J. G. Reid, M. Rho, R. Rhodes, K. P. Riehle, M. C. Rivera, B. Rodriguez-Mueller, Y.-H. Rogers, M. C. Ross, C. Russ, R. K. Sanka, P. Sankar, J. Fah Sathirapongsasuti, J. A. Schloss, P. D. Schloss, T. M. Schmidt, M. Scholz, L. Schriml, A. M. Schubert, N. Segata, J. A. Segre, W. D. Shannon, R. R. Sharp, T. J. Sharpton, N. Shenoy, N. U. Sheth, G. A. Simone, I. Singh, C. S. Smillie, J. D. Sobel, D. D. Sommer, P. Spicer, G. G. Sutton, S. M. Sykes, D. G. Tabbaa, M. Thiagarajan, C. M. Tomlinson, M. Torralba, T. J. Treangen, R. M. Truty, T. A. Vishnivetskaya, J. Walker, L. Wang, Z. Wang, D. V. Ward, W. Warren, M. A. Watson, C. Wellington, K. A. Wetterstrand, J. R. White, K. Wilczek-Boney, Y. Wu, K. M. Wylie, T. Wylie, C. Yandava, L. Ye, Y. Ye, S. Yooseph, B. P. Youmans, L. Zhang, Y. Zhou, Y. Zhu, L. Zoloth, J. D. Zucker, B. W. Birren, R. A. Gibbs, S. K. Highlander, B. A. Methé, K. E. Nelson, J. F. Petrosino, G. M. Weinstock, R. K. Wilson, O. White, and The Human Microbiome

Project Consortium. 2012. Structure, function and diversity of the healthy human microbiome. Nature 486:207–214.

Huxley, E. J., J. Viroslav, W. R. Gray, and A. K. Pierce. 1978. Pharyngeal aspiration in normal adults and patients with depressed consciousness. The American Journal of Medicine 64:564–568.

Ichinohe, T., I. K. Pang, Y. Kumamoto, D. R. Peaper, J. H. Ho, T. S. Murray, and A. Iwasaki. 2011. Microbiota regulates immune defense against respiratory tract influenza A virus infection.

Jackson, M. A., S. Verdi, M.-E. Maxan, C. M. Shin, J. Zierer, R. C. E. Bowyer, T. Martin, F. M. K. Williams, C. Menni, J. T. Bell, T. D. Spector, and C. J. Steves. 2018. Gut microbiota associations with common diseases and prescription medications in a population-based cohort. Nature Communications 9:2655.

Jacobson, A., L. Lam, M. Rajendram, F. Tamburini, J. Honeycutt, T. Pham, W. Van Treuren, K. Pruss, S. R. Stabler, K. Lugo, D. M. Bouley, J. G. Vilches-Moure, M. Smith, J. L. Sonnenburg, A. S. Bhatt, K. C. Huang, and D. Monack. 2018. A Gut Commensal-Produced Metabolite Mediates Colonization Resistance to Salmonella Infection. Cell Host & Microbe 24:296–307.e7.

Jang, S.-O., H.-J. Kim, Y.-J. Kim, M.-J. Kang, J.-W. Kwon, J.-H. Seo, H. Y. Kim, B.-J. Kim, J. Yu, and S.-J. Hong. 2012. Asthma Prevention by Lactobacillus Rhamnosus in a Mouse Model is Associated With CD4+CD25+Foxp3+ T Cells. Allergy, Asthma & Immunology Research 4:150–156.

Janiak, M. C., M. J. Montague, C. I. Villamil, M. K. Stock, A. E. Trujillo, A. N. DePasquale, J. D. Orkin, S. E. Bauman Surratt, O. Gonzalez, M. L. Platt, M. I. Martínez, S. C. Antón, M. G. Dominguez-Bello, A. D. Melin, and J. P. Higham.

2021. Age and sex-associated variation in the multi-site microbiome of an entire social group of free-ranging rhesus macaques. Microbiome 9:1–17.

Jo, R., K. Yama, Y. Aita, K. Tsutsumi, C. Ishihara, M. Maruyama, K. Takeda, E. Nishinaga, K. Shibasaki, and S. Morishima. 2021. Comparison of oral microbiome profiles in 18-month-old infants and their parents. Scientific Reports 11:861.

Johnson, B. M., M. C. Gaudreau, R. Gudi, R. Brown, G. Gilkeson, and C. Vasu. 2020. Gut microbiota differently contributes to intestinal immune phenotype and systemic autoimmune progression in female and male lupus-prone mice. Journal of Autoimmunity 108:102420.

Jovel, J., L. A. Dieleman, D. Kao, A. L. Mason, and E. Wine. 2018. Chapter 10 - The Human Gut Microbiome in Health and Disease. Pages 197–213 *in* M. Nagarajan, editor. Metagenomics. Academic Press.

Kamphorst, K., B. C. Oosterloo, A. M. Vlieger, N. B. Rutten, C. M. Bunkers, E. C. Wit, and R. M. Van Elburg. 2019. Antibiotic Treatment in the First Week of Life Impacts the Growth Trajectory in the First Year of Life in Term Infants. Journal of Pediatric Gastroenterology and Nutrition 69:131–136.

Kempler, C. 2022, November. FDA Approves First Fecal Microbiota Product. https://www.fda.gov/news-events/press-announcements/fda-approves-first-fecal-microbiota-product; FDA.

Khan, I., N. Ullah, L. Zha, Y. Bai, A. Khan, T. Zhao, T. Che, and C. Zhang. 2019. Alteration of Gut Microbiota in Inflammatory Bowel Disease (IBD): Cause or Consequence? IBD Treatment Targeting the Gut Microbiome. Pathogens 8:126.

Kim, M., E. Vogtmann, D. A. Ahlquist, M. E. Devens, J. B. Kisiel, W. R. Taylor, B. A. White, V. L. Hale, J. Sung, N. Chia, R. Sinha, and J. Chen. 2020. Fecal Metabolomic Signatures in Colorectal Adenoma Patients Are Associated with Gut Microbiota and Early Events of Colorectal Cancer Pathogenesis. mBio 11:10.1128/mbio.03186–19.

Kim, S. Y., and D. Y. Yi. 2020. Components of human breast milk: From macronutrient to microbiome and microRNA. Clinical and Experimental Pediatrics 63:301–309.

Kim, Y. S., T. Unno, B.-Y. Kim, and M.-S. Park. 2019. Sex Differences in Gut Microbiota. The World Journal of Men's Health 38:48–60.

Klein, S. L. 2000. The effects of hormones on sex differences in infection: From genes to behavior. Neuroscience and Biobehavioral Reviews 24:627–638.

Knoop, K. A., K. G. McDonald, D. H. Kulkarni, and R. D. Newberry. 2016. Antibiotics promote inflammation through the translocation of native commensal colonic bacteria. Gut 65:1100–1109.

Koenig, J. E., A. Spor, N. Scalfone, A. D. Fricker, J. Stombaugh, R. Knight, L. T. Angenent, and R. E. Ley. 2011. Succession of microbial consortia in the developing infant gut microbiome. Proceedings of the National Academy of Sciences 108:4578–4585.

Koppen, I. J. N., A. A. T. M. Bosch, E. A. M. Sanders, M. A. van Houten, and D. Bogaert. 2015. The respiratory microbiota during health and disease: A paediatric perspective. Pneumonia 6:90–100.

Korpela, K., A. Salonen, L. J. Virta, R. A. Kekkonen, K. Forslund, P. Bork, and W. M. de Vos. 2016. Intestinal microbiome is related to lifetime antibiotic use in Finnish pre-school children. Nature Communications 7:10410.

Köster, J., and S. Rahmann. 2012. Snakemake-a scalable bioinformatics workflow engine. Bioinformatics 28:2520–2522.

Kostric, M., K. Milger, S. Krauss-Etschmann, M. Engel, G. Vestergaard, M. Schloter, and A. Schöler. 2018. Development of a Stable Lung Microbiome in Healthy Neonatal Mice. Microbial Ecology 75:529–542.

Kozyrskyj, A. L., R. Kalu, P. T. Koleva, and S. L. Bridgman. 2016. Fetal programming of overweight through the microbiome: Boys are disproportionately affected. Journal of Developmental Origins of Health and Disease 7:25–34.

Kubinak, J. L., W. Z. Stephens, R. Soto, C. Petersen, T. Chiaro, L. Gogokhia, R. Bell, N. J. Ajami, J. F. Petrosino, L. Morrison, W. K. Potts, P. E. Jensen, R. M. O'Connell, and J. L. Round. 2015. MHC variation sculpts individualized microbial communities that control susceptibility to enteric infection. Nature Communications 6:8642.

Kuek, L. E., and R. J. Lee. 2020. First contact: The role of respiratory cilia in host-pathogen interactions in the airways. American Journal of Physiology-Lung Cellular and Molecular Physiology 319:L603–L619.

Kuperman, A., A. Zimmerman, S. Hamadia, O. Ziv, V. Gurevich, B. Fichtman, N. Gavert, R. Straussman, H. Rechnitzer, M. Barzilay, S. Shvalb, J. Bornstein, I. Ben-Shachar, S. Yagel, I. Haviv, and O. Koren. 2020. Deep microbial analysis of multiple placentas shows no evidence for a placental microbiome. BJOG: An International Journal of Obstetrics & Gynaecology 127:159–169.

Kuthyar, S., K. Watson, S. Huang, L. J. N. Brent, M. Platt, J. Horvath, J. Gonzalez-Martinez, M. Martínez, F. Godoy-Vitorino, R. Knight, M. G. Dominguez-Bello, and K. R. Amato. 2022. Limited microbiome differences in captive and semi-wild primate populations consuming similar diets. FEMS Microbiology Ecology 98:fiac098.

Lamberte, L. E., and W. van Schaik. 2022. Antibiotic resistance in the commensal human gut microbiota. Current Opinion in Microbiology 68:102150.

Lau, A., N. Yanagisawa, Y. Y. Hor, L. C. Lew, J. S. Ong, L. O. Chuah, Y. Lee, S. B. Choi, F. Rashid, N. Wahid, H. Sugahara, and M. T. Liong. 2017, May. Bifidobacterium longum BB536 alleviated upper respiratory illnesses and modulated gut microbiota profiles in Malaysian pre-school children. https://www.wageningenacademic.com/doi/epdf/10.3920/BM2017.0063?role=tab.

Lebeche, D., S. Malpel, and W. V. Cardoso. 1999. Fibroblast growth factor interactions in the developing lung. Mechanisms of Development 86:125–136.

Lee, S. Y., M. M. Aogáin, K. D. Fam, K. L. Chia, N. A. B. M. Ali, M. M. C. Yap, E. P. H. Yap, S. H. Chotirmall, and C. L. Lim. 2019. Airway microbiome composition correlates with lung function and arterial stiffness in an age-dependent manner. PLOS ONE 14:e0225636.

Levan, S. R., K. A. Stamnes, D. L. Lin, A. R. Panzer, E. Fukui, K. Mccauley, K. E. Fujimura, M. Mckean, D. R. Ownby, E. M. Zoratti, H. A. Boushey, M. D. Cabana, C. C. Johnson, and S. V. Lynch. 2019. Elevated faecal 12,13-diHOME concentration in neonates at high risk for asthma is produced by gut bacteria and impedes immune tolerance.

References

Levy, M., A. A. Kolodziejczyk, C. A. Thaiss, and E. Elinav. 2017. Dysbiosis and the immune system. Nature Reviews Immunology 17:219–232.

Li, G., J. Lin, C. Zhang, H. Gao, H. Lu, X. Gao, R. Zhu, Z. Li, M. Li, and Z. Liu. 2021. Microbiota metabolite butyrate constrains neutrophil functions and ameliorates mucosal inflammation in inflammatory bowel disease. Gut Microbes 13:1968257.

Li, N., F. He, B. Liao, Y. Zhou, B. Li, and P. Ran. 2017. Exposure to ambient particulate matter alters the microbial composition and induces immune changes in rat lung. Respiratory Research 18:143.

Liu, S., R. Cao, L. Liu, Y. Lv, X. Qi, Z. Yuan, X. Fan, C. Yu, and Q. Guan. 2022. Correlation Between Gut Microbiota and Testosterone in Male Patients With Type 2 Diabetes Mellitus. Frontiers in Endocrinology 13:836485.

Liu, X., T. H. Nguyen, L. Sokulsky, X. Li, K. Garcia Netto, A. C.-Y. Hsu, C. Liu, K. Laurie, I. Barr, H. Tay, F. Eyers, P. S. Foster, and M. Yang. 2021. IL-17A is a common and critical driver of impaired lung function and immunopathology induced by influenza virus, rhinovirus and respiratory syncytial virus. Respirology (Carlton, Vic.) 26:1049–1059.

Lloyd-Price, J., G. Abu-Ali, and C. Huttenhower. 2016. The healthy human microbiome. Genome Medicine 8:1–11.

Lührs, H., T. Gerke, J. G. Müller, R. Melcher, J. Schauber, F. Boxberge, W. Scheppach, and T. Menzel. 2002. Butyrate inhibits NF-kappaB activation in lamina propria macrophages of patients with ulcerative colitis. Scandinavian Journal of Gastroenterology 37:458–466.

Ma, R., L. Cheng, Y. Song, Y. Sun, W. Gui, Y. Deng, C. Xie, and M. Liu. 2022. Altered Lung Microbiome and Metabolome Profile in Children With Pulmonary Arterial Hypertension Associated With Congenital Heart Disease. Frontiers in Medicine 9.

Mammen, M. J., and S. Sethi. 2016. COPD and the microbiome. Respirology 21:590–599.

Manichanh, C., J. Reeder, P. Gibert, E. Varela, M. Llopis, M. Antolin, R. Guigo, R. Knight, and F. Guarner. 2010. Reshaping the gut microbiome with bacterial transplantation and antibiotic intake. Genome Research 20:1411.

Markle, J. G. M., D. N. Frank, S. Mortin-Toth, C. E. Robertson, L. M. Feazel, U. Rolle-Kampczyk, M. Von Bergen, K. D. McCoy, A. J. Macpherson, and J. S. Danska. 2013. Sex differences in the gut microbiome drive hormone-dependent regulation of autoimmunity. Science 339:1084–1088.

Marques, T. M., R. Wall, R. P. Ross, G. F. Fitzgerald, C. A. Ryan, and C. Stanton. 2010. Programming infant gut microbiota: Influence of dietary and environmental factors. Current Opinion in Biotechnology 21:149–156.

Marsland, B. J., A. Trompette, and E. S. Gollwitzer. 2015. The Gut–Lung Axis in Respiratory Disease. Annals of the American Thoracic Society 12:S150–S156.

Mayhew, D., N. Devos, C. Lambert, J. R. Brown, S. C. Clarke, V. L. Kim, M. Magid-Slav, B. E. Miller, K. K. Ostridge, R. Patel, G. Sathe, D. F. Simola, K. J. Staples, R. Sung, R. Tal-Singer, A. C. Tuck, S. Van Horn, V. Weynants, N. P. Williams, J.-M. Devaster, and T. M. A. Wilkinson. 2018. Longitudinal profiling of the lung microbiome in the AERIS study demonstrates repeatability of bacterial and eosinophilic COPD exacerbations. Thorax 73:422–430.

Moerlooze, L. D., B. Spencer-Dene, J.-M. Revest, M. Hajihosseini, I. Rosewell, and C. Dickson. 2000. An important role for the IIIb isoform of fibroblast growth factor receptor 2 (FGFR2) in mesenchymal-epithelial signalling during mouse organogenesis. Development 127:483–492.

Moffatt, M. F., and W. O. Cookson. 2017. The lung microbiome in health and disease. Clinical Medicine 17:525–529.

Mueller, N. T., E. Bakacs, J. Combellick, Z. Grigoryan, and M. G. Dominguez-Bello. 2015. The infant microbiome development: Mom matters. Trends in Molecular Medicine 21:109–117.

Mueller, S., K. Saunier, C. Hanisch, E. Norin, L. Alm, T. Midtvedt, A. Cresci, S. Silvi, C. Orpianesi, M. C. Verdenelli, T. Clavel, C. Koebnick, H. J. F. Zunft, J. Doré, and M. Blaut. 2006. Differences in fecal microbiota in different European study populations in relation to age, gender, and country: A cross-sectional study. Applied and Environmental Microbiology 72:1027–1033.

Natividad, J. M., B. Marsaux, C. L. G. Rodenas, A. Rytz, G. Vandevijver, M. Marzorati, P. Van den Abbeele, M. Calatayud, and F. Rochat. 2022. Human Milk Oligosaccharides and Lactose Differentially Affect Infant Gut Microbiota and Intestinal Barrier In Vitro. Nutrients 14:2546.

Needell, J. C., and D. Zipris. 2016. The Role of the Intestinal Microbiome in Type 1 Diabetes Pathogenesis. Current Diabetes Reports 16:1–8.

Niu, J., M. Cui, X. Yang, J. Li, Y. Yao, Q. Guo, A. Lu, X. Qi, D. Zhou, C. Zhang, L. Zhao, and G. Meng. 2023. Microbiota-derived acetate enhances host antiviral response via NLRP3. Nature Communications 14:642.

Nobel, Y. R., L. M. Cox, F. F. Kirigin, N. A. Bokulich, S. Yamanishi, I. Teitler, J. Chung, J. Sohn, C. M. Barber, D. S. Goldfarb, K. Raju, S. Abubucker, Y. Zhou, V. E. Ruiz, H. Li, M. Mitreva, A. V. Alekseyenko, G. M. Weinstock, E. Sodergren, and M. J. Blaser. 2015. ARTICLE Metabolic and metagenomic outcomes from early-life pulsed antibiotic treatment. Nature Communications.

Öberg, M., M. S. Jaakkola, A. Woodward, A. Peruga, and A. Prüss-Ustün. 2011. Worldwide burden of disease from exposure to second-hand smoke: A retrospective analysis of data from 192 countries. The Lancet 377:139–146.

Org, E., M. Mehrabian, B. W. Parks, P. Shipkova, X. Liu, T. A. Drake, and A. J. Lusis. 2016. Sex differences and hormonal effects on gut microbiota composition in mice. Gut Microbes 7:313–322.

Park, J., M. Kim, S. G. Kang, A. H. Jannasch, B. Cooper, J. Patterson, and C. H. Kim. 2015. Short-chain fatty acids induce both effector and regulatory T cells by suppression of histone deacetylases and regulation of the mTOR-S6K pathway. Mucosal Immunology 8:80–93.

Pascale, A., N. Marchesi, C. Marelli, A. Coppola, L. Luzi, S. Govoni, A. Giustina, and C. Gazzaruso. 2018. Microbiota and metabolic diseases. Endocrine 61:357–371.

Pattaroni, C., M. L. Watzenboeck, S. Schneidegger, S. Kieser, N. C. Wong, E. Bernasconi, J. Pernot, L. Mercier, S. Knapp, L. P. Nicod, C. P. Marsland, M. Roth-Kleiner, and B. J. Marsland. 2018. Early-Life Formation of the Microbial and Immunological Environment of the Human Airways. Cell Host & Microbe 24:857–865.e4.

Pembrey, L., M. L. Newell, and P. A. Tovo. 2008. Age-related lymphocyte and neutrophil levels in children of hepatitis C-infected women. Pediatric Infectious

Disease Journal 27:800–807.

Peng, C., X. Xu, Y. Li, X. Li, X. Yang, H. Chen, Y. Zhu, N. Lu, and C. He. 2020. Sex-specific association between the gut microbiome and high-fat diet-induced metabolic disorders in mice. Biology of Sex Differences 11:5.

Pérez-Cobas, A. E., J. Rodríguez-Beltrán, F. Baquero, and T. M. Coque. 2023. Ecology of the respiratory tract microbiome. Trends in Microbiology 0.

Peterson, S. W., N. C. Knox, G. R. Golding, S. D. Tyler, A. D. Tyler, P. Mabon, J. E. Embree, F. Fleming, S. Fanella, G. Van Domselaar, M. R. Mulvey, and M. R. Graham. 2016. A Study of the Infant Nasal Microbiome Development over the First Year of Life and in Relation to Their Primary Adult Caregivers Using Cpn60 Universal Target (UT) as a Phylogenetic Marker. PLoS ONE 11:e0152493.

Phillips, K. A., K. L. Bales, J. P. Capitanio, A. Conley, P. W. Czoty, B. A. 't Hart, W. D. Hopkins, S.-L. Hu, L. A. Miller, M. A. Nader, P. W. Nathanielsz, J. Rogers, C. A. Shively, and M. L. Voytko. (n.d.). Why Primate Models Matter.

PrabhuDas, M., B. Adkins, H. Gans, C. King, O. Levy, O. Ramilo, and C. A. Siegrist. 2011. Challenges in infant immunity: Implications for responses to infection and vaccines. Nat Immunol 12:189–194.

Prakash, A., B. A. Peters, E. Cobbs, D. Beggs, H. Choi, H. Li, R. B. Hayes, and J. Ahn. 2021. Tobacco Smoking and the Fecal Microbiome in a Large, Multi-ethnic Cohort. Cancer Epidemiology, Biomarkers & Prevention 30:1328–1335.

Ratajczak, W., A. Rył, A. Mizerski, K. Walczakiewicz, O. Sipak, and M. Laszczyńska. 2019. Immunomodulatory potential of gut microbiome-derived short-chain fatty acids (SCFAs). Acta Biochimica Polonica 66.

Rautava, S., R. Luoto, S. Salminen, and E. Isolauri. 2012. Microbial contact during pregnancy, intestinal colonization and human disease. Nature Reviews Gastroenterology & Hepatology 9:565–576.

Raymond, S. L., J. C. Rincon, J. L. Wynn, L. L. Moldawer, and S. D. Larson. 2017. Impact of early-life exposures to infections, antibiotics, and vaccines on perinatal and long-term health and disease. Frontiers in Immunology 8:1–7.

Rhoades, N. S., M. Davies, S. A. Lewis, I. R. Cinco, S. G. Kohama, L. E. Bermudez, K. L. Winthrop, C. Fuss, J. A. Mattison, E. R. Spindel, and I. Messaoudi. 2022. Functional, transcriptional, and microbial shifts associated with healthy pulmonary aging in rhesus macaques. Cell Rep 39:110725.

Rhoades, T. Barr, S. Hendrickson, K. Prongay, A. Haertel, L. Gill, L. Garzel, K. Whiteson, M. Slifka, and I. Messaoudi. 2019. Maturation of the infant rhesus macaque gut microbiome and its role in the development of diarrheal disease. Genome Biology 20:1–16.

Roager, H. M., and T. R. Licht. 2018. Microbial tryptophan catabolites in health and disease. Nature Communications 9:3294.

Rouhani, S., N. W. Griffin, P. P. Yori, M. P. Olortegui, M. Siguas Salas, D. Rengifo Trigoso, L. H. Moulton, E. R. Houpt, M. J. Barratt, M. N. Kosek, and J. I. Gordon. 2020. Gut Microbiota Features Associated With Campylobacter Burden and Postnatal Linear Growth Deficits in a Peruvian Birth Cohort. Clinical Infectious Diseases 71:1000–1007.

Ruf, B. R., and M. Knuf. 2014. The burden of seasonal and pandemic influenza in infants and children. European Journal of Pediatrics 173:265–276.

References

Sagar, S., M. E. Morgan, S. Chen, A. P. Vos, J. Garssen, J. van Bergenhenegouwen, L. Boon, N. A. Georgiou, A. D. Kraneveld, and G. Folkerts. 2014. Bifidobacterium breve and Lactobacillus rhamnosus treatment is as effective as budesonide at reducing inflammation in a murine model for chronic asthma. Respiratory Research 15:46.

Schittny, J. C. 2017. Development of the lung. Cell and Tissue Research 367:427–444.

Segal, L. N., A. V. Alekseyenko, J. C. Clemente, R. Kulkarni, B. Wu, H. Chen, K. I. Berger, R. M. Goldring, W. N. Rom, M. J. Blaser, and M. D. Weiden. 2013. Enrichment of lung microbiome with supraglottic taxa is associated with increased pulmonary inflammation. Microbiome 2013 1:1 1:1–12.

Segata, N., J. Izard, L. Waldron, D. Gevers, L. Miropolsky, W. S. Garrett, and C. Huttenhower. 2011. Metagenomic biomarker discovery and explanation. Genome Biology 12:R60.

SeungHye, H., and R. Mallampalli. 2015, February. The Role of Surfactant in Lung Disease and Host Defense against Pulmonary Infections. https://www.atsjournals.org/doi/epdf/10.1513/AnnalsATS.201411-507FR?role=tab.

Seyedian, S. S., F. Nokhostin, and M. D. Malamir. 2019. A review of the diagnosis, prevention, and treatment methods of inflammatory bowel disease. Journal of Medicine and Life 12:113–122.

Shastri, P., J. McCarville, M. Kalmokoff, S. P. J. Brooks, and J. M. Green-Johnson. 2015. Sex differences in gut fermentation and immune parameters in rats fed an oligofructose-supplemented diet. Biology of Sex Differences 6:1–12.

Shields-Cutler, R. R., G. A. Al-Ghalith, M. Yassour, and D. Knights. 2018. SplinectomeR Enables Group Comparisons in Longitudinal Microbiome Studies. Front Microbiol 9:785.

Sidener, H. M., B. Park, and L. Gao. 2017. Effect of antibiotic administration during infancy on growth curves through young adulthood in rhesus macaques (Macaca mulatta). Comparative Medicine 67:270–276.

Siracusa, M. C., M. G. Overstreet, F. Housseau, A. L. Scott, and S. L. Klein. 2008. 17β-Estradiol Alters the Activity of Conventional and IFN-Producing Killer Dendritic Cells1. The Journal of Immunology 180:1423–1431.

Sivaprakasam, S., P. D. Prasad, and N. Singh. 2016. Benefits of short-chain fatty acids and their receptors in inflammation and carcinogenesis. Pharmacology & Therapeutics 164:144–151.

Stepanauskaite, L., M. Birgersson, N. Brusselaers, I. Schuppe-Koistinen, A. Archer, L. Engstrand, and C. Williams. 2023. High-fat diet and estrogen modulate the gut microbiota in a sex-dependent manner in mice. Communications Biology 6:1–12.

Strömberg Celind, F., G. Wennergren, S. Vasileiadou, B. Alm, and E. Goksör. 2018. Antibiotics in the first week of life were associated with atopic asthma at 12 years of age. Acta Paediatrica (Oslo, Norway : 1992) 107:1798–1804.

Sulaiman, I., B. G. Wu, Y. Li, J.-C. Tsay, M. Sauthoff, A. S. Scott, K. Ji, S. B. Koralov, M. Weiden, J. C. Clemente, D. Jones, Y. J. Huang, K. A. Stringer, L. Zhang, A. Geber, S. Banakis, L. Tipton, E. Ghedin, and L. N. Segal. 2021. Functional lower airways genomic profiling of the microbiome to capture active microbial metabolism. European Respiratory Journal 58:2003434.

Takahashi, Y., A. Saito, H. Chiba, K. Kuronuma, K. Ikeda, T. Kobayashi, S. Ariki, M. Takahashi, Y. Sasaki, and H. Takahashi. 2018. Impaired diversity of the lung microbiome predicts progression of idiopathic pulmonary fibrosis. Respiratory Research 19:1–10.

Tamburini, S., N. Shen, H. C. Wu, and J. C. Clemente. 2016. The microbiome in early life: Implications for health outcomes. Nature Medicine 22:713–722.

Tang, C., and S. Offermanns. 2017. FFA2 and FFA3 in Metabolic Regulation. Handb Exp Pharmacol 236:205–220.

Thorpe, J. E., R. P. Baughman, P. T. Frame, T. A. Wesseler, and J. L. Staneck. 1987. Bronchoalveolar Lavage for Diagnosing Acute Bacterial Pneumonia. The Journal of Infectious Diseases 155:855–861.

Tong, X., F. Su, X. Xu, H. Xu, T. Yang, Q. Xu, H. Dai, K. Huang, L. Zou, W. Zhang, S. Pei, F. Xiao, Y. Li, and C. Wang. 2019. Alterations to the Lung Microbiome in Idiopathic Pulmonary Fibrosis Patients. Frontiers in Cellular and Infection Microbiology 9.

Tremlett, H., K. C. Bauer, S. Appel-Cresswell, B. B. Finlay, and E. Waubant. 2017. The gut microbiome in human neurological disease: A review. Annals of Neurology 81:369–382.

Trompette, Eva S Gollwitzer, Koshika Yadava, Anke K Sichelstiel, Norbert Sprenger, Catherine Ngom-Bru, Carine Blanchard, Tobias Junt, Laurent P Nicod, Nicola L Harris, and Benjamin J Marsland. 2014. Gut microbiota metabolism of dietary fiber influences allergic airway disease and hematopoiesis. nature medicine 2:159–169.

Turta, O., and S. Rautava. 2016. Antibiotics, obesity and the link to microbes - what are we doing to our children? BMC Medicine 14:57.

Uzan-Yulzari, A., O. Turta, A. Belogolovski, O. Ziv, C. Kunz, S. Perschbacher, H. Neuman, E. Pasolli, A. Oz, H. Ben-Amram, H. Kumar, H. Ollila, A. Kaljonen, E. Isolauri, S. Salminen, H. Lagström, N. Segata, I. Sharon, Y. Louzoun, R. Ensenauer, S. Rautava, and O. Koren. 2021. Neonatal antibiotic exposure impairs child growth during the first six years of life by perturbing intestinal microbial colonization. Nature Communications 12:1–12.

Valeri, F., and K. Endres. 2021. How biological sex of the host shapes its gut microbiota. Frontiers in Neuroendocrinology 61:100912.

Vallender, E. J., and G. M. Miller. 2013. Nonhuman Primate Models in the Genomic Era: A Paradigm Shift. ILAR Journal 54:154–165.

van Nimwegen, F. A., J. Penders, E. E. Stobberingh, D. S. Postma, G. H. Koppelman, M. Kerkhof, N. E. Reijmerink, E. Dompeling, P. A. van den Brandt, I. Ferreira, M. Mommers, and C. Thijs. 2011. Mode and place of delivery, gastrointestinal microbiota, and their influence on asthma and atopy. Journal of Allergy and Clinical Immunology 128:948–955.e3.

Vangay, P., T. Ward, J. S. Gerber, and D. Knights. 2015. Antibiotics, pediatric dysbiosis, and disease. Cell Host and Microbe 17:553–564.

Venegas, D. P., M. K. De La Fuente, G. Landskron, M. J. González, R. Quera, G. Dijkstra, H. J. M. Harmsen, K. N. Faber, and M. A. Hermoso. 2019. Short chain fatty acids (SCFAs)mediated gut epithelial and immune regulation and its relevance for inflammatory bowel diseases. Frontiers in Immunology 10.

Vinolo, M. A. R., H. G. Rodrigues, R. T. Nachbar, and R. Curi. 2011. Regulation of Inflammation by Short Chain Fatty Acids. Nutrients 3:858–876.

Wang, B., M. Yao, L. Lv, Z. Ling, and L. Li. 2017. The Human Microbiota in Health and Disease. Engineering 3:71–82.

Wang, J., F. Li, R. Sun, X. Gao, H. Wei, L.-J. Li, and Z. Tian. 2013. Bacterial colonization dampens influenza-mediated acute lung injury via induction of M2 alveolar macrophages. Nature Communications 4:2106.

Weibel, E. R. 1963. Morphometry of the Human Lung. Springer, Berlin, Heidelberg.

Weiss, G. A., and T. Hennet. 2017. Mechanisms and consequences of intestinal dysbiosis. Cellular and Molecular Life Sciences 74:2959–2977.

Wlodarska, M., A. D. Kostic, and R. J. Xavier. 2015. An integrative view of microbiome-host interactions in inflammatory bowel diseases. Cell Host and Microbe 17:577–591.

Yildiz, S., B. Mazel-Sanchez, M. Kandasamy, B. Manicassamy, and M. Schmolke. 2018. Influenza A virus infection impacts systemic microbiota dynamics and causes quantitative enteric dysbiosis. Microbiome 6:9.

Yoon, K., and N. Kim. 2021. Roles of Sex Hormones and Gender in the Gut Microbiota. Journal of Neurogastroenterology and Motility 27:314–325.

Yurkovetskiy, L., M. Burrows, A. A. Khan, L. Graham, P. Volchkov, L. Becker, D. Antonopoulos, Y. Umesaki, and A. V. Chervonsky. 2013. Gender bias in autoimmunity is influenced by microbiota. Immunity 39:400–412.

Zhang, D., S. Li, N. Wang, H.-Y. Tan, Z. Zhang, and Y. Feng. 2020. The Cross-Talk Between Gut Microbiota and Lungs in Common Lung Diseases. Frontiers in

Microbiology 11.

Zhang, L., D. Dong, C. Jiang, Z. Li, X. Wang, and Y. Peng. 2015. Insight into alteration of gut microbiota in Clostridium difficile infection and asymptomatic C. Difficile colonization. Anaerobe 34:1–7.

Zhang, X., H. Zhong, Y. Li, Z. Shi, H. Ren, Z. Zhang, X. Zhou, S. Tang, X. Han, Y. Lin, F. Yang, D. Wang, C. Fang, Z. Fu, L. Wang, S. Zhu, Y. Hou, X. Xu, H. Yang, J. Wang, K. Kristiansen, J. Li, and L. Ji. 2021. Sex- and age-related trajectories of the adult human gut microbiota shared across populations of different ethnicities. Nature Aging 1:87–100.

Zhao, L., J.-L. Luo, M. K. Ali, E. Spiekerkoetter, and M. R. Nicolls. 2023. The Human Respiratory Microbiome: Current Understandings and Future Directions. American Journal of Respiratory Cell and Molecular Biology 68:245–255.

Zhu, Q., N. Qi, L. Shen, C. C. Lo, M. Xu, Q. Duan, N. J. Ollberding, Z. Wu, D. Y. Hui, P. Tso, and M. Liu. 2023. Sexual Dimorphism in Lipid Metabolism and Gut Microbiota in Mice Fed a High-Fat Diet. Nutrients 15:2175.

Zuany-Amorim, C., E. Sawicka, C. Manlius, A. Le Moine, L. R. Brunet, D. M. Kemeny, G. Bowen, G. Rook, and C. Walker. 2002. Suppression of airway eosinophilia by killed Mycobacterium vaccae-induced allergen-specific regulatory T-cells. Nature Medicine 8:625–629.

Zuo, T., X. Wu, W. Wen, and P. Lan. 2021. Gut Microbiome Alterations in COVID-19. Genomics, Proteomics & Bioinformatics 19:679–688.